Załącznik nr 1/1
do Zarządzenia Rektora PG nr 30/2022
z 14 kwietnia 2022r.

GDAŃSK UNIVERSITY OF TECHNOLOGY | FACULTY OF CHEMISTRY

The author of the PhD dissertation: **Dorota Dulko**

Scientific discipline: chemical sciences

DOCTORAL DISSERTATION

Title of PhD dissertation:

Application of human bile salts for *in vitro* digestion models

Title of PhD dissertation (in Polish):

Wykorzystanie ludzkich soli żółciowych w modelach trawienia *in vitro*

Supervisor:

Adam Macierzanka DSc PhD

Associate Professor

……

Supervisor's Signature

Załącznik nr 2/2
do Zarządzenia Rektora PG nr 30/2022
z 14 kwietnia 2022r.

GDAŃSK UNIVERSITY OF TECHNOLOGY | FACULTY OF CHEMISTRY

STATEMENT

The author of the PhD dissertation: **Dorota Dulko**

I, the undersigned, declare that I am aware that in accordance with the provisions of Art. 27 (1) and (2) of the Act of 4th February 1994 on Copyright and Related Rights (Journal of Laws of 2021, item 1062), the university may use my doctoral dissertation entitled: **„Application of human bile salts for *in vitro* digestion models"** for scientific or didactic purposes.[1]

Kraków,..... .....
signature of the PhD student

Aware of criminal liability for violations of the Act of 4th February 1994 on Copyright and Related Rights and disciplinary actions set out in the Law on Higher Education and Science(Journal of Laws 2021, item 478), as well as civil liability, I declare, that the submitted doctoral dissertation is my own work.

I declare, that the submitted doctoral dissertation is my own work performed under and in cooperation with the supervision of **Adam Macierzanka**.

This submitted PhD dissertation has never before been the basis of an official procedure associated with the awarding of a PhD degree.

All the information contained in the above thesis which is derived from written and electronic sources is documented in a list of relevant literature in accordance with art. 34 of the Copyright and Related Rights Act.

I confirm that this PhD dissertation is identical to the attached electronic version.

Kraków,..... .....
signature of the PhD student

I, the undersigned, agree/~~do not agree~~* to include an electronic version of the above doctoral dissertation in the open, institutional, digital repository of Gdańsk University of Technology.

Kraków,..... .....
signature of the PhD student

*) delete where appropriate.

[1] Art 27. 1. Educational institutions and entities referred to in art. 7 sec. 1 points 1, 2 and 4–8 of the Act of 20 July 2018 – Law on Higher Education and Science, may use the disseminated works in the original and in translation for the purposes of illustrating the content provided for didactic purposes or in order to conduct research activities, and to reproduce for this purpose disseminated minor works or fragments of larger works. 2. If the works are made available to the public in such a way that everyone can have access to them at the place and time selected by them, as referred to in para. 1, is allowed only for a limited group of people learning, teaching or conducting research, identified by the entities listed in paragraph 1.

Załącznik nr 3/2
do Zarządzenia Rektora PG nr 30/2022
z 14 kwietnia 2022r.

GDAŃSK UNIVERSITY OF TECHNOLOGY | FACULTY OF CHEMISTRY

DESCRIPTION OF DOCTORAL DISSERTATION

The Author of the PhD dissertation: Dorota Dulko
Title of PhD dissertation: Application of human bile salts for *in vitro* digestion models

Title of PhD dissertation in Polish: Wykorzystanie ludzkich soli żółciowych w modelach trawienia *in vitro*

Language of PhD dissertation: English

Supervision: Adam Macierzanka

Date of doctoral defense: ……
Keywords of PhD dissertation in Polish: ludzka żółć, sole żółciowe, trawienie *in vitro*, proteoliza, lipoliza
Keywords of PhD dissertation in English: human bile, bile salts, *in vitro* digestion, proteolysis, lipolysis

Summary of PhD dissertation in Polish:

W niniejszej pracy wykorzystano eksperymentalne modele *in vitro*, symulujące środowisko ludzkiego przewodu pokarmowego, celem oceny wpływu fizjologicznych surfaktantów, takich jak sole żółciowe, na kinetykę trawienia. Sole żółciowe są biosurfaktantami syntezowanymi w wątrobie i wydzielanymi wraz z żółcią do jelita cienkiego. Istnieje wiele doniesień dotyczących udziału soli żółciowych w lipolizie, natomiast wiedza dotycząca ich wpływu na inne składniki odżywcze, jak np. białka jest bardzo ograniczona. Przeprowadzone przeze mnie eksperymenty obejmowały porównanie systemu modelowego (indywidualne sole żółciowe) z ludzką żółcią (zawierającą różne stężenia soli żółciowych, fosfolipidów i innych substancji) podczas lipolizy i proteolizy w warunkach *in vitro*. Próbki ludzkiej żółci uzyskano dzięki współpracy z ośrodkiem klinicznym. Po raz pierwszy dokonano ilościowej analizy wpływu ludzkie żółci na trawienie modelowego białka spożywczego oraz tłuszczu. Po raz pierwszy dokonano także walidacji stosowanych obecnie, statycznych modeli trawienia *in vitro,* z punktu widzenia fizjologicznego odwzorowywania roli soli żółciowych w ludzkim przewodzie pokarmowym. W tym względzie wykazano *in vitro*, jak wpływ prawdziwej żółci ludzkiej na proteolizę i lipolizę można wiarygodnie odtworzyć poprzez zastosowanie mieszaniny indywidualnych soli żółciowych i fosfolipidów.

Summary of PhD dissertation in English:

In this study, experimental *in vitro* models simulating the environment of the human gastrointestinal tract were used to assess the impact of physiological surfactants, such as bile salts, on the kinetics of digestion. Bile salts are biosurfactants synthesised in the liver and secreted together with bile into the small intestine. There are many reports on the role of bile salts in lipolysis, but the knowledge of their influence on other nutrients, such as proteins, is very limited. The experiments I conducted included the comparison of a model system (individual bile salts) with real human bile (containing different concentrations of bile salts, phospholipids, and other substances) during *in vitro* lipolysis and proteolysis. Human bile samples were obtained in cooperation with a clinical hospital. For the first time, a quantitative analysis of the effects of human bile on the digestion of a model food protein and lipid was performed. Moreover, for the first time, the currently used static *in vitro* digestion models were validated from the point of view of the physiological role of bile salts in the human digestive tract. In this respect, it has been demonstrated *in vitro* how the effect of human bile on the proteolysis and lipolysis can be reliably reproduced by applying mixtures of individual bile salt and phospholipids.

Table of contents

List of abbreviations:

ANOVA – analysis of variance

ATP – adenosine triphosphate

BS – bile salt(s)

BTEE – bis(triethoxysilyl)ethane

C - cholate

CD – circular dichroism

CDC - chemodeoxycholate

CMC - critical micelle concentration

DAD – diode array detector

DPPC - dipalmitoylphosphocholine

DTT - ditiotreitol

E – enzymes

ELSD - evaporative light scattering detector

ERCP - endoscopic retrograde cholangiopancreatography

ESIN - Engineered Stomach and Small Intestine

FFA – free fatty acid

GC - glycocholate

GCDC - glycochenodeoxycholate

GDC - glycodeoxycholate

GE- gastric emptying

GHDC - glycohyodeoxycholate

HB – human bile

HCl – hydrochloric acid

HPLC – high performance liquid chromatography

IgG – immunoglobulin G

LC – liquid chromatography

NaGDC - sodium glycodeoxycholate

NaCl – sodium chloride

NaTC - sodium taurocholate

OVA – ovalbumin

PC - phosphatidylcholine

PE – phosphatidylethanolamine

PMSF – phenylmethanesulfonyl fluoride

PS - phosphatidylserine

RT – room temperature

SD – standard deviation

SDS - sodium dodecyl sulphate

SDS-PAGE – sodium dodecyl sulphate polyacrylamide gel electrophoresis

SGF - simulated gastric fluid

SHIME - Simulator of Human Intestinal Microbial Ecosystem

SIF - simulated intestinal fluid

SSF - simulated salivary fluid

TC - taurocholate

TCDC - taurochenodeoxycholate

TDC - taurodeoxycholate

TDC – taurodeoxycholate

TG - trigliceryde

TIC - total ion current

TJ - tight junction

UV – ultraviolet

WPI – whey protein isolate

αLA – alpha lactalbumin

βLg – beta lactoglobulin

1. Introduction

Every day we ingest food consisting of different nutrients, which play an essential role in maintaining many functions of our body; carbohydrates and fats are predominantly the source of energy, and proteins are major building blocks for the body tissues. Once the nutrients present in food are ingested they take part in a number of physicochemical processes and chemical reactions, beginning in the mouth, through the stomach, and finally the small and large intestines. In the following sections, there is a summary of the digestion processes that take place in the human gastrointestinal tract. The emphasis has been predominantly on the small intestinal compartment, where the majority of digestive enzymes are present and where physiological surfactants, such as bile salts, contribute to the food digestion processes.

1.1. General characterisation of food digestion conditions

1.1.1. Physicochemical aspects of food digestion

Food digestion processes can be, in principle, divided into four compartments in which different conditions impact the food transformation: mouth, stomach, small intestine, and large intestine (Fig. 1). In the following sections of this work, the physicochemical aspects of food digestion in each of the mentioned compartments of the digestive tract have been described.

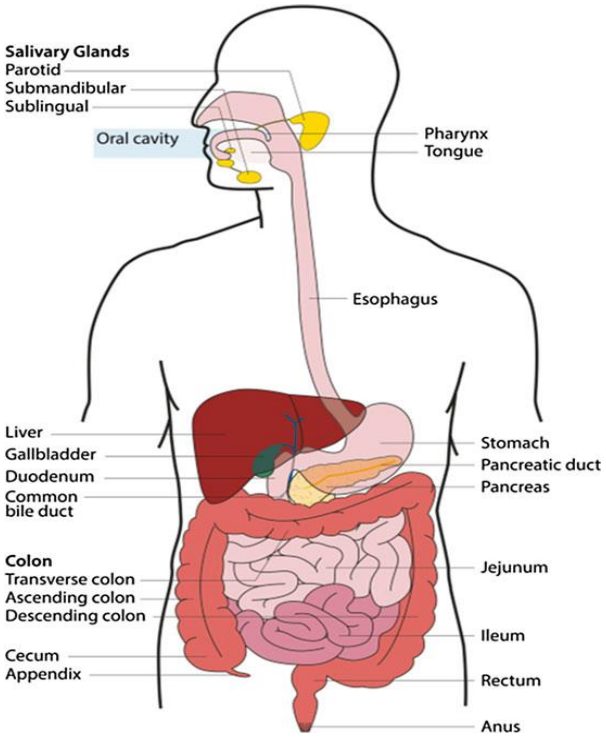

Figure 1. Schematic representation of the human gastrointestinal tract (Alegría et al., 2015).

The mouth

After ingestion, food processing starts in the mouth, where the food undergoes a mechanical treatment with the help of the tongue and teeth. There are three main processes occurring during the oral phase of digestion: mastication, lubrication, and enzymatic hydrolysis (Bornhorst & Singh, 2013). After the first bite, food is transported, chewed, and lubricated with saliva, forming at this stage a “bolus”. Oral food processing can differ depending on the individual oral physiology (i.e. depending on age, sex, health, dental hygiene, etc.) and on the food properties (i.e. moisture, texture, hardness, particle size, rheology, etc.). Both sets of factors play an important role in bolus processing (Bornhorst & Singh, 2012). The mastication along with the action of the tongue allows for increasing the contact of bolus with saliva and lubricates the food, which impacts its physical properties. Moreover, the saliva acts as a medium between a bolus and the taste receptor cells. Mastication reduces the size of the bolus to make it easier for swallowing and for further transportation in the oral cavity and through the esophagus. Using bread as an example, a previous study showed that after ingestion and during mastication, bread loses its viscid structure. The maximal particle size of the degraded bolus decreases more than twice after 27 s of mastication

(Hoebler et al., 1998). Chewing of food with the teeth starts with the first bite. The force applied to the bite depends on the type of food (e.g., the food consistency, the volume of the bite, etc.) – the harder the bolus the longer time is needed for chewing and more force needs to be applied. The chewing time is correlated with the effectiveness of bolus degradation. The longer the mastication the lower the size of the bolus. Similarly, the smaller the initial bolus size the shorter the time of mastication (Chen, 2009). Besides the bolus size reduction, the other aspect of chewing is saliva incorporation. Saliva incorporates bolus particles and can modify its viscosity. The saliva consists of 98% of water and 2% of organic and inorganic ingredients such as electrolytes, glycoproteins, and enzymes. The most important salivary enzyme is α-amylase, which is responsible for the initial (and limited) hydrolysis of carbohydrates. The enzyme is secreted mainly by the parotid salivary glands. It hydrolyses 1,4-α-glycoside bonds with the disengagement of maltose. Up to 30% of starch is typically hydrolysed in the mouth within 20-30 seconds. The pH of saliva ranges between 5.6 and 7.6, which corresponds with the optimal pH for the α-amylase activity. The saliva also has an antibacterial function due to the presence of lysozyme, lactoferrin, and immunoglobulin A (Dawes et al., 2015), (Nater et al., 2005).

The stomach

After the oral processing, when the bolus is reduced to a size that can be easily swallowed, it is moved to the back of the oral cavity. Next, the bolus enters the stomach through the pharynx and esophagus due to the action of primary and secondary peristalsis (Buettner et al., 2001). In the stomach, pH ranges typically from 1 to 4, depending on the fasted or fed state. Just after meal consumption, the pH of gastric content is similar to the meal pH due to the buffering effect of the food. The pH is decreasing along with the secretion of gastric acid. The secretion is stimulated by the action of hormones, which are activated after consumption (Camilleri & Vazquez Roque, 2014). Under acidic conditions, bolus acts as a partly digested, semi-fluid mixture of food, salivary and gastric fluids, from now on called “chyme”. The function of the stomach is to store, mix and digest food, as well as deliver the resulting, partially digested chyme to the duodenum. There are three main anatomical parts of this organ (Fig. 2). The first is the fundus – an upper proximal curvature of the stomach closest to the esophagus. This upper part is filled with air and along with the fundic contractions moves chyme from the fundus to the pylorus of the stomach. These

contractions are responsible for mixing chyme with gastric juices, which are secreted by the glands lining the gastric epithelium (Kong & Singh, 2008). The next, middle part is the body. It is responsible for the storage of food content. The third, called the antrum of the stomach, acts as a grinder, mixer, and pump. It is the place where chyme is fragmented and is gradually moved through the pyloric sphincter into the proximal small intestine (i.e., the duodenum). The stomach capacity of an adult human is about 1.5 litre (Bellmann et al., 2016). The gastric phase of digestion comprises three principal processes: the diffusion of gastric juices into food structure, its mechanical degradation by peristaltic movements, and enzymatic hydrolysis. Looking at the mechanical degradation of the chyme it is important to consider multiple processes such as mixing, grinding, sieving (i.e. separation of liquid and solid contents), and pumping. All of that happens due to the smooth muscles' action and is known as peristaltic movements. The muscle contractions are regulated by hormones and the nervous system. Under the aforementioned conditions, the chyme can be degraded to smaller particles, which increases the surface area of the food available for gastric enzymes. The acidic environment of the stomach along with mechanical forces, enzymatic action, and body temperature optimal for pepsin activity have synergistic effect on solid food breakdown. Similar to the oral phase of digestion, the physical properties of ingested food play an important role in the kinetics of food breakdown. From the example of the study on gastric digestion of carrots (raw and cooked) and ham, it can be concluded, that soft foods disintegrate more rapidly than hard ones (Kong & Singh, 2008).

Particle size influences the gastric emptying rate and time. The smaller the particle size of the chyme, the faster the gastric emptying (Guo et al., 2015). A good example here is a study that compares the gastric digestion of brown and white rice. Brown rice, because of the higher amount of dietary fibres, forms more viscous and thus bigger chyme particles, which in turn delay gastric emptying. The other subject correlated with the physical properties of chyme is the mechanism of nutrient release, as a result of mechanical and chemical chyme degradation. There are two main steps. First, nutrients are transported from the food interior to the food surface. In the second step nutrient diffusion occurs from the food surface to the gastric juices. Nevertheless, the precise mechanism of nutrient release is still unclear (Somaratne et al., 2020).

From the biochemical point of view, gastric digestion includes the initial enzymatic hydrolysis of proteins, lipids, and nucleic acids. The main enzyme secreted and activated in

the stomach is proteolytic pepsin. Pepsin is most active at pH 2 and is inactive above pH 6.5 (Johnston et al., 2007). This enzyme hydrolyses the peptide bonds of aromatic (e.g. phenylalanine), acidic (e.g. glutamic acid), and hydrophobic (e.g. leucine, valine) amino acids. The action of pepsin produces short polypeptides by cleaving phenylalanine, tyrosine, tryptophan, and leucine in position P1 or P1' with a cleavage probability between 17 and 51%, respectively. Moreover, there is up to 24% cleavage probability for the enzyme at the peptide bonds of some other amino acid residues i.e. cysteine, glutamine, and alanine. It means pepsin is efficient in proteolysis, but does not have a strong site-specific preference in cleaving peptide bonds (Macierzanka et al., 2012), (Singh & Ye, 2013).

Pepsin is also involved in the metabolism of nucleic acids ingested with food. DNA is denatured (at least partially) to a single strand at a pH below 4. More accurate depurination of DNA occurs under strongly acidic gastric juices (pH <3), and thus phosphodiester bonds are more exposed. A single strand of DNA has a structure similar to polypeptide chains containing aromatic amino acids, which means that pepsin can, bind to nucleobases and hydrolyse the phosphodiester bond, resulting in short fragments with 3'-phosphate and 5'-OH ends. Previous studies have shown that the catalytic efficiency of pepsin in cleaving nucleic acids is ca. 10,000 times lower than against proteins, suggesting that for effective DNA hydrolysis, a higher concentration of pepsin is required (Stankiewicz & Bartoszek, 2017), (Liu et al., 2015).

Gastric lipase is a surface-active enzyme stable in the pH range of 3-6. It can adsorb at the oil-water interface, gaining access to the triacylglycerol substrate. It releases fatty acids by hydrolysing the ester bond in the sn-3 position of triacylglycerols. Due to the action of gastric lipase triacylglycerols are hydrolysed to free fatty acids, diacylglycerols, and 2-monoacylglycerols (Singh & Ye, 2013), (Armand, 2007). Gastric lipolysis leads to the hydrolysis of 5-40% of the total fats consumed. The limitation in hydrolysis is due to the product inhibition of gastric lipase (Pafumi et al., 2002). Lipolysis products occupy the lipid surface preventing access for lipase. In the gastric environment, there is a lack of physiological, surface-active agents that could remove the lipolysis products from the interface, and thus enable unhindered access of the gastric lipase to the triacylglycerol substrate. A different situation is during small intestinal lipolysis, where surface-active bile salts can enhance the action of pancreatic lipase by solubilizing the lipolysis products. This will be described in more detail in the next sections.

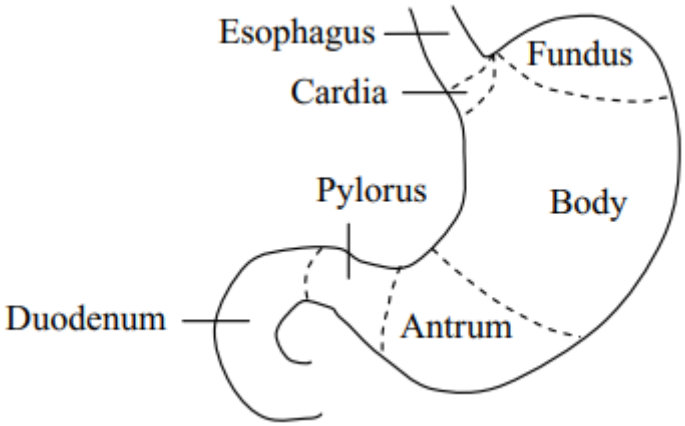

Figure 2. The schematic representation of the stomach compartments (Kong & Singh, 2008).

The small intestine

The acidic chyme from the stomach is transported to the small intestine, more precisely, to the duodenum, where the chyme is neutralised with sodium bicarbonate to a pH of around 7 at which small intestinal enzymes are active. The small intestine is divided into three parts. The first one, already mentioned, is the duodenum. Duodenum has around 25-30 cm in length with around 4 cm diameter (Helander & Fändriks, 2014). It is connected with the pancreas through the pancreatic duct and with the liver and the gallbladder through the common bile duct (Fig. 3). These ducts deliver, respectively, the pancreatic juice (containing enzymes), and the bile, which is described in detail in the following sections. The next parts of the small intestine are jejunum and ileum with a mean, total length of around 6.5 m and a mean diameter of ca. 2 cm (Olivares-Morales et al., 2015). All three parts are responsible for the digestion and absorption of nutrients. Additionally, in the terminal ileum, vitamin B12 and bile salts absorption occurs (Duerksen et al., 2006). In each part, the peristalsis and segmentation contractions are responsible for propelling digesta and for mixing it with intestinal juices (Tharakan et al., 2010).

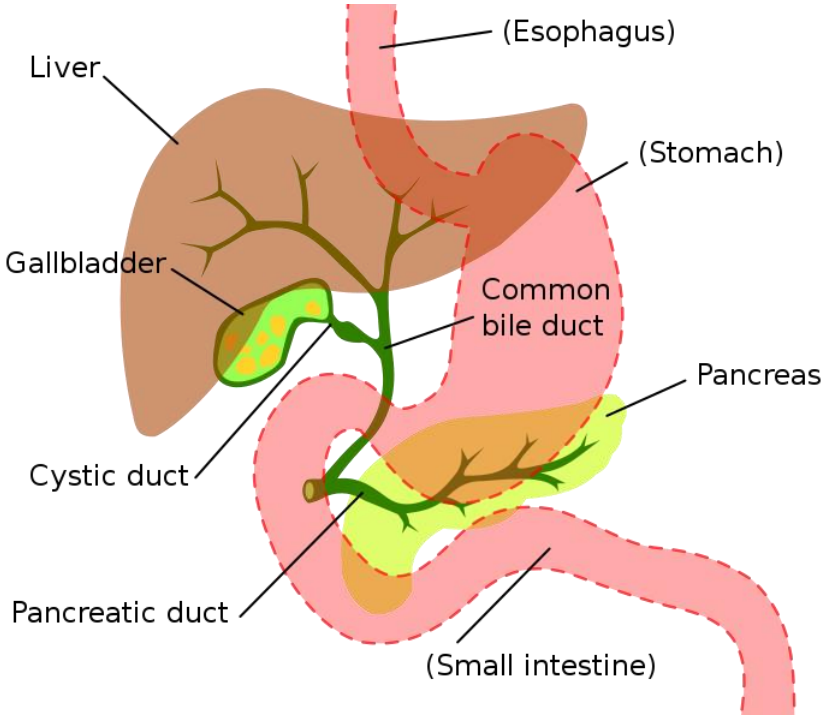

Figure 3. Human digestive system with the representation of bile and pancreatic ducts. https://upload.wikimedia.org/wikipedia/commons/9/96/Digestive_system_showing_bile_duct.svg (accessed: 08.03.21)

The inner surface of the small intestine is lined with mucosa and epithelial tissue, which together form folds, villi, and microvilli (Fig. 4). The microvilli-covered surface is called the brush border membrane. It makes a large surface area available for the absorption of nutrients (total of 260 - 300 m^2 (Walton et al., 2016)).

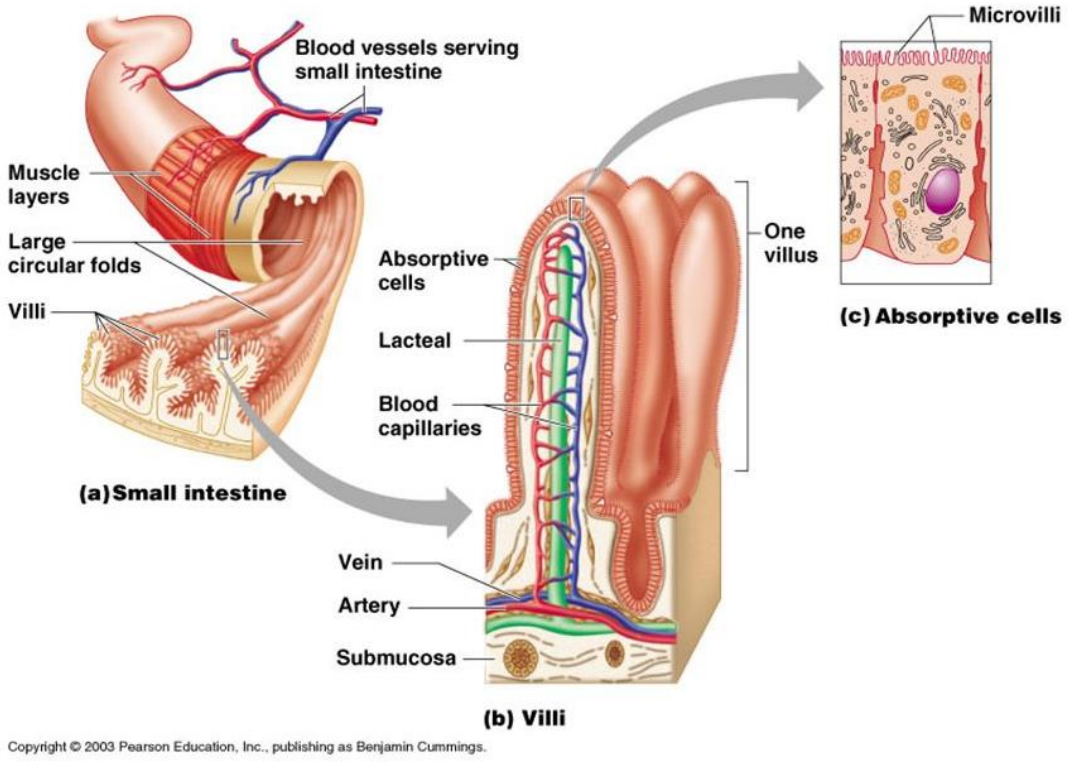

Figure 4. Schematic representation of the inner surface of the small intestine (a). Images (b) and (c) show villi and microvilli, respectively (Copyright © 2003 Pearson Education, Inc., publishing as Benjamin Cummings).

In the small intestine, the proteins that have been partially digested in the stomach are further hydrolysed by proteolytic enzymes secreted by the pancreas. The pancreatic juice contains several enzymes responsible for proteolysis, which are initially in an inactive form: trypsinogen, chymotrypsinogen, proelastase, and procarboxypeptidases (Bhutia & Ganapathy, 2018). In the lumen of the small intestine and under the impact of enteropeptidase presented in the intestinal epithelial cells, trypsinogen is partially hydrolysed to the active form - trypsin. Trypsin, in turn, activates chymotrypsin, elastase, and carboxypeptidases (Bhutia & Ganapathy, 2018). Trypsin and chymotrypsin are called endopeptidases. They hydrolyse internal peptide bonds. Trypsin catalyses the hydrolysis of peptide chains at the sites where the carbonyl groups belong to arginine and lysine. Chymotrypsin hydrolyses the peptide bonds at the carboxyl side of amino acids tyrosine, phenylalanine, tryptophan, and leucine (Hinsberger & Sandhu, 2004). Peptide bonds formed by the carboxyl group of aromatic amino acids (phenylalanine, tyrosine, and tryptophan) are hydrolysed by elastase. Carboxypeptodases also take part in the biosynthesis of peptides but in comparison to other proteolytic enzymes they act to a smaller extent (Bhutia &

Ganapathy, 2018), (Hornbuckle et al., 2008). These different modes of action make intestinal proteolysis efficient in generating a range of peptides containing 6-8 amino acids (Bhutia & Ganapathy, 2018).

The small intestine is also the place where lipids are digested. Pancreatic lipase is responsible for the breakdown of triacylglycerols to free fatty acids and 2-monoacylglycerols (Fig. 5).

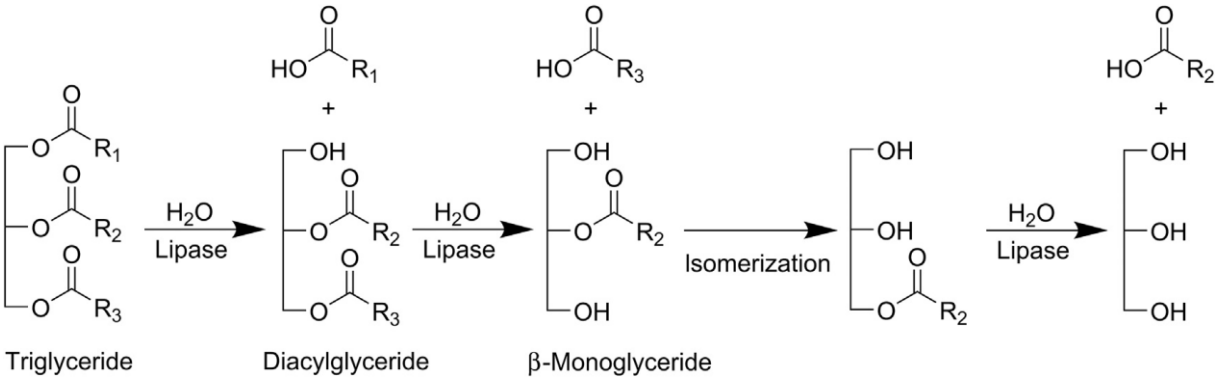

Figure 5. The hydrolysis of triacylglycerol (triglyceride) by the pancreatic lipase (Cotten, 2020)

The enzyme is involved in the digestion of emulsified fats and acts at the oil-water interface (Fig.6). It is most efficient with the participation of colipase secreted by the pancreas. The efficiency of intestinal lipolysis is additionally enhanced by the bile salts.

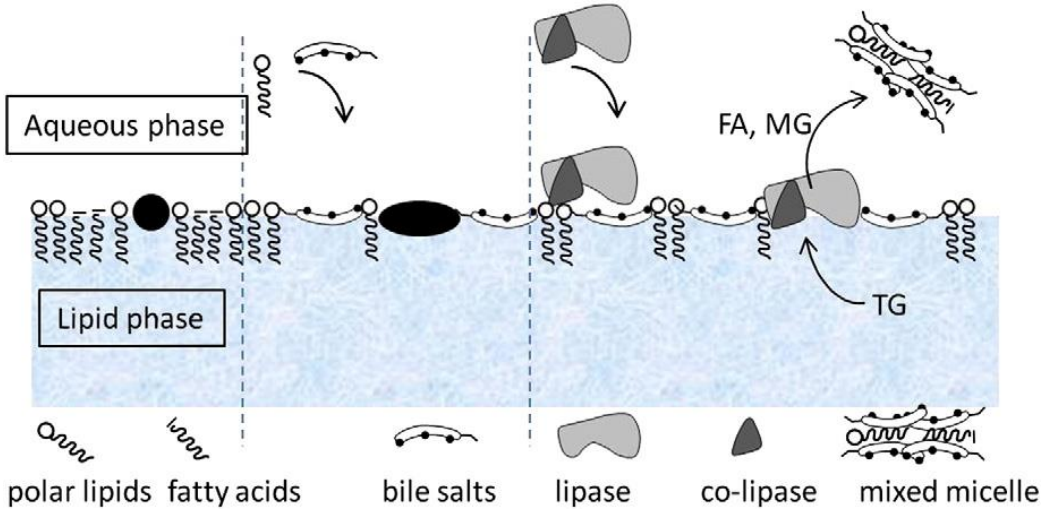

Figure 6. Schematic representation of the interfacial aspects of lipolysis in the small intestine with the participation of bile salts. (Wilde & Chu, 2011)

Bile salts are capable of removing surface-active molecules occupying the interface via orogenic displacement and enabling the access of lipase and co-lipase to the interface (Hornbuckle et al., 2008), (Wilde & Chu, 2011). The presence of bile salts can significantly influence the electrostatic interactions with colipase. Due to these interactions co-lipase can adsorb onto the disrupted interface, as a complex with pancreatic lipase, improving the hydrolysis of lipids. Human bile and bile salts are described in more detail in the following section (Section 1.1.2).

Another lipolytic enzyme in the small intestine is pancreatic phospholipase. It is responsible for the hydrolysis of phospholipids. More precisely, it hydrolyses glycerphosholipids in the sn-2 position resulting in the creation of free fatty acids and lysophospholipids (Molendi-Coste et al., 2011). The reaction does not express preferences towards specific fatty acids. The efficiency of hydrolysis is related to the concentrations of calcium ions and pH (within the range of 7-9.) (Kudo & Murakami, 2002). Phospholipases from subfamily A_2 (i.e. $sPLA_2$-IB) act more likely on anionic phospholipids i.e. phosphatidylethanolamine (PE), phosphatidylserine (PS) but emphatically on phosphatidylcholine (PC). The hydrolysis is enhanced by the presence of biosurfactants such as deoxycholate (Hanasaki et al., 1999). Phospholipids also undergo hydrolysis by 1,3-regioselective pancreatic lipase in the sn-1 position. The phosphatidylcholine is deacetylated on the acyl ester bond to 1-acyl-2-lyso-glycerophosphocholine (Mnasri et al., 2017). Hydrolysis products get transported through epithelium cells, bind to albumin, and can further serve as building blocks for membrane phospholipids (Taylor et al., 2010).

In addition to fats and proteins, the digestion of carbohydrates also takes place in the small intestine. The primary enzyme responsible for the hydrolysis is pancreatic amylase. As a result of its action, carbohydrates pre-digested in the oral cavity are hydrolysed to the form of disaccharides. Then, disaccharides (maltose, lactose, sucrose, etc.) are hydrolysed by appropriate enzymes of the small intestine into monosaccharides: the enzyme maltase breaks down maltose into two glucose molecules, sucrase breaks down sucrose into glucose and fructose, and lactase breaks down lactose into glucose and galactose (Jenkins, 2007). The mentioned enzymes are located in the brush border membrane. They are transported from the endoplasmic reticulum through the Golgi apparatus where undergo modification before taking part in the hydrolysis. They are anchored into the apical plasma membrane (Hooton et al., 2015).

Apart from the mentioned nutrients, the digestion of nucleic acids should also be considered. Pancreatic nucleases (oligonucleotidases), present in the duodenum, degrade nucleic acids into mono-, di-, tri-, and oligonucleotides. In the next step, phosphodiester bonds are broken down by the action of phosphoesterases to nucleosides. Phosphoesterases detach the orthophosphate group. As a result of the breakdown of nucleic acids in the small intestine, purine and pyrimidine bases are obtained, which, after absorption in the jejunum, are metabolised into uric acid and β-amino acids. Nucleic acids are used that way in the human body for the production of new nucleic acids (Głazowska et al., 2017).

Digested nutrients (carbohydrates, proteins, lipids, and nucleic acids) are absorbed through the epithelium of the small intestine and transported into the bloodstream. They are used as building blocks and energy sources for the body. The absorption relies on diffusion or active transport through the intestinal mucosal barrier (Fig. 7). Enterocytes in the intestinal mucosa act as a selective columnar cells, in which occludins, claudins, and junctional adhesion molecules occur. These proteins mediate by paracellular permeability, i.e. caludin-17 acts as an anion channel (Rosenthal et al., n.d.). These paracellular channels are known as the tight junction (TJ) (Anderson & Van Itallie, 2009). TJ moves molecules from the intestinal lumen to the bloodstream (Falasca et al., 2019).

Some substances, e.g. water and small water-soluble particles, pass freely through the membrane (Fig. 7a). Others undergo active transport, which is supported by ATP and Na^+/K^+ pomp in the brush border (Fig. 7b). Carbohydrates (e.g. glucose) are absorbed by an active transport. They are transformed by brush border membrane hydrolases, e.g. lactase hydrolases lactose to glucose and galactose. Also, amino acids (glycine, praline, alanine, taurine) are transported by an active transport with the help of sodium co-transporter. Dipeptides and tripeptides, in turn, are H^+ co-transported. Another type of adsorption needs support, more precisely a carrier. Some amino acids undergo diffusion through the membrane with the help of transporter protein PAT-1 (Nada et al., 2016). Lipids are absorbed in three steps: (i) diffusion through the intestinal mucus layer, (ii) passive transport through the brush border membrane, and (iii) binding to intracellular proteins (i.e. CD36 which binds to digested lipids by hydrophobic interactions) (Woudstra & Thomson, 2002), (Nada et al., 2016). Fatty acids, 2-monoacylglycerols, triacylglycerols, and cholesterol esters are re-synthesised in enterocytes and thus form lipoprotein particles called chylomicrons, which are transported in this form to the circulation.

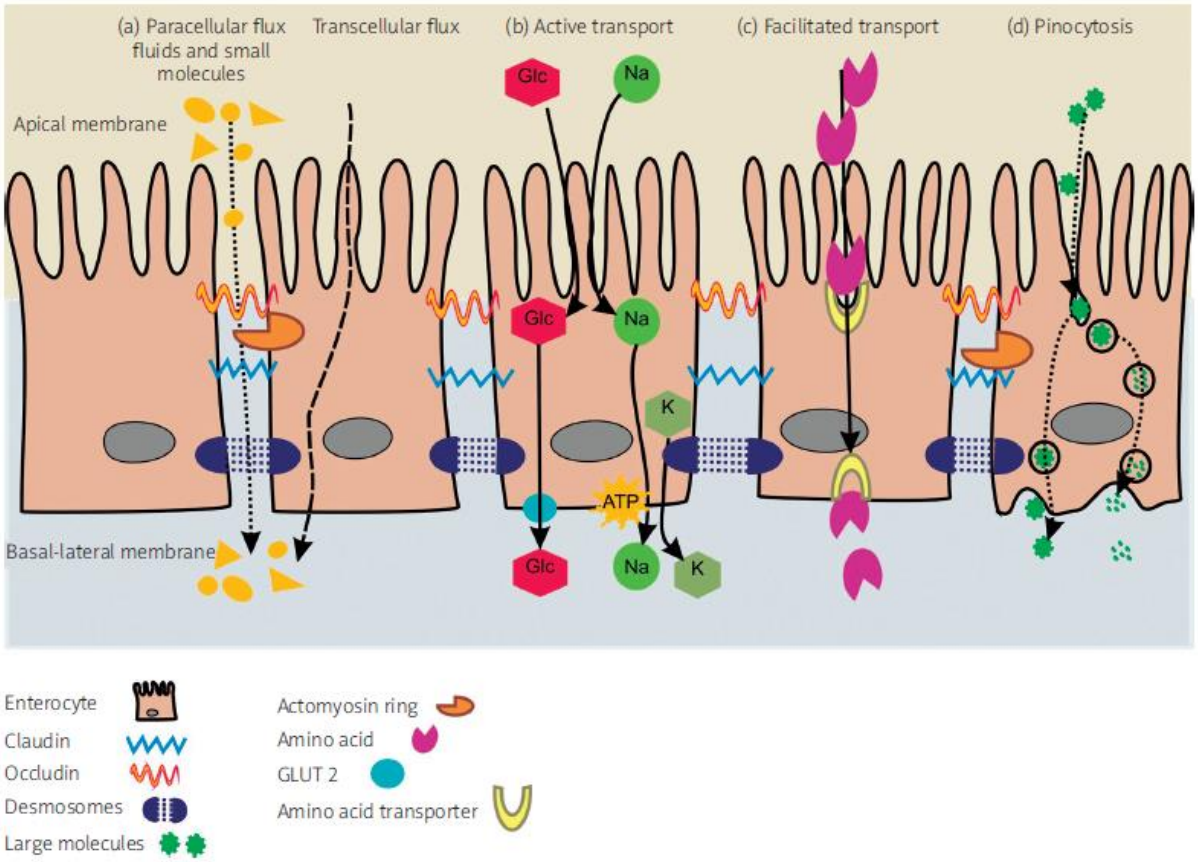

Figure 7. Schematic representation of the absorption of nutrients in the human small intestine (Szefel et al., 2015)

The large intestine

The last part of the digestive system is the large intestine, which consists of four segments: the cecum, colon, rectum, and anus. The basic functions of the large intestine are the absorption of water and electrolytes that have not been absorbed in the small intestine, compaction of the intestinal contents, and the accumulation and periodic excretion of faeces. The large intestine is home to commensal bacteria (e.g. faecal streptococcus, hay cane, anaerobic cocci, and others) that feed on undigested debris. The amount of bacteria is estimated to range from 10^{11} to 10^{12} cells/g (Brooks & Kalmokoff, 2012). The large intestine microorganisms are responsible for the production of certain vitamins (K and B), protein fermentation processes, and softening of the stool (Value & Used, 2010), (Gibson & Roberfroid, 1995). An important element of the physiology of the large intestine is a contraction of intestinal muscles, which is responsible for moving the content forward. The segmentation increases the efficiency of water and mineral substances absorption and,

together with the peristalsis, is also responsible for the defecation process (Barrett et al., 2010).

1.1.2. The human bile and bile salts

Human bile is produced in the liver, stored in the gallbladder, and transported to the small intestine through the bile duct. Hepatic bile consists of water (around 95%), bile salts, bilirubin, cholesterol, fatty acids, inorganic salts, fats, and others (Hornbuckle et al., 2008), (Boyer, 2013). Apart from water, bile salts are the most abundant ingredient of human bile. Bile salts or bile acids synthesised from the cholesterol, with the help of 17 enzymes, can be divided into two categories: primary (cholic acid, chenodeoxycholic acid) and secondary (deoxycholic acid, litocholic acid). Next, they are conjugated with amino acids (glycine or taurine) and form conjugated primary and secondary bile acids. In the large intestine, bile acids are metabolised by bacteria by deconjugation and decarboxylation into the secondary and tertiary forms. These are easier to be dissolved in water and thus recycled or excreted from our body. Around 85-90% of bile salts are present in the small intestine while only 1% in the liver and 10-15% in the gallbladder (Macierzanka et al., 2019), (Hebanowska, 2010).

Bile salts are biological surfactants with unusual structures. They do not possess a hydrophilic head–hydrophobic tail structure, which is typical for conventional surfactants. Instead, they are flat, with one site having a strong affinity to hydrophobic substances and the other site to hydrophilic ones (Fig. 8).

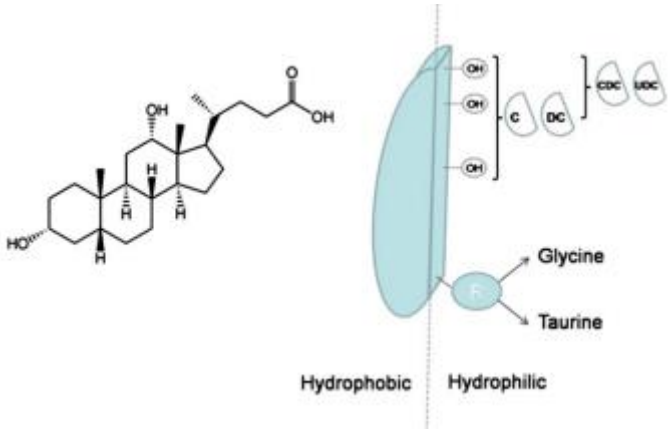

Figure 8. Representation of bile acids structure. (a) Chemical structure of deoxycholic acid and (b) a schematic view of the bile acid structure oriented at the interface (Maldonado-Valderrama et al., 2011).

The hydrophobicity of bile salts decreases with the conjugation. Because of their planar structure, bile salts form different types of micelles than conventional head–tail surfactants (Maldonado-Valderrama et al., 2011). Different bile salt micelles can be formed depending on the bile salt structure, its concentration, pH, or temperature. Since the 1960s, three models of bile salts micelles were proposed (Warren et al., 2006). The first one shows the micelles formed by the back-to-back connection (Fig. 9). Hydrophobic sites are exposed to each other between bile salt molecule and hydrophilic sites are exposed outside. This model represents “primary micelles”. For larger micelles made of more than 10 bile salt molecules, there are probably additional interactions between hydrophilic sites which form “secondary micelles”. This secondary bonding consists of lipophilic groups connected by hydrophobic weak interactions and hydrophilic regions connected by hydrogen bonds (Carey & Small, 1972). Next, a disk-like model represents bile salts with lipophilic sites oriented to the micelle interior, where hydrophobic substances could be solubilised, and with the hydrophilic sites oriented towards the solvent (Nagadome et al., 2001). The third model shows unusual helical shape micelles with hydrophobic moieties displayed in the aqueous phase at low bile salt concentrations (Giglio et al., 1988).

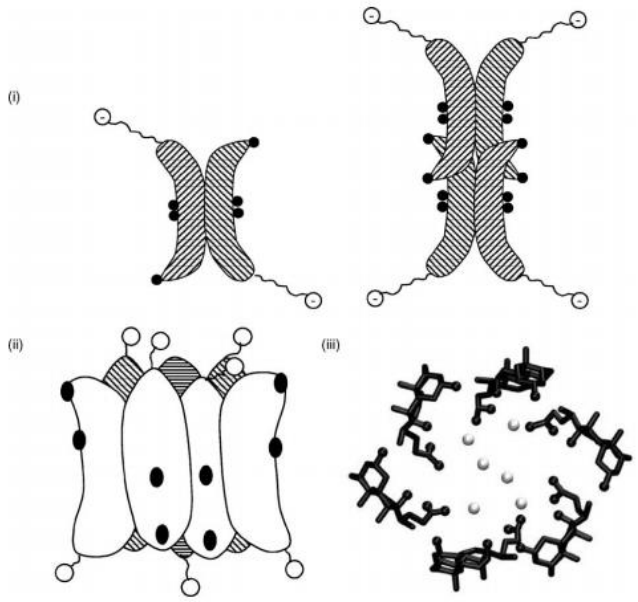

Figure 9. Proposed structures of bile salt micelles: (i) primary micelles, (ii) secondary micelles, and (iii) disk-like structure (Warren et al., 2006).

In the human small intestine, the most common bile salt micelles are mixed micelles. The mixed micelles consist of bile salts with phospholipids and surface active lipolysis products

(fatty acids and monoglycerides). The concentration of bile salts in the human small intestine can differ between fed or fasted state or between healthy and ill (i.e. bile stones, pancreatic cancer) subjects. It can typically vary between 2.6 and 15 mM. The critical micelle concentration (CMC) of bile salts is different for different types of bile salts and usually is estimated as a range. For the primary bile salts, the CMC values range usually between 5.9 and 17 mM, for conjugated primary ones 4 – 15 mM, for secondary 2.8 – 7.5 mM and for secondary conjugated 1.9 – 8 mM (Macierzanka et al., 2019).

The first proposed model showed a "mixed disk" with drum shape perimeter where bile salt molecules are outside the drum (Fig. 10). The model was later modified by adding phospholipids between bile salts dimers. In contrast with described models, the next version showed bile salts molecules lying flat on the surface in the form of rod shape micelles. The radial shell model was confirmed with the use of small-angle neutron scattering (Hofmann & Hagey, 2014).

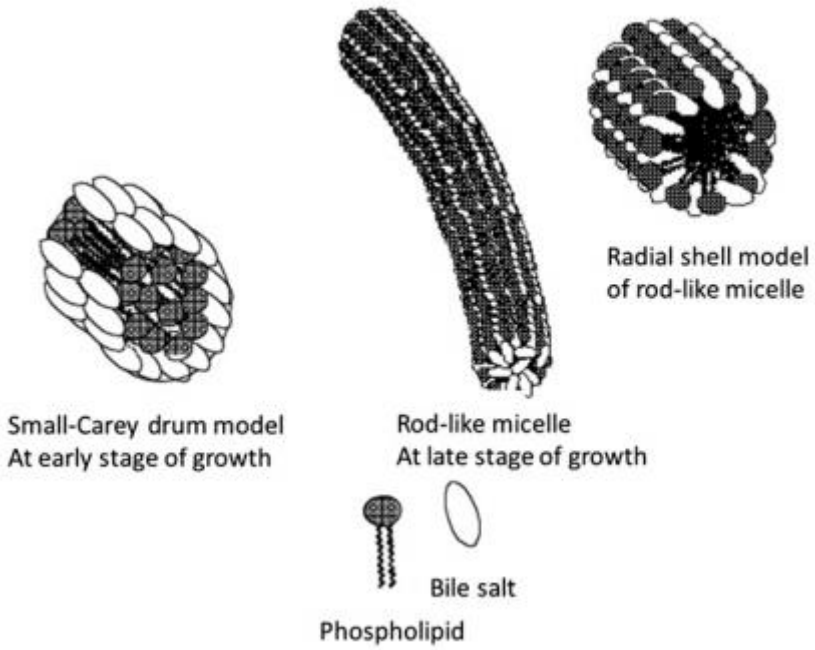

Figure 10. Comparison of models showing the bile salt–phospholipid mixed micelles (Hofmann & Hagey, 2014).

Bile salts have a very strong affinity to the interfaces. Thanks to the unique structure characterised by hydroxyl groups on one side and methyl groups on the other, they have specific behaviour. Depending on concentration, temperature, and pH, different surface

tension isotherms can be observed. Additionally, the final surface tension of conventional head-tail surfactants is often higher than for bile salts. Based on isotherms characteristics, it was concluded that bile salts aggregation occurs in a stepwise manner (O'Connor et al., 1983). The lower values of surface tension occurs also due to the flat structure of bile salts and flat conformation at the interfaces (Matubayasi et al., 1996), (Maldonado-Valderrama et al., 2008).

Thanks to the unique structure, bile salts are responsible for (i) the displacement of materials adsorbed at the interface (e.g. proteins from emulsion's interface), (ii) facilitating the access of lipase and co-lipase and (iii) transport of lipolysis product through the intestinal mucous.

Bile salts are involved in the emulsification of fat droplets in the small intestine. The emulsification can occur as a result of lipolysis products displacement. The literature shows that the presence of bile salts during simulated lipolysis increases free fatty acids release compared with control experiments without them (Mun et al., 2006). It means that during the removal of products from the interface, bile salts enable access for lipase and co-lipase to the triacylglycerol substrate, enabling an ongoing hydrolysis.

Calvo-Lerma and co-workers, who investigated simulated pH-stat lipolysis under different conditions showed that the rate of free fatty acids release is correlated with the differences between bile salts concentration, bile origin (porcine or bovine), lipids concentration, and pH. They concluded that porcine and low-taurocholic bile had the highest impact on the lipolysis rate (Calvo-Lerma et al., 2019). It is probably due to the adsorption characteristics of different bile salt types. Generally, based on that they are split into two main groups: reversibly adsorbed (i.e. NaGDC, NaTDC) and partially irreversibly adsorbed (i.e. NaTC, NaGC). The longer the bile salt occupies the interface the more it facilitates the adsorption of lipase (Mun et al., 2006).

Bile salts play an important role in the transport of lipolysis products. They can modulate interactions of particulate material with mucus. Experiments measuring the charge (ζ-potential) and the location (confocal microscopy) of bile salt-covered particles during the penetration through the porcine intestinal mucus, showed that the negative charge imparted to the particles by bile salts change the electrostatic interactions with mucus, enhancing the passive transport of particles through the mucus (Macierzanka et al.,

2011). The same study showed that mucus penetration is not only limited to very small particles, which suggested that lipolysis can take place even after the mucus has been penetrated by, for example, partially digested lipid droplets.

Simulating the intestinal environment helps to understand the overall processes occurring during digestion and absorption of food particles. *In vitro* digestion models are still under development for improving our knowledge.

1.2. *In vitro* models of digestion

It is well-know that the food digestion is a complex process occurring in several compartments of the digestive tract with different physiological, physical and chemical conditions. To follow the fate of food, scientists all over the world try to reconstruct *in vivo* the gastrointestinal environment on a laboratory scale. The use of *in vitro* models compared to *in vivo* is much cheaper, simpler, has no ethical restrictions, and allows for continuous monitoring of simulated digestion. Currently, *in vitro* models are used not only for food study and design but also in pharmacy, toxicology, and microbiology. There are several types of *in vitro* digestion models used to mimic the human gastrointestinal tract: static models, semi-dynamic models, and dynamic models. This chapter presents a brief review of commonly used *in vitro* digestion models.

1.2.1. Static models

Typical static models mimic digestion in the mouth, stomach, small intestine, and, in a few cases, fermentation processes in the large intestine. When simulating these individual phases of digestion, factors such as temperature, the presence of bile salts and enzymes, their concentrations, pH, and digestion time are taken into account and usually they are constant (static) over time, for each of the digestion compartments. The different phases of *in vitro* digestion vary mainly in the composition of digestive fluids, pH, and time of digestion. Moreover, static models do not reflect the geometry and peristalsis of individual compartments of the digestive system.

The phase that simulates the physicochemical processes taking place in the oral cavity is often the first step of *in vitro* static digestion models. Solid food is firstly grounded to reflect

the chewing process, and then SSF (simulated salivary fluids) containing α-amylase is added. The duration of this phase may be approximately 2 minutes at pH 7. In the case of studying liquid foods, the digestive phase in the mouth is often omitted. The oral digesta goes directly to the gastric digestion phase (Brodkorb et al., 2019).

Models representing the oral phase can be divided into two groups. First, covering only this stage of digestion is used, for example, to test the flavour and texture of food upon the simulated mastication processes. The second group consists of models in which the digestive stage in the oral cavity is the initial stage for the study of further stages of digestion (stomach, intestine) (Verhoeckx et al., 2015).

Food portions that have been pre-treated in one stage are subjected to the next stage of digestion. In the gastric digestion phase, a low pH neutralizes the effect of salivary amylase. SGF (salivary gastric fluids) consists mainly of hydrochloric acid, gastric lipase, and pepsin solution (most often of animal origin). This gastric phase is simulated by continuously mixing the chyme with SGF. The entire phase generally takes about 2 hours at pH 3 (Verhoeckx et al., 2015). In the next step, the digestion content of the gastric phase is mixed with simulated intestinal fluids (SIF) which, thanks to the presence of sodium bicarbonate, neutralise the acidic pH of the gastric content. When simulating physicochemical processes in the human small intestine, enzymes such as pancreatic lipase, colipase, trypsin, and chymotrypsin are used. Additionally, SIF contains bile extracts or individual bile salts mixture. The intestinal digestion phase usually lasts about 2 hours at a pH 7 under a constant agitation. It does not mimic intestinal peristalsis or nutrient absorption (Brodkorb et al., 2019).

Static models are characterised by repeatability, low cost, and the simplicity in controlling conditions. Due to the lack of the dynamic characteristics of the real digestive system (peristalsis, changes in pH, changes in enzyme concentration, etc.), they are often used for basic research such as preliminary screening of the digestibility and bioaccesibility of nutrients.

1.2.2. Semi-dynamic models

Semi-dynamic models are an upgrade of static ones. They are not mimicking the peristaltic motion in the gut but they take into account dynamic changes in the gastric pH and the secretion of gastric enzymes over time. According to the literature data, immediately after ingesting food, the pH value in the stomach of a human on the "Western Pattern Diet" rises to values above pH 5 (Kong & Singh, 2008). The gradual secretion of hydrochloric acid lowers

the pH, which is important for the optimal activity of gastric enzymes. The semi-dynamic models also simulate gastric emptying and further digestion under small intestinal conditions (Fig. 11). Those models are used, for example, for studies on the behaviour of probiotics in the stomach (De Carvlho et al., 2009), tracking the digestion and phase separation processes of proteins and fats in the acidic, gastric environment (Bourlieu et al., 2014), etc.

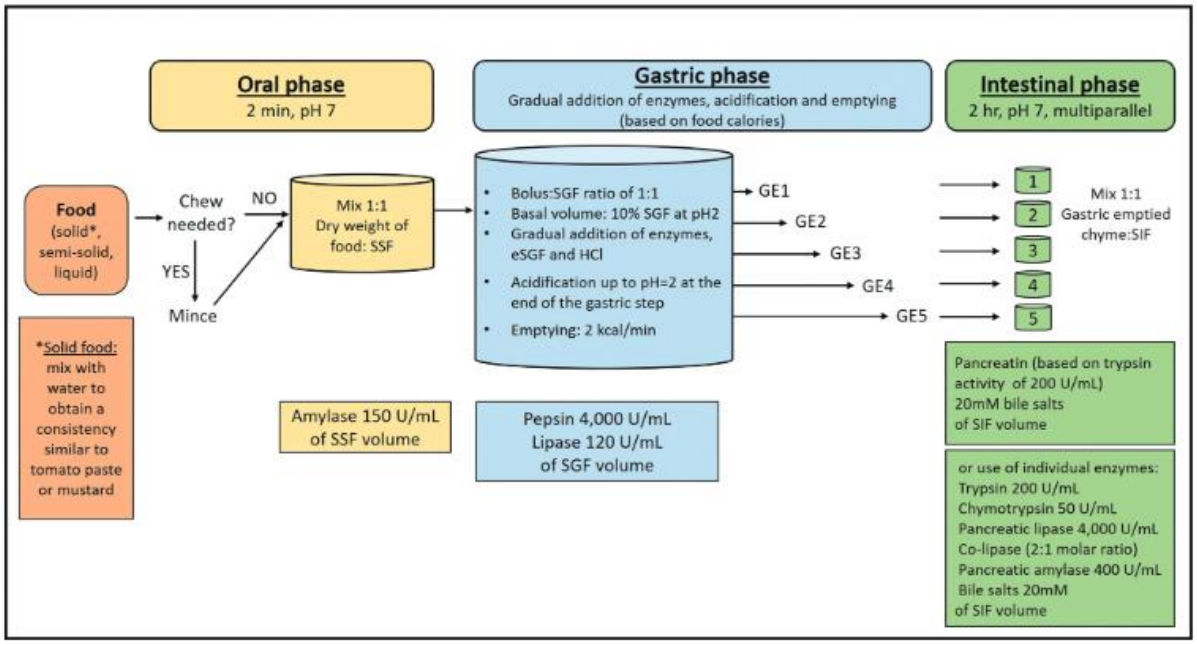

Figure 11. Overview diagram of an exemplary semi-dynamic digestion model, showing the content of simulated digestion fluids (SSF – Simulated Salivary Fluid, SGF – Simulated Gastric Fluid, SIF – Simulated Intestinal Fluid) and the gastric emptying (GE) schedule during the gastric phase of simulated digestion (Mulet-Cabero et al., 2020).

1.2.3. Dynamic models

Dynamic models are characterised by simulating the gastrointestinal tract while considering temporal variations in physical conditions, e.g. variable pH of the stomach after meal ingestion and variable enzyme concentrations depending on the fed or fasted state. Additionally, dynamic models can mimic the peristaltic movements, the physiological geometry of digestive compartments, or can even employ dialysis of digested product, which mimics the absorption of nutrients. Dynamic models are divided into two main groups: monocompartmental and multicompartmental (Guerra et al., 2012).

Monocompartmental models most often focus on reflecting the physiology of the stomach. They consist of two parts: the cone shaped elastic body, where gastric juices are mixed with the digestive content, and the antrum, where the shearing and grinding forces are simulated (Fig. 12). They are equipped with a pH electrode positioned in the fundus, a hoop for acids and enzymes delivery (depending on luminal meal content), and temperature controlled water bath (water jacket). In addition, gastric dynamic models mimic gastric emptying using antral sieving. They are equipped with a valve that allows smaller food particles to leave the stomach earlier, whereas larger ones are returned to the chamber for further gastric digestion/disintegration. The gastric digestion parameters e.g. time, concentration of enzymes, and pH are computer-controlled (Wickham et al., 2012).

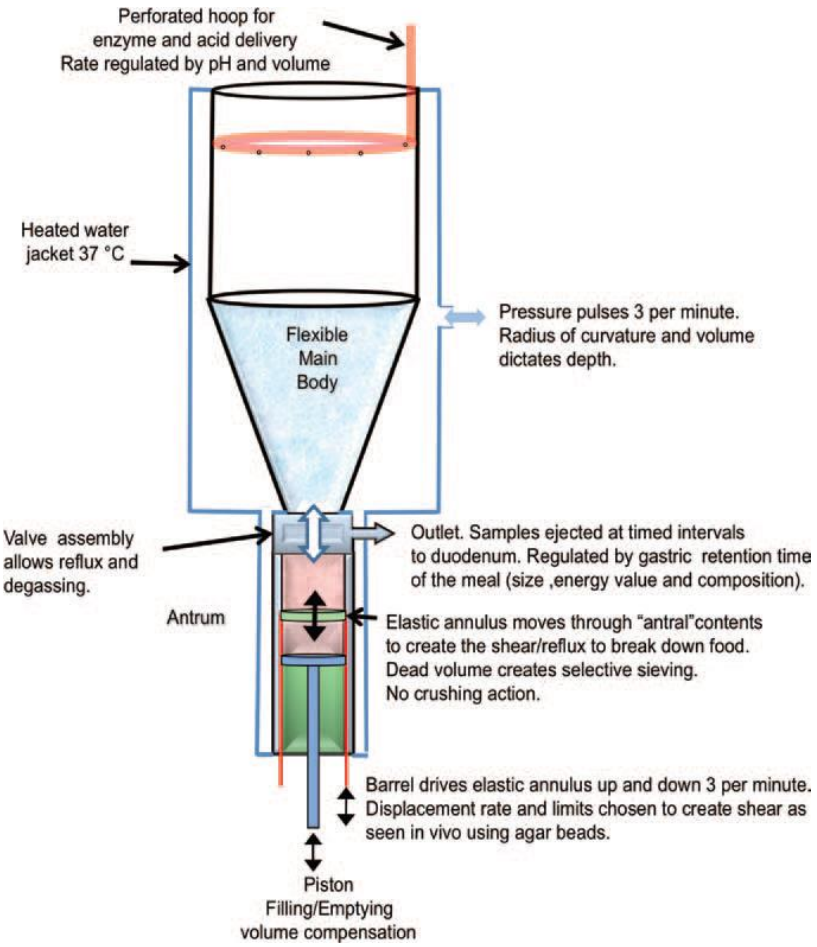

Figure 12. Schematic representation of an exemplary monocompartmental dynamic digestion model – Dynamic Gastric Model (Wickham et al., 2012).

Multicompartmental models often consist of artificial compartments of the upper gastrointestinal tract: the stomach and the whole small intestine. They are computer-controlled systems simulating in real time the pH, temperature, food transit times, sequential addition of gastric and intestinal secretions, the flow rates of all fluids, and the peristalsis (Reynaud et al., 2021). In the example of DIDGI® system (Fig. 13), each compartment is surrounded by a water jacket. A teflon membrane mimics the connection between the stomach and duodenum with the option of sieving. The flow rates of the meal, enzymes, acids, salts, bile, and pH are controlled with pumps along with the emptying rate. All of these data are implemented in the software based on the studies on animals and human volunteers, so it is possible to simulate factors like duration of the meal, secretions, emptying rates, or pH curve (Ménard et al., 2014).

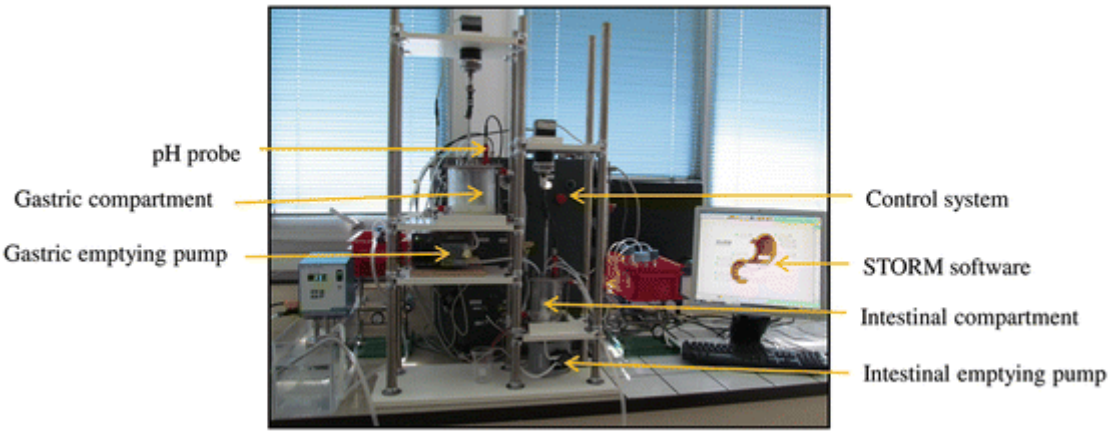

Figure 13. The setup of gastrointestinal dynamic model DIDGI®.

There is another example of multicompartmental dynamic model – TIM 1. The model was being developed over time (Minekus et al., 1995), (Venema, 2015), and now it comprises of the stomach, duodenum, jejunum, and ileum compartments connected with peristaltic valves and semi-permeable membranes (Fig. 14). Each of these environments is controlled by software. The authors of the TIM 1 model also designed the tinyTIM digestion model, which is a simplified version of TIM 1 (Havenaar et al., 2013). The TIM system is a pioneer in dynamic simulations of the digestion conditions. All of the collected data are highly reproducible and show a good correlation with *in vivo* human data, e.g. bioaccessibility of

amino acids (Schaafsma, 2005) and fat-soluble vitamins (De et al., 2009), digestion of carbohydrates (Venema et al., 2003), folate intake predictions (Verwei et al., 2006), and much more.

Among the systems mentioned above, we can list some other examples simulating human gastrointestinal conditions, i.e. SHIME (Simulator of Human Intestinal Microbial Ecosystem) (Molly et al., 1993) or ESIN (Engineered Stomach and Small Intestine) (Alric & Denis, 2009).

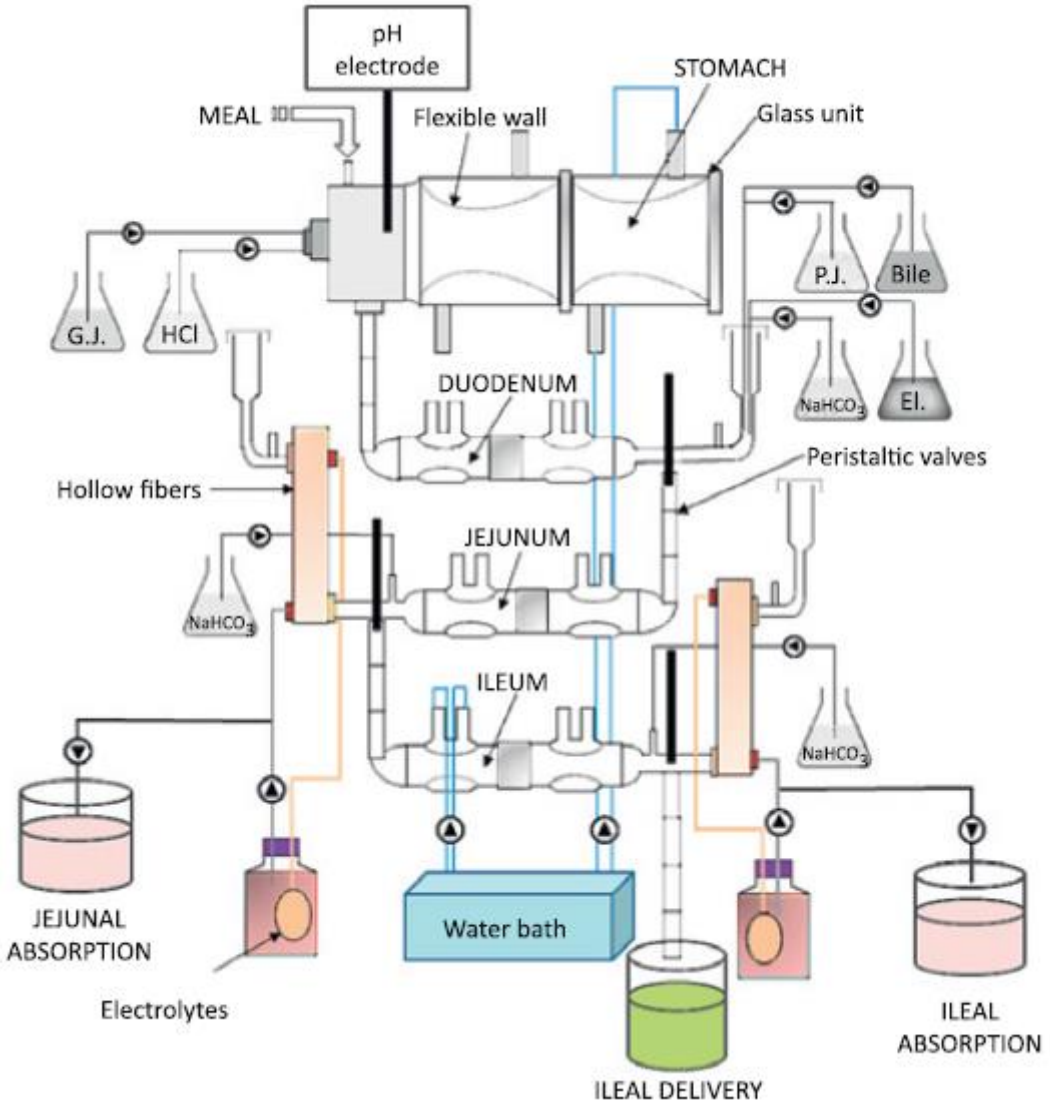

Figure 14. Schematic representation of TIM 1 dynamic multicompartmental model (Guerra et al., 2012)

1.2.4. Mimicking human bile with bile substitutes

In vitro digestion protocols recommend the use of commercially available porcine or bovine bile extracts. In such a case, there is a need to determine the exact concentration of bile salts because it is not provided by the supplier due to variations between bile samples used for different batches of the product. Hence, additional reagents and equipment, e.g. enzymatic assays, are needed for the quantitative analysis of the bile salt content (Brodkorb et al., 2019). Because of that, some laboratories use individual, purified bile salts to prepare recommended bile salt concentration for the intestinal phase of simulated digestion. In both cases, bile salts are of bovine or porcine source. In Tab. 1, there is a comparison between the bile salt composition (the most abundant bile salts) of human bile and those of bovine bile and porcine bile, which are most commonly used (in the form of bile extracts) in *in vitro* digestion methods to mimic the human bile.

Table 1. The bile salt composition of human bile relative to bovine and porcine bile (Mackie & Rigby, 2015).

Bile salt	Human bile [%]	Bovine bile [%]	Porcine bile [%]
Taurodeoxycholate (TDC)	0	0	37
Glycohyodeoxycholate (GHDC)	0	0	34
Taurocholate (TC)	11	31	0
Glycocholate (GC)	26	46	0
Taurochenodeoxycholate (TCDC)	13	2	2
Glycochenodeoxycholate (GCDC)	25	3	26
Taurodeoxycholate (TDC)	5	8	0
Glycodeoxycholate (GDC)	11	10	0
Other	9	0	0

According to the data present in Tab. 1, it might be difficult to mimic the human bile salt profile by using the animal substitutes. As mentioned earlier, different bile salts can exhibit different interfacial properties. Moreover, human bile also contains other components, which might influence the digestion processes, but are vastly ignored in *in vitro* digestion models. Currently applied human bile substitutes are not validated in terms of a reliable simulation of physiological roles of human bile in the human digestive tract.

2. The aim of the PhD research project

The primary aim of my research was to investigate whether any influence of real human bile on the extent of the intestinal proteolysis and lipolysis processes could be effectively replicated by using simplified mixtures of individual bile salts and other organic constituents found in bile.

I hypothesise that human bile has the ability to impact both the intestinal proteolysis and lipolysis, and that this impact can be emulated by utilising specific individual components of bile (i.e., biliary biosurfactants), resulting in the protein and lipid degradation extents that are comparable to those exerted in the presence of real human bile. If confirmed, this would potentially endorse the use of individual bile salts (and other biosurfactants) as reliable, human-relevant substitutes for a difficult-to-obtain human bile in future *in vitro* studies focused on proteolysis and lipolysis.

3. Materials and methods

Methodology used in *in vitro* proteolysis study

3.1. Human bile collection for *in vitro* proteolysis study

The Ethics Committee of the Regional Medical Chamber in Rzeszów (Poland) granted approval for the collection and analysis of human bile (HB) (certificate 15/B/2016). The Declaration of Helsinki's ethical guidelines were followed in the design and execution of the research. During the endoscopic retrograde cholangiopancreatography (ERCP) examination, samples of HB were taken from 76 patients (Tab.2). The aspiration was conducted by expert endoscopists at the Department of Gastroenterology and Hepatology (Teaching Hospital No 1, Rzeszów, Poland).

Table 2. Group profiles of the ERCP patients recruited for bile collection

ERCP indication code	Number of subjects	Averaged age (yrs) ± SD
A. Choledocholithiasis	43	67 ± 18
B. Pancreatic neoplasm	15	71 ± 14
C. Benign biliary stricture	13	65 ± 19
D. Cholangiocarcinoma	5	73 ± 14

Prior to the ERCP, all patients fasted for at least 8 hours. All subjects gave their informed consent for the collection and use of their bile samples in planned research. The technique of bile collecting during the ERCP examinations was chosen to lessen the possibility of bile contamination by digestive enzymes from the pancreatic juice and intestinal lumen. ERCP is an endoscopic treatment that involves diagnosing and treating the pancreatic and/or bile ducts (Kozarek, 2017). During the procedure, the ampulla of Vater must be located in the duodenum, where a duodenoscope is introduced into the second section of the duodenum (Fig. 15a). The pancreatic duct and the common bile duct meet together in the ampulla of Vater, and in this location it is possible to cannulate the bile duct.

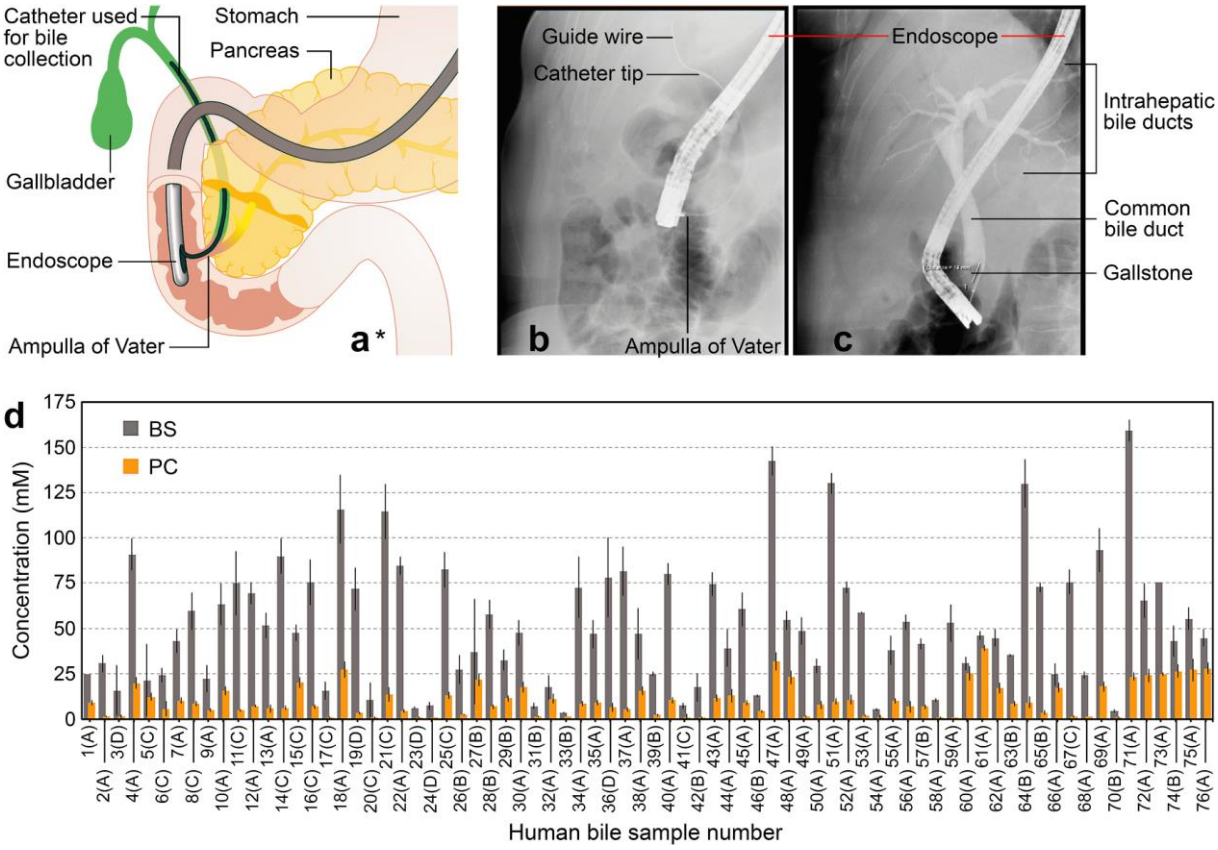

Figure 15. Collection and composition of human bile (HB). Endoscopic retrograde cholangio-pancreatography (ERCP) HB collection is shown schematically in (a). (b, c) Fluoroscopy images of a patient with choledocholithiasis – images collected during an ERCP procedure. The common bile duct is cannulated using a catheter, and the catheter is positioned for bile aspiration (b). The same patient is shown in the image (c) after applying a contrast post-aspiration to visualise the intrahepatic and extrahepatic bile ducts and pinpoint the location of a biliary gallstone. (d) The total bile salt (BS) and phosphatidylcholine (PC) concentrations of HB samples obtained from 76 patients (means ± SD, n = 3). An ERCP indication code is placed after a patient number (see Tab. 1). These results have already been published in Dulko, et al. (2021). *The diagram was modified from the original material – ©Detailed diagram of an endoscopic retrograde cholangio pancreatography (ERCP) by Cancer Research UK (original email from CRUK, https://commons.wikimedia.org/w/index.php?curid=34332566 / CC BY-SA 4.0, https://creativecommons.org/licenses/by-sa/4.0/deed.en) – and is available to use after modifications under the same license as the original.

In the procedure used in the study, a sterile catheter was used to cannulate the bile duct. After the guided pipe's position had been verified under fluoroscopy (under X-ray guidance, see Fig. 15b), the catheter was placed selectively over it. All of the patients (n = 76) had their catheter positions verified. The catheter had a syringe attached to one end. The accompanying endoscopy nurse applied a gentle suction with a syringe to aspirate the bile.

The catheter was operated back and forth from the extrahepatic bile ducts to the intrahepatic bile ducts (Fig. 15c). An aliquot of 2 – 3 mL of bile was aspirated from each individual. The collected materials were immediately poured into 0.5 mL polypropylene test tubes. For snap freezing, the tubes were immediately sealed and submerged in liquid nitrogen. Prior to further analysis, samples were kept at -80°C.

3.2. Human bile composition and bile salt profile for *in vitro* proteolysis study

The amount of total bile salts (BS) in HB was determined using the bile acids (enzymatic cycling) test kit (Alpha laboratories in Hampshire, UK), according to the published procedure (Mackie, Rigby, Harvey, & Bajka, 2016).

The BS profile (i.e., the quantities of individual bile salts) of HB samples was determined using an Agilent 1260 HPLC system connected to an AB Sciex 4000 QTrap triple quadrupole mass spectrometer (Sciex, Cheshire UK). An amount of 990 µL of 0.9% NaCl was added to 10 µL of HB (i.e., a 100-fold dilution). Next, 50 µL of methanol and 50 µL of diluted HB were combined in an HPLC container. The analysis was conducted using previously published methodology (Mackie et al., 2016). The following BS reference standards were used: sodium chenodeoxycholate (C8621, Sigma-Aldrich, Dorset, UK), sodium glycodeoxycholate (G9910, Sigma-Aldrich), sodium glycochenodeoxycholate (G0759, Sigma-Aldrich), sodium glycocholate (G7132, Sigma-Aldrich), sodium taurodeoxycholate (T0875, Sigma-Aldrich), sodium taurochenodeoxycholate (T6260, Sigma-Aldrich), sodium cholate (C6445, Sigma-Aldrich) and sodium taurocholate (86339, Sigma-Aldrich). Representative chromatograms of the BS standards, as well as of individual BS species in an exemplary HB sample, have been shown in Fig. 16.

A modified version of the protocol reported by Persson et al. (Persson et al., 2007) was used to quantify the concentration of phosphatidylcholine (PC) in HB, using HPLC (Shimadzu x1 HPLC 4FLC XR, Shimadzu, Japan) equipped with an evaporative light scattering detector (Shimadzu ELSD LT II). An aliquot of HB (100 µL) was diluted with 1 mL of ethyl ether-acetic acid mixture (98:2, v/v) and then evaporated to dryness under nitrogen. Evaporated samples were dissolved in 1 mL of hexane-isopropanol mixture (80:20, v/v), centrifuged (14.8k rpm, 2 min, Thermo Fresco 21 Heraeus), and 200 µl of supernatant was taken for HPLC-ELSD analysis. The analytical column (250 × 4.6 mm) with silica particles (LiChrospher 100-5 Diol,

Knauer) was used at 55°C and the system pressure was between 30 and 80 bar. The chromatographic separation was performed with the following mobile phases: (A) 81.42 vol% n-hexane, 17 vol% isopropanol, 1.5 vol% acetic acid, 0.08 vol% trimethylamine, and (B) 84.42 vol% isopropanol, 14 vol% water, 1.5 vol% acetic acid, 0.08 vol% triethylamine. The following gradient elution programme was used: a linear decrease from 95% to 80% A over 6 min (flow rate 1 mL/min), a linear decrease from 80% to 60% A over 4 min (1 mL/min) followed by a linear decrease from 60% to 0% A over 10 min (1 mL/min); next, a linear increase from 0% to 95% A over 1 min (1 mL/min) followed by an increase in the flow rate from 1 to 2 mL/min over 0.6 min, and the 2 mL/min flow rate was maintained for another 5.4 min. Finally, the flow rate was reduced back to 1 mL/min over 2 min. The injection volume was 20 µL. The detection parameters were as follows: nebulizer gas (nitrogen) pressure, 2.5 bar; drift tube temperature, 50°C; gain, 5.

The PC was identified by retention times matching with the PC standard (Sigma-Aldrich, P3556). The concentration of PC was determined from a calibration curve (R^2 = 0.9901) prepared with the PC standard. Additionally, the presence/concentration of phosphatidylethanolamine (PE) in HB was determined. The PE standard (Sigma-Aldrich, P0399) was used to determine the retention time of the phospholipid and to prepare a calibration curve. Fig. 15d displays the combined BS and PC concentrations of all HB samples. Results are shown as means ± SD (n = 3).

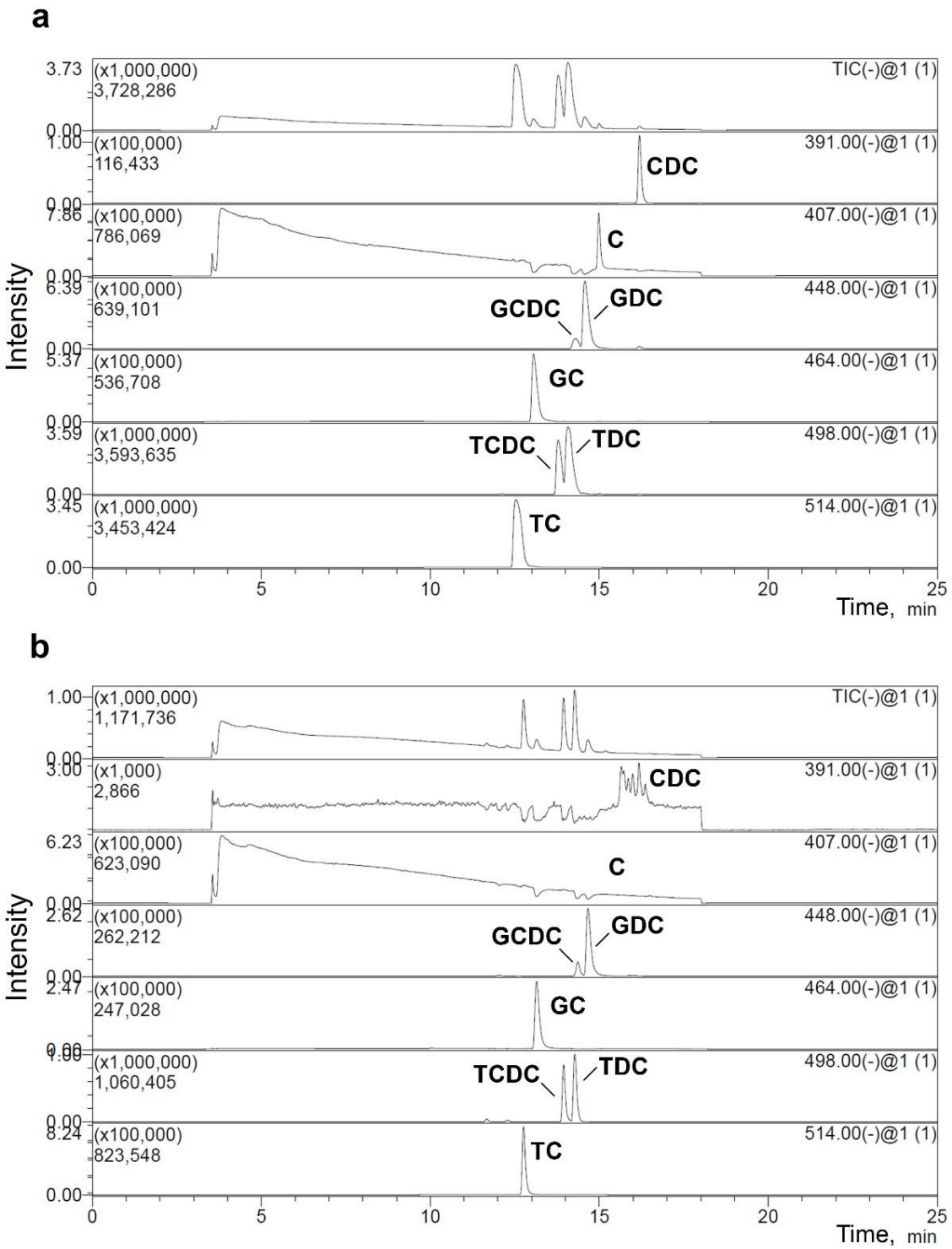

Figure 16. LC-MS analysis of human bile (HB). Representative chromatograms of (a) BS standards and of (b) individual BS species in HB sample no. 51(A). The top graphs in both panels show the total ion current (TIC) chromatograms, followed by chromatograms obtained for individual BS species: chenodeoxycholate, CDC; cholate, C; glycochenodeoxycholate, GCDC; glycodeoxycholate, GDC; glycocholate, GC; taurochenodeoxycholate, TCDC; taurodeoxycholate, TDC; taurocholate, TC. These results have been published (Dulko, et al. 2021).

3.3. Selection of human bile samples for *in vitro* proteolysis study

The HB samples were tested for any remaining proteolytic activity that might have been a result of contamination with human pancreatic enzymes during the bile aspiration. For this purpose, bovine milk β-lactoglobulin (βLg; L3908, Sigma-Aldrich, Germany) was put through simulated intestinal proteolysis (for experimental details, see Section 3.4.1.) for 120 min while being exposed to HB without the addition of any proteolytic enzymes. If the concentration of the protein remained constant throughout the experiment, indicating that the protein was not digested, the applied HB sample was deemed free of proteolytic enzymes. SDS-PAGE and HPLC were used to examine samples collected during the experiment, using the procedures described in detail in Section 3.5.

3.4. *In vitro* static human digestion models: proteolysis study

A static intestinal *in vitro* proteolysis model was employed for the initial assessment of the impact of individual BS concentration and the BS content of HB on the small intestinal proteolysis progress and extent. The procedure that was previously described (Gass et al., 2007) was used to create the model (see Section 3.4.1.).

In order to include both the gastric and the small intestinal phases of proteolysis in *in vitro* simulation, the *in vitro* intestinal proteolysis was eventually replaced by a gastrointestinal proteolysis model. The impact of the BS and PC contents in HB as well as of individual BS was assessed using a method that mimics the gastrointestinal digestion in humans. The procedures described previously (Mandalari, Adel-Patient, et al., 2009), (Moreno, Mackie, & Mills, 2005), (Böttger et al., 2019) served as the foundation for the gastrointestinal model used in this study (see Section 3.4.2.). Ultra-pure water (HLP5s system, Hydrolab, Poland) was used to make all required buffers and simulated digestive fluids.

3.4.1. Simulated intestinal proteolysis

Protein stock solutions (4 mg/mL) of either food-grade whey protein isolate (BiPRO®, Davisco Foods International Inc., Eden Prairie, MN) or β-lactoglobulin (βLg) purified from bovine milk (90%, L3908, Sigma-Aldrich, Germany) were made in a 20 mM sodium phosphate buffer (pH 7.0) containing 0.01% (w/v) sodium azide. The next step involved transferring 0.5 mL aliquots of a protein stock into 1.5 mL screw-cap Eppendorf tubes and adding a stock of individual bile salts (50 mM or 100 mM), which was made up of equimolar quantities of two different, individual BS – sodium taurocholate (NaTC; 95%, T4009, Sigma-

Aldrich, Germany) and sodium glycodeoxycholate (NaGDC; 97%, G9910, Sigma-Aldrich, Germany) – dissolved in the sodium phosphate buffer. These two individual BS were selected as they had previously been used to mimic bile in *in vitro* digestion models (Mandalari, Adel-Patient, et al., 2009; Dupont et al., 2009; Chu et al., 2009; Krupa et al., 2020). The tubes were handled individually during the digestion (Brodkorb et al., 2019), and after adding digestive enzymes to the tubes, the final concentration of BS in the digestion mixture was 0, 1, 2, 3, 3.64, 4, 6, 8 or 10 mM.

Alternatively, the tubes containing a protein stock were filled with 50 µL of a selected human bile sample. The HB samples no. 46(B), 65(B), and 51(A) (Fig. 15d) were selected for the proteolysis studies. The addition of HB resulted in the total BS concentrations of 0.65 mM, 3.64 mM, or 6.51 mM, respectively, and 0.18-0.49 mM PC in the final digestion mix.

The digestion was carried out with intestinal enzymes, trypsin from porcine pancreas (T0303, Sigma-Aldrich, Germany; activity of 13,800 U/mg of protein calculated using BAEE as substrate) and α-chymotrypsin from bovine pancreas (C7762, Sigma-Aldrich, Germany; activity of 40 U/mg of protein calculated using BTEE as substrate), at 37°C and 170 rpm (Heratherm IMH60 incubator, Thermo Scientific, Waltham, MA). The enzymes were individually dissolved in a cold (4°C) sodium phosphate buffer before use. To prevent enzymes autolysis, the enzyme stocks (5 mg/mL each) were made right before the digestion experiments. They were then kept on ice until needed.

Sample tubes were topped up to a volume of 980 µL with the sodium phosphate buffer and then incubated for 10 minutes at 37°C (170 rpm) before the enzyme stock solutions were added. The following addition of the enzyme stocks (10 µL aliquot of each enzyme stock) produced a final, total concentration of 0.1 mg/mL of trypsin and chymotrypsin (1:1 w/w) in the digestion mixture. The overall digestion mixture volume in each sample tube was 1 mL, and the initial protein concentration (βLg or WPI) was 2 mg/mL. The duration of the intestinal proteolysis was 0.25, 1, 2, 5, 10, 15, 30, 60, or 120 minutes at pH 7.0 (37°C, 170 rpm). The digestion in individual time-point samples was halted by mixing with PMFS (0.1 M stock in ethanol, 93482, Sigma-Aldrich, Germany) to the final 3 mM concentration of the protease inhibitor. Control experiments were also conducted without the use of enzymes, BS, or HB, by substituting these compounds in the digestion mixture with the sodium phosphate buffer. Before further examination, all post-digestion samples were stored at -80°C. Purified βLg with the individual BS was examined in all *in vitro* intestinal digestion

tests, which were carried out in triplicate (n = 3) for each set of the condition tested (e.g., presence/absence of BS, different BS concentrations, etc.). N = 5 was employed for other intestinal digesting tests (e.g., βLg or WPI with HB samples or WPI with the individual BS).

3.4.2. Simulated gastrointestinal proteolysis

Protein stock solutions (pH 3.0) of purified βLg or WPI (protein concentration, 2 mg/mL) were made using simulated gastric fluid (SGF; 150 mM NaCl, pH 3.0), which also contained sodium azide at a concentration of 0.01% (w/v). A stock of porcine pepsin (P6887, Sigma-Aldrich, Germany; activity: 3,300 U/mg of protein calculated using haemoglobin as substrate), prepared in SGF (20 mg pepsin per mL), was added after 10 min of pre-incubation of the protein solution (10 mL) at 37°C (170 rpm), resulting in the final enzyme concentration of 100 µg/mL (pepsin:protein, 1:20, w/w). The enzyme stock solution was made just before the experiment using a cold (4°C) SGF and kept on ice until required in order to prevent the autolysis of pepsin. Protein samples were digested for 60 minutes under *in vitro* gastric conditions (pH 3.0, 170 rpm, 37°C). At various times, ranging from 0.25 to 60 min of the gastric digestion, aliquots (0.5 mL) of the digestion mixture were removed from the digestion vial to individual 1.5 mL Eppendorf tubes and mixed with 100 mL of 0.5 M ammonium bicarbonate (09830, Sigma-Aldrich) aqueous solution. This quickly raised the pH to around 7.5, inactivating the pepsin in the collected time-point samples. The digestion in the vial was stopped after 60 min by bringing the pH up to 7.5 with 0.1 M NaOH (maintained for 10 min at 37°C). A 0.5 mL aliquot of the original protein stock solution was combined with 100 mL of 0.5 M ammonium bicarbonate solution to create a control sample (i.e., an undigested sample).

The mixture of the post-gastric digestion (5 mL) was then transferred to a fresh vial for the following intestinal digestion. The mixture was topped up with 275 µL of 0.5 M Bis-Tris HCL (B6032, Sigma-Aldrich, Germany) buffer that had been prepared with simulated intestinal fluid (SIF; 150 mM NaCl, pH 7.0).

For experiments with HB, 283 µL of the HB sample no. 65(B) (Fig. 15d) was added to the digestion vial to make the final (i.e., after the addition of intestinal enzymes, etc., as described below) 20-fold dilution of the HB, which produced 3.64 mM BS and 0.18 mM PC concentrations in the final digestion mix. Alternatively, for experiments with individual BS with/without PC, the stock solution of individual BS (i.e., NaTC and NaGDC; prepared as in section 3.4.1, but with SIF) and/or the vesicular PC dispersion were added to obtain the

same, final BS and/or PC concentrations as in the digestion experiments with HB, i.e., BS 3.64 mM and PC 0.18 mM. The mixture was toped up with SIF in order to replicate the volume brought about with the HB sample. If the digestion was carried out in the presence of PC, the vesicular dispersion of the lipid was prepared first, according to the method adapted from previous studies (Moreno et al., 2005), (Mandalari et al., 2008), (Macierzanka et al., 2009). Namely, egg yolk L-α-phosphatidylcholine (61755, Sigma-Aldrich, Germany) was dissolved in a chloroform/methanol mixture (1:1 v/v) to the PC concentration of 4.62 mg/mL. After transferring 5 mL of the mixture to a 50 mL round bottom flask, the solvents were evaporated using a rotary evaporator in order to form a thin film of PC. Any residual solvent was removed at RT under vacuum after three purges with nitrogen. The lipid film was then suspended in 5 mL of SIF (170 rpm, 10 min at 37°C), and finally the dispersion (PC conc. 4.62 mg/mL) was sonicated in an ice bath for 5 min using a sonication probe (80% intensity, 2 s impulses with 5 s breaks between them; Vibra-Cell Ultrasonic Liquid Processor, Sonics, CT). The size of PC vesicles was determined by a dynamic light scattering method using a Nano-ZS Zetasizer (Malvern Instruments Ltd., Malvern, UK) operating in size-measure mode. The mean particle size (Z-average) was 146.4 ± 2.4 nm (n = 4). The vesicular PC dispersion was added to the digestion mix in quantities required to obtain 0.18 mM PC concentration.

Subsequently, the pH of the digestion vial content was adjusted to 7.0, if required. After 10 min pre-incubation at 37°C, the intestinal proteolysis was carried out at pH 7.0 for up to 120 min (37°C, 170 rpm) using trypsin from porcine pancreas (T0303, Sigma-Aldrich, Germany) and α-chymotrypsin from bovine pancreas (C7762, Sigma-Aldrich, Germany). Stock solutions of both enzymes were prepared as in Section 3.4.1, but with chilled SIF. The intestinal digestion was initiated by a simultaneous addition of 50 µL of the trypsin stock and 50 µL of the chymotrypsin stock, which produced a comparable ratio of the protein being digested to the intestinal enzymes as in the procedure described in section 3.4.1. Time-point samples (500 µL) were withdrawn after 0.25, 1, 2, 5, 10, 15, 30, 60 and 120 min, and digestion in the samples stopped by mixing with 0.1 M PMSF inhibitor solution to its final concentration of 3 mM. Control experiments without enzymes, BS/PC or HB were carried out by replacing those components of digestion mixture with SGF or SIF. All post-digestion samples were stored at -80°C before further analysis. All *in vitro* gastrointestinal digestion experiments of purified βLg and WPI were done five times (n = 5) for each condition used.

Comparative gastrointestinal digestion experiments have also been done for bovine milk caseins from various sources: β-casein purified from bovine milk (98%, C6905, Sigma-Aldrich, Germany), food-grade sodium caseinate (90% protein, DMV International, The Netherlands) as well as Micellar Casein (Reflex Nutrition, UK) – a food supplement containing 80% protein (casein/whey protein, 80/20 w/w), 4% carbohydrate and 1.5% fat. Protein stock solutions (protein conc., 10 mg/mL) were prepared individually for all three casein sources by gentle mixing of protein powders in 150 mM NaCl (pH 7.0) containing 0.01% (w/v) sodium azide. Finally, stock solutions were diluted with SIF to give the protein conc. of 2 mg/mL, and pH adjusted to 3.0, if required. All *in vitro* gastrointestinal digestions of caseins were carried out in the same way as described above in this section for the purified βLg or WPI. They were done in triplicate (n = 3) for each condition used.

3.5. Characterisation of digestion samples: *in vitro* proteolysis study

3.5.1. Qualitative analysis of proteolysis progress

The collected time-point samples were first characterised by sodium dodecyl sulphate polyacrylamide gel electrophoresis (SDS-PAGE), which was used to qualitatively assess the proteolysis progress (Böttger et al., 2019).

Most of the chemicals used for the SDS-PAGE analysis were purchased from Invitrogen Ltd.: 40% acrylamide solution (HC2040), resolving buffer (HC2212), stacking buffer (HC2112), APS (HC2005), TEMED (HC2006), SeeBlue pre-Stained Protein Standard (LC5625), DTT (10x) (NP0004), LDS sample buffer (4x) (NP0007), MES SDS running buffer (20x) (NP0002). Aliquots (50 µL) of time-point samples taken during the digestion experiments were mixed with 15 µl of 0.5M DTT (D9163, Sigma-Aldrich), 30 µl of LDS Sample Buffer (x4) and with 50 µl of an intestinal buffer (20 mM sodium triphosphate buffer or SIF). Subsequently, the samples were heated in a hot block (Benchmark MyBlock BSH 5002-E) at 70°C for 10 min and cooled to RT before loading onto a polyacrylamide gel. The gels were prepared using the Invitrogen SureCast™ Handcast System user guide (MAN0014073, Thermo Fisher Scientific, https://assets.thermofisher.com/TFS-Assets/LSG/manuals/surecast_system_UG.pdf). Briefly, the resolving gel (10% acrylamide) was prepared, poured between glass plates, and left for 15 min to allow the acrylamide to polymerise. Subsequently, the stacking gel (4% acrylamide) was prepared and poured on top of the resolving gel. The 10-well comb was

inserted and the gel was left for 15 min to polymerise. Protein samples were loaded onto a freshly prepared gel (10 µg protein per well). SeeBlue Plus pre-stained molecular weight marker was used, containing a mix of proteins ranging from 3 to 188 kDa. Gels were run for 25 min at 150 mA/gel and 200 V. A continuous buffer system, consisting of 50 mL MES SDS running buffer and 950 mL ultra-pure water was used. Afterwards, gels were stained for 30 min in 0.1% w/v Brilliant Blue R (Sigma-Aldrich, 27816) solution of methanol (STANLAB 60300100X), acetic acid (POCH 568760114) and ultra-pure water (45:10:45, v/v/v). After the staining, gels were left overnight in a fixing solution (ultra-pure water/methanol/acetic acid, 70/20/10, v/v/v). Gels were scanned using a Gel Doc XR+ System (Bio-Rad). At least two replicate gels of each digestion were run.

3.5.2. Quantitative analysis of proteolysis progress

Using a modified version of the approach described by Hernandez-Ledesma et al. (Hernández-Ledesma, Dávalos, Bartolomé, & Amigo, 2005), a quantitative HPLC examination of the proteolysis progress and extent was performed. The Agilent 1100 Series LC (Agilent Technologies Inc., Santa Clara, CA) system, which included a vacuum degassing unit, a binary pump, an autosampler injector, a column thermostat, and a diode array detector (DAD), was used to analyse the digestion time-point samples. Zorbax 300SB-C8 column (4.6 mm 250 mm, 5 µm; Agilent Technologies Inc., Santa Clara, CA) was used for the chromatographic separation. The sample injection volume was 5 µL. The column was kept at 30°C. The 0.1% v/v trifluoroacetic acid solution in water (solvent A) and the 0.1% v/v trifluoroacetic acid solution in acetonitrile (solvent B) were prepared for use in a binary gradient elution system. In order to elute the samples, a flow rate of 0.8 mL/min was used. The applied gradient for solvent B was 5% (0 min), 20% (20 min), 60% (50 min), and 60% (53 min). Detection was done at 214 and 280 nm. In digestion time-point samples, the concentration of βLg (the sum of βLg variants A and B) was quantified and normalised against the value recorded for the undigested control (Meyer, 1995; Vincent, Elkins, Condina, Ezernieks, & Rochfort, 2016).

The analysis was done for time-point samples obtained from either five (n = 5) or three (n = 3) individual digestion experiments carried out for every individual set of digestion conditions. These have been specified in Sections 3.4.1 and 3.4.2. The HPLC results have been displayed as mean ± SD. A Student's *t*-test was used to evaluate statistical differences between two groups, and a 1-way ANOVA was used to compare the differences between

three or more groups (significance level, α = 0.05). GraphPad Prism 5.0 (GraphPad Software, San Diego, California) was used to conduct the statistical analysis.

3.6. Circular dichroism spectroscopy

A Jasco J-710 Spectropolarimeter (Jasco, Tokyo, Japan) equipped in a quartz cell (0.1 mm path length; Hellma UK Ltd, Essex, UK) was used to record far-UV CD spectra. βLg (L3908, Sigma-Aldrich, Germany; final concentration of 2 mg/mL) was dissolved in 20 mM sodium phosphate buffer (pH 7.0) and evaluated in the presence or absence of the individual BS (i.e., NaTC and NaGDC – 1:1, mol/mol; total 3.64 mM) and/or PC (0.18 mM and 0.5 mM). The BS stock solution and the PC dispersion were prepared as in Sections 3.4.1 and 3.4.2, respectively, but with the 20 mM sodium phosphate buffer, and added in quantities required to obtain the above concentrations of BS and/or PC. The protein was incubated with the BS and/or PC for 5 min at 37°C (170 rpm) before analysis. The average of four accumulations taken at a rate of 20 nm/min, between 185 and 260 nm, with a 4 s time constant and a 0.5 nm resolution, was used to create CD spectra. They have been presented as molar CD after the buffer blank was subtracted.

3.7. Human bile and other materials for *in vitro* emulsion lipolysis study

A detailed procedure of the collection of human bile (HB) samples and their examination for the phosphatidylcholine (PC) contents, total bile salt (BS) contents and the BS profiles have been described in Sections 3.1. and 3.2. as well as in (Dulko et al., 2021). Only those selected samples that lacked proteolytic and lipolytic activity were used in further research, as described below in Section 3.8.

Individual BS, sodium glycodeoxycholate (NaGDC, G-9910, ≥97% pure) and sodium taurocholate (NaTC, T4009, ≥95% pure) were obtained from Sigma-Aldrich. Egg yolk L-α-Phosphatidylcholine (PC, 61755), tributyrin (W222305), porcine pancreatin (P7545), phosphate buffered saline (PBS, P4417), Bis-Tris (14879), Tris-(hydroxymethyl)-aminomethane (252859), phenylmethanesulfonyl fluoride solution (PMFS, 93482), Coomassie blue (27816), and sodium azide (NaN_3, S2002) were also from Sigma-Aldrich. NaCl, $CaCl_2$, NaOH, HCl, and acetic acid were purchased from POCh S.A. (Gliwice, Poland). Ultra-pure water was prepared with a HLP5s purification system (Hydrolab, Straszyn, Poland).

Whey protein isolates (WPI, 93% of protein, BiPRO Davisco Foods International Inc.) were used to emulsify refined sunflower oil (Fabiola, FSF Poland) that had been purchased locally in Gdańsk (Poland). Prior to the use in emulsion preparation, the oil was purified with Florisil adsorbent (60–100 mesh; Fluka, 46385; 2:1 w/w) by continuous mixing (140 rpm, 30 min) followed by centrifugation (9 000 rpm, 40 min) and decantation of the adsorbent. The purified oil was stored under nitrogen at 4°C until needed. The fatty acid (FA) profile of the oil was analysed. For that purpose, the FAs of the oil were converted to FA methyl esters (FAMEs) according to previously published method (ISO 12966-2:2017(E)), and analysed with GC-FID using a Perkin Elmer Autosystem XL instrument and under the following conditions: 50 m x 0.2 mm x 0.2 µm CP-Sil 88 capillary column (Agilent Technology), helium carrier gas (1 mL/min); temperatures: injector, 250°C; detector, 250°C; column, 170°C, split ratio 60:1. The obtained FA composition of the oil was as follows: 56.8±0.3% $C_{18:2}$, 31.8±0.04% $C_{18:1}$, 6.5±0.2% $C_{16:0}$, 3.6±0.02% $C_{18:0}$, and 1.3±0.01% of other FAs, which is typical for sunflower oils (Gupta, 2002).

3.8. Assaying residual proteolytic and lipolytic activity of HB and selecting HB samples for *in vitro* emulsion lipolysis studies

HB samples were examined for residual proteolytic activity using the method described in detail Section 3.3. and in (Dulko et al., 2021).

Those HB samples that did not reveal proteolytic activity were further examined for any residual lipolytic activity (LA). The LA assay was adapted from Minekus et al. (Minekus et al., 2014). Namely, 3.865 mL of the assay solution (0.3 mM Tris-(hydroxymethyl)-aminomethane, 150 mM NaCl, 2 mM $CaCl_2$, 4 mM sodium taurodeoxycholate (Sigma-Aldrich, T0875), pH 8.0) and 0.135 mL of tributyrin were equilibrated at 37±0.1°C under continuous mixing (1500 rpm). The pH of the mixture was adjusted to 8.0 with 0.1 M NaOH. The LA monitoring started after addition of a HB solution (prepared by dissolving 1 mg HB per 1 mL of ultra-pure water) to the reaction mixture. LA was measured for two different volumes of the HB solution (i.e., 26.7 µL and 53.3 µL), each analysed in triplicate, and the results were presented as the mean ± SD. The rate of 0.1 M NaOH addition, required to maintain the pH constant at 37±0.1°C during any eventual release of free fatty acids (FFAs), was measured with a thermo-regulated pH-stat device (Cerko Lab System, Gdynia, Poland). The kinetics of FFA release was monitored for at least 5 min (37±0.1°C, 1500 rpm). Ultra-pure water and lipase from porcine pancreas (Sigma-Aldrich, L3126; specific LA of 69 ±15 U/mg) were used as negative and positive controls, respectively. The residual LA of HB (U/mg) was calculated using the following equation: $LA = R_{NaOH} \times 1000 / (v \times C_{HB})$, where R_{NaOH} is the rate of delivery of 0.1 M NaOH, i.e., µmol of FFA titrated per minute, v (µL) is the volume of HB solution, and C_{HB} (mg/mL) is the concentration of HB solution. The residual LA of each analysed HB sample was normalised against the mean specific LA of the lipase (Tab. 3), which had been assayed in the same fashion. Only those HB samples that did not express mean residual LA larger than 1% of the LA detected for the lipase were considered free of lipolytic activity and qualified for the use in *in vitro* lipolysis studies (Section 3.10).

Eliminating HB samples that expressed residual proteolytic and/or lipolytic activities was necessary before including any HB in the *in vitro* lipolysis experiments because otherwise the lipolysis progress of the protein-stabilised emulsion studied here could have been significantly affected by any uncontrolled addition of digestive enzymes delivered potentially with HB.

Apart from not being allowed to express proteolytic and lipolytic activities, HB samples were also required to contain low and comparable amounts of PC but different total amounts of BS. By selecting such HB samples, I aimed to concentrate primarily on any potential impact of the BS content of HB on the lipolysis progress and extent. Finally, three HB samples were selected for the lipolysis experiments after all the aforementioned screening procedures had been finished and the criteria met: samples denoted by codes 57(B), 56(A) and 11(C); see Fig. 15. In this *in vitro* emulsion lipolysis study, they have been referred to as 'HB-4.16', 'HB-5.35' and 'HB-7.43', respectively (Tab. 3), to reflect the different, total BS concentrations (mM) they produced in the *in vitro* digestion environment.

Table 3. BS and PC concentrations produced with selected HB samples in the digestion mixture for the lipolysis experiments, and the residual lipolytic activities of the HB samples (the activates have also been normalised against the lipolytic activity of pancreatic lipase).

Sample	BS, mM * (mean ± SD, n = 3)	PC, mM * (mean ± SD, n = 3)	Lipolytic activity, U/mg (mean ± SD, n = 6)	Normalised activity, % (mean ± SD)
Lipase from porcine pancreas (positive control)	-	-	69±15	100
Ultra-pure water (negative control)	-	-	0.002±0.004	0.003±0.005
HB-4.16	4.16±0.29	0.69±0.12	0.6±0.4	0.9±0.6
HB-5.35	5.35±0.43	0.69±0.29	0.4±0.3	0.6±0.4
HB-7.43	7.43±0.58	0.48±0.07	0.6±0.4	0.9±0.6

* Total BS and PC concentrations obtained under the *in vitro* lipolysis conditions (i.e., after a 10-fold dilution of a HB sample in the digestion mix).

3.9. Emulsion preparation and analysis before *in vitro* emulsion lipolysis study

WPI was dissolved (0.5% w/w) in saline (150 mM NaCl, 0.02% (w/w) NaN_3 in ultra-pure water) and used as an aqueous phase in emulsion preparation. The Florisil-cleaned sunflower oil was used as an oil phase. A fixed amount of emulsion was prepared (24 g) in a glass vial. An oil-in-aqueous phase premix (20:80 w/w) was emulsified using an ultrasound homogenizer (VCX500 ultrasonic liquid processor, 20 kHz, 500 W, Sonics & Materials Inc., CT) over 3.5 min by applying consecutive 2-s pulses at 80% amplitude separated with 5-s pauses.

The vial with emulsion was immersed in an iced water bath (5°C) during the emulsification process.

Droplet size of emulsions was determined from the dynamic light scattering using a Zetasizer Nano ZS (Malvern Instruments, Malvern, United Kingdom) operated in a size-measure mode. Prior to measurement, emulsions were diluted with the saline (1:2.5k, v/v). In total, 13 emulsions were prepared and examined for determining the mean droplet size (Z-Average) ± SD. Each emulsion was analysed twice.

3.10. *In vitro* small intestinal lipolysis in emulsion

The progress of lipolysis in emulsion was monitored using a pH-stat automatic mini-titration unit (Cerko Lab System, Gdynia, Poland) and under the simulated small intestinal digestion conditions specified previously in the Infogest protocol (Brodkorb et al., 2019), with some modifications. Total volume of digestion mixture was 3 mL and contained: 0.375 mL of emulsion, 1.2 mL of lipolysis buffer (2 mM Bis-Tris, 150 mM sodium chloride, pH 7.0 (Chu et al., 2009)), 1 mL of pancreatin solution in the lipolysis buffer (at the concentration required to provide the pancreatic lipase activity of 2000 U/mL in the final mixture (Brodkorb et al., 2019)), 0.3 mL of undiluted HB sample or 0.3 mL of the PBS stock of individual BS (NaTC and NaGDC, 1:1, mol/mol) with/without co-dissolved PC, 3µL of 0.3 M $CaCl_2$ aqueous solution, predetermined volume of 0.1 M HCl required to adjust the pH to 7.0, and the lipolysis buffer in amounts required to reach the final volume of the reaction mixture (i.e., 3 mL). This resulted in a 10-fold dilution of HB used for experiment and produced the final, total BS and PC concentrations that differed between experiments, depending on the HB sample used (Tab. 3). When the lipolysis experiments were carried out in the presence of a BS/PC mixture (i.e., instead of HB), the amounts of BS and PC introduced to the digestion mix were the same as if they had been produced by using a particular HB sample (Tab. 3). Additionally, a series of lipolysis experiments were done with the individual BS (i.e., NaTC and NaGDC, 1:1, mol/mol) being the sole biliary surfactants used (i.e., without PC) in order to investigate the effect of increasing BS concentration on the lipolysis progress. In that case, the total concentration of individual BS in the digestion mix ranged from 0 to 15 mM.

The lipolysis experiment was carried out in a 20-mL, conical, glass vessel, thermostated at 37±0.1°C. The digestion was started by addition of the pancreatin solution (i.e., the source of digestive enzymes) to the digestion mixture and conducted for 2 h at 37±0.1°C. The pH 7.0

was kept constant by adding 0.1 M NaOH under continuous mixing (500 rpm). Experiments were done in triplicate for each set of analysed conditions (e.g., for individual HB samples, BS at different concentrations, with/without PC, etc.) and the results presented in each case as the mean concentration (±SD) of released FFAs in the function of digestion time. Control experiments were also done without HB, BS and/or PC by replacing those components with PBS. Additionally, blank experiments were conducted with the pancreatin solution replaced by a pure buffer. Any limited addition of NaOH required during the blank experiments to keep the pH 7.0 was monitored and the recorded NaOH volumes taken into account when evaluating the lipolysis experiments.

The emulsion lipolysis progress was monitored by continuous recording of the volume of 0.1 M NaOH required to neutralise FFAs released from the emulsified triglyceride (TG) substrate and maintain constant pH (i.e., pH 7.0). The recorded volume of titrant was used to calculate the percentage of liberated FFAs (%) (Sarkar, Li, Cray, & Boxall, 2018), (Y. Li & McClements, 2010):

$$FFA\ (\%) = \frac{(V_{NaOH} - V_{blank}) \cdot C \cdot MW}{m_{oil} \cdot N \cdot 1000} \cdot 100\% \quad (1)$$

where *C* is the molar concentration of the NaOH titrant (0.1 M), *MW* is the average molecular weight of sunflower oil TGs (885.69 g/mol; based on the average composition of fatty acids determined with GC-FID), m_{oil} is the amount (g) of the oil delivered in emulsion to the digestion mixture, *N* is the number of FFA released from a TG molecule (i.e., *N* = 2, considering two FFAs are released from one TG molecule by the action of pancreatic lipase), V_{NaOH} is the volume (mL) of NaOH needed to neutralise the FFAs produced, and V_{blank} is the mean volume (mL) of NaOH required to neutralise a blank sample.

In the experiments carried out in the presence of HB or BS/PC mixture, the volume (mL) of NaOH needed to neutralise FFAs released in a reference digestion experiment (i.e., an experiment without TG emulsion, which was replaced with saline) was first investigated. Those experiments aimed at detecting any possible release of FFAs from PC that might have occurred during the digestion with pancreatin (i.e., by the pancreatic phospholipase that might have been delivered with pancreatin). The V_{NaOH} values recorded for every time point of a reference digestion experiment were subtracted from corresponding V_{NaOH} values recorded for a relevant digestion experiment on emulsion. The final V_{NaOH} values obtained

that way were used to calculate (eq. 1) the percent of FFAs liberated solely from the emulsified TGs.

Statistical comparisons between two groups of data were made using a Student's *t* test, and 1-way ANOVA was used for comparing three (or more) groups of data (significance level, *P* value < 0.05).

Methodology used in *in vitro* interfacial study of lipolysis

3.11. Human bile collection and analysis for interfacial studies

Comprehensive details regarding the collection and characterisation of human bile (HB) have been presented in Sections 3.1. and 3.2., and published in (Dulko et al., 2021).

The concentration of total bile salts (BS) in HB was assessed using the bile acids (enzymatic cycling) test kit (Alpha laboratories, Hampshire, UK) following the method described by (Mackie, Rigby, Harvey, & Bajka, 2016; Section 3.2). The BS profiles of HB samples, as well as their phosphatidylcholine (PC) contents, were determined by as outlined in Section 3.2.

3.12. Selection of HB samples for interfacial studies

Based on the results of total BS and total PC concentrations (Section 3.1; Fig. 15d), a subset of HB samples was chosen for interfacial measurements, including *in vitro* digestion experiments. This research specifically required selected HB samples to exhibit both low and similar concentrations of PC, while also displaying substantial variation in total BS concentrations. By selecting such samples, I intended to focus predominantly on a potential effect of the BS content of HB on interfacial properties during lipolysis.

Before being employed for any further investigations, HB samples underwent testing to identify potential residual lipolytic and proteolytic activity (refer to Sections 3.12.1 and 3.12.2) that could have arisen from pancreatic enzyme contamination during bile aspiration. HB samples were considered suitable for the study only if they did not display evident indications of lipolytic and proteolytic enzyme contamination.

After completion of the aforementioned screening process, three HB samples were chosen for the interfacial studies. These HB samples (coded as 9(A), 56(A), and 36(D); see Fig. 15d) were collected from patients with choledocholithiasis and cholangiocarcinoma, conditions known to impact bile composition (Li & Apte, 2015), (Costi, Gnocchi, Di Mario, & Sarli, 2014), thus providing distinct variations in total BS content. For the purpose of my research, the

selected HB samples were designated as HB-2.23, HB-5.35, and HB-7.81, respectively, reflecting the total BS concentrations (mM) they brought about in the interfacial experiments. Fig. 17 illustrates the maximum BS and PC concentrations generated under the experimental conditions involving the selected HB samples, along with their corresponding BS profiles.

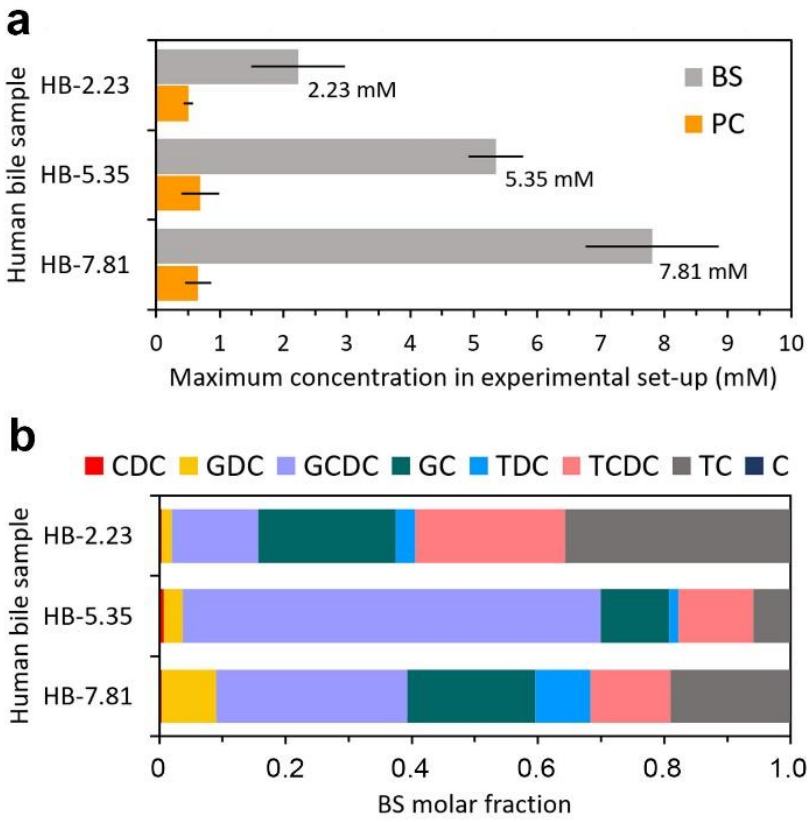

Figure 17. The human bile (HB) samples used in interfacial studies. (a) The maximum concentrations of total bile salts (BS) and phosphatidylcholine (PC) generated by three selected HB samples during the interfacial experiments, following a 10-fold dilution of HB within the experimental setup. (b) The BS profiles of the HB samples, highlighting the molar fractions of particular BS in the total BS tested. The BS species encompassed in the profiles include chenodeoxycholate (CDC), glycodeoxycholate (GDC), glycochenodeoxycholate (GCDC), glycocholate (GC), taurodeoxycholate (TDC), taurochenodeoxycholate (TCDC), taurocholate (TC), and cholate (C).

3.12.1. Assessment of residual lipolytic activity in HB samples selected for interfacial studies

The evaluation of pancreatic lipase activity was adapted from (Brodkorb et al., 2019) and conducted in the same way as for the purpose of *in vitro* emulsion lipolysis studies. The method has been described in detail in Section 3.8.

The lipolytic activity of HB samples was normalised against the mean activity of pancreatic lipase (Tab. 4). Only HB samples with a mean activity less than 1% of the activity detected for the lipase were considered suitable for subsequent experiments.

Table 4. Lipolytic activity of HB samples selected for interfacial studies, relative to the activity of purified porcine pancreatic lipase

Sample	**Lipolytic activity, U/mg (mean ± SD, n = 6),**	**Normalised activity, % (mean ± SD)**
Lipase from porcine pancreas (positive control)	69 ± 15	100
Ultra-pure water (negative control)	0.002 ± 0.004	0.003 ± 0.006
HB-2.23	0.6 ± 0.18	0.9 ± 0.3 *
HB-5.35	0.4 ± 0.3	0.6 ± 0.4 *
HB-7.81	0.5 ± 0.5	0.7 ± 0.7 *

* All three HB samples exhibited lipolytic activity that was less than 1% of the activity detected for pancreatic lipase (refer to Section 3.12.1.). Consequently, they were deemed appropriate for the interfacial experiments.

3.12.2. Assessment of residual proteolytic activity in HB samples selected for interfacial studies

HB samples were further examined for residual proteolytic activity using the method described in detail in Section 3.3. and published previously in (Dulko et al., 2021).

3.13. Critical micelle concentration (CMC) of individual BS mixture

The CMC of the mixture of two individual BS (sodium glycodeoxycholate (NaGDC, 97% purity; Sigma-Aldrich, G9910) and sodium taurocholate (NaTC, 95% purity; Sigma-Aldrich, T4009)) was determined with the use of Nano-Isothermal Titration Calorimeter III (N-ITC III, CSC, USA). This involved measuring heat fluctuations in the sample cell during titration and comparing them to a reference (control) cell. The BS stock solution, containing equimolar quantities of NaGDC and NaTC, was prepared in simulated intestinal fluid (SIF; 1.13 mM sodium phosphate, 150 mM sodium chloride, 2 mM calcium chloride, 0.01% sodium azide; pH 7) by dissolving the two BS together to the concentration exceeding the expected CMC. The experiments were conducted in a 952-µL sample cell at 37°C with stirring at 250 rpm. Injections (5 µL) of the BS stock were sequentially made every 300 s to incrementally increase the BS concentration. The reference cell contained SIF. The heating rate necessary to maintain a constant temperature difference between the sample and reference cells was recorded after each injection using Titration Bindworks software (CSC, USA). The injection peaks were integrated and normalised with respect to the number of moles of the BS injected. The enthalpogram comprised three segments: initial dilution of BS micellar solution in SIF (i.e., a demicellisation process), sharp decrease in the heat effect reflecting CMC attainment, and subsequent addition of concentrated BS solution to the existing micellar solution in the sample cell. The heat of micellisation was calculated from the difference between the enthalpies of the two linear parts of the sigmoidal curve. The first derivative of the integrated peaks was analysed with respect to total BS concentration to determine the CMC, indicated by the minimum point of the curve (Łuczak, Jungnickel, Joskowska, Thöming, & Hupka, 2009). The CMC determination experiment was done in triplicate (n = 3), and the resultant data were employed to compute the mean ± SD.

3.14. Oil-water interfacial studies

3.14.1. Preparation of phospholipid vesicles for interfacial studies

The preparation of vesicles was essentially done as already outlined in Section 3.4.2., with some modifications. Briefly, egg yolk L-α-phosphatidylcholine (Sigma-Aldrich, 61755) was dissolved in a mixture of chloroform and methanol (1:1 v/v) to achieve a concentration of 5 mg/mL of phosphatidylcholine (PC). Subsequently, 5 mL of this solution was transferred to a round-bottom flask and subjected to solvent evaporation using a rotary evaporator

(Autobac, General Diagnostic) to create a thin PC film. The lipid film was then suspended in 5 mL of simulated intestinal fluid (SIF) under continuous stirring (170 rpm, 10 min) at 37°C. An ultrasound homogenization process (20 min) followed this step, and the resulting dispersion (PC concentration: 5 mg/mL) was subsequently filtered using a Sartorius syringe filter (0.2 µm, PTFE). The size of the PC vesicles was determined using dynamic light scattering through a Zetasizer Nano-ZS system (Malvern Instruments, UK) operating in the size-measure mode. The obtained mean particle size was measured at 156 ± 4 nm (n = 4). This vesicular PC dispersion was incorporated into the experimental setup for interfacial studies, with quantities adjusted to yield PC concentrations corresponding to those introduced by the chosen HB samples (Fig. 17).

3.14.2. Oil purification for interfacial studies

Sunflower oil (Fabiola, FSF Poland) was purified with Florisil resins (60–100 mesh, Fluka, 46385) prior to its utilisation to remove surface-active impurities (Macierzanka et al., 2012). The procedure involved combining the adsorbent with the oil in a ratio of 1:2 (w/w) under continuous stirring (500 rpm) for a duration of 9 h at 1000 rpm. Subsequently, the mixture was subjected to centrifugation (12000 rpm, 30 min; Centrikon T-124, Kronton Instruments). The oil phase was decanted and then filtered through Millex filters (0.1 µm PDVF) using a vacuum pump, after which it was stored under a nitrogen atmosphere in darkness until its intended use. Control measurements of the interfacial tension of pure SIF/sunflower oil were performed before each experiment detailed in Sections 3.14.3. and 3.14.4. These measurements consistently yielded a stable value of 23.5 ± 1.5 mN/m at 37.0 ± 0.1^{o}C.

3.14.3. Adsorption/desorption at oil–water interface

This experimental work has been done by me in collaboration with the University of Granada (Biocolloid and Fluid Physics Group, Department of Applied Physics), during my research visit to Granada, Spain (Section 7).

The adsorption/desorption experiments were conducted using the Octopus device, a pendant drop film balance equipped with a subphase multi-exchange device, and controlled by Dinaten software (Maldonado-Valderrama, Torcello-Gómez, del Castillo-Santaella, Holgado-Terriza, & Cabrerizo-Vílchez, 2015). A comprehensive description of the experimental setup has been provided elsewhere (Maldonado-Valderrama, Terriza, Torcello-

Gómez, & Cabrerizo-Vílchez, 2013), (Maldonado-Valderrama, del Castillo Santaella, Holgado-Terriza, & Cabrerizo-Vílchez, 2022).

Initially, the experiments encompassed the three selected HB samples, which were subjected to a 10-fold dilution with SIF. This led to the attainment of the BS and PC concentrations as illustrated in Fig. 17a. Furthermore, investigations were carried out involving a blend of individual BS. The stock solution comprising equimolar quantities of two BS (NaGDC and NaTC) was prepared in SIF to achieve a total concentration of 25 mM. Subsequently, this BS stock solution was diluted with SIF to match the same total concentrations of BS as in the three HB samples used initially (Fig. 17a). Additionally, measurements were executed for combinations of individual BS and PC (BS/PC; PC prepared as detailed in Section 3.14.1.). In this regard, the dispersion of PC vesicles was employed in quantities that mirrored the PC concentrations within the chosen HB samples (Fig. 17a). All the aforementioned solutions/mixtures were also subjected to subsequent 10-fold and 100-fold dilutions with SIF, and examined individually.

The following experimental procedure was applied. A droplet of HB, BS, or BS/PC solution was formed at the tip of a coaxial double capillary (Patent ES 2 153 296 B1) immersed in purified sunflower oil situated in a glass cuvette (Hellma, OG, 10-mm optical path length, type 6030). The cuvette was maintained at a temperature of 37.0 ± 0.1^{o}C. The measurement of the interfacial tension (IFT) for various solutions was carried out at a consistent interfacial area of 30 mm^2, spanning a period of 32 min. Following this, dilatational rheology was assessed by controlled deformation of the interfacial area.

The dilatational modulus (E) of the interfacial layer was determined, encompassing both real (E') and imaginary (E'') components: E = E' + iE'', wherein E' corresponds to the storage modulus reflecting elasticity, and E'' signifies the loss modulus representing interfacial viscosity. The amplitude of oscillation was maintained below 5% variation, and the frequencies applied were 0.01, 0.1, and 1 Hz. Frequencies beyond this range would predominantly manifest elastic behaviour in the adsorbed layer due to longer relaxation times, rendering the imaginary part negligible. The dilatational rheology assessment required approximately 20 min, encompassing 10 cycles for each frequency examined.

Subsequently, the stability of the interfacial film was gauged by monitoring the spontaneous desorption of HB, BS, or BS/PC via bulk concentration depletion. This involved the substitution of the bulk solution with SIF using a subphase exchange method, where a 10-

fold replacement of droplet content with SIF guaranteed complete exchange of the bulk solution (Maldonado-Valderrama, Muros-Cobos, Holgado-Terriza, & Cabrerizo-Vílchez, 2014). Throughout the entire subphase exchange process, the IFT was recorded. Additionally, the dilatational rheology of the resultant interfacial film was assessed following the replacement procedure and after the IFT reached a stabilised state, typically around 32 min into the desorption phase.

3.14.4. Monitoring the oil-water IFT under simulated small intestinal lipolysis conditions

This experimental work has been done by me in collaboration with the University of Granada (Biocolloid and Fluid Physics Group, Department of Applied Physics), during my research visit to Granada, Spain (Section 7).

The *in vitro* simulation of small intestinal lipolysis conditions at the oil-water interface was conducted using the Octopus apparatus as outlined by (Maldonado-Valderrama et al., 2013). The comprehensive simulation encompassed three distinct experimental steps conducted in a temperature-controlled glass cuvette at 37 ± 0.1^{o}C: (1) protein adsorption, (2) lipolysis, and (3) desorption (Fig. 18). Throughout the entire experiment, the evolution of IFT was continuously monitored *in situ*.

In the initial stage (step 1), a droplet (4.5–6.0 µL) of bovine milk β-lactoglobulin (βLg; Sigma-Aldrich, L3908) solution (0.1 g/L in SIF) was generated within purified sunflower oil. The process of protein adsorption was tracked at a consistent interfacial area until equilibrium IFT was attained. This established an oil/water interface stabilised by protein, mimicking a single droplet of protein-stabilised emulsion. The protein adsorption phase (n = 15) extended for 62 min.

Moving on to the subsequent stage (step 2), the droplet was exposed to conditions emulating small intestinal lipolysis via subphase exchange. This entailed 10 cycles of droplet content exchange with solutions of either:

(i) Freshly prepared in SIF (and pre-stored on ice) porcine pancreatic lipase (Sigma-Aldrich, L3126) at the 0.16 mg/mL concentration (Maldonado-Valderrama et al., 2013), (Aguilera-Garrido, del Castillo-Santaella, Galisteo-González, José Gálvez-Ruiz, & Maldonado-Valderrama, 2021),

(ii) Lipase with vesicular PC prepared in SIF (with PC quantities adjusted to give the concentration of 0.6 mM, which represented an average PC concentration in the selected HB samples; refer to Fig. 17a),

(iii) Lipase with individual BS (NaTC + NaGDC; total equimolar concentration of 2.23, 5.35, or 7.81 mM in SIF, matching total BS concentrations in selected HB samples; refer to Fig. 17a),

(iv) Lipase with individual BS and PC (BS/PC) in SIF (utilising the above BS concentrations as well as PC quantities adjusted to mirror the PC concentrations in the selected HB samples; refer to Fig. 17a), or

(v) Lipase with HB (i.e., with the selected HB samples diluted 10x with SIF, resulting in total BS concentration of 2.23, 5.35, or 7.81 mM, and 0.5–0.7 mM PC concentration; refer to Fig. 17a).

The inclusion of co-lipase was omitted due to prior evidence showing its negligible influence on comparable interfacial experiments (Torcello-Gómez et al., 2011), (Maldonado-Valderrama et al., 2013). The lipolysis step lasted for 32 min.

In the final stage (step 3; 34 min), the droplet content was substituted with SIF (15 cycles of droplet volume exchange). This led to bulk solution depletion and allowed assessing the ability of surface-active material to desorb from the interface.

At the conclusion of each step (once IFT had stabilised), dilatational rheology was measured (Fig. 18) using the conditions specified in Section 3.14.3.

All experiments were conducted in triplicate (n = 3) for each condition tested. Statistical comparison between two groups of data was made using a Student's *t* test (significance level, P value < 0.05).

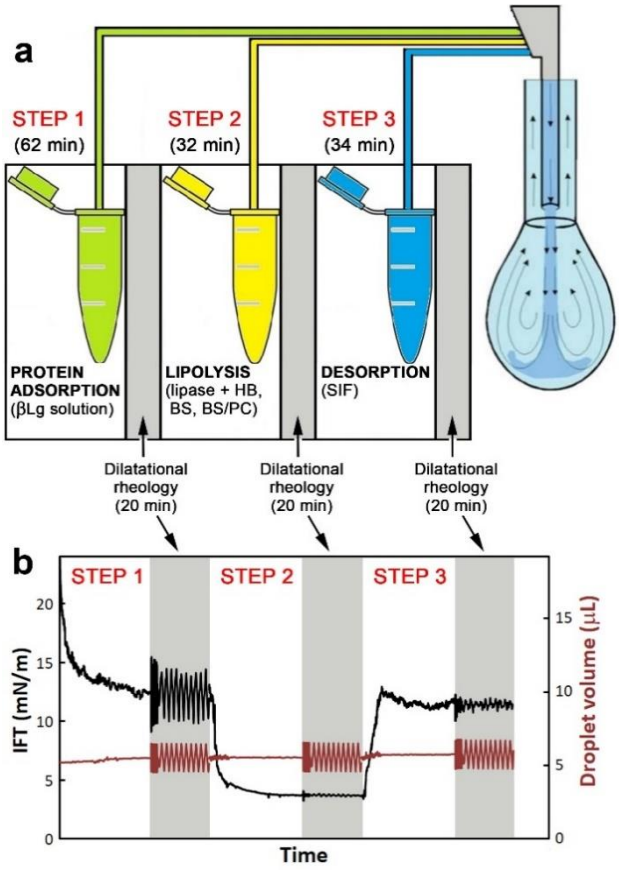

Figure 18. (a) Schematic representation of the experimental setup for monitoring oil-water interfacial tension (IFT) under simulated small intestinal lipolysis conditions. Progression to subsequent experiment steps involved replacing the content of the solution droplet using the Octopus subphase multi-exchange device. Image adapted from (Maldonado-Valderrama et al., 2013). (b) Exemplary outcomes illustrating the changes in IFT and droplet volume across the stages of protein adsorption, lipolysis, and desorption. The grey-shaded intervals indicate the time periods during which dilatational rheology measurements were taken.

4. Results and discussion

4.1. *In vitro* proteolysis

4.1.1. Effect of bile salt concentration on *in vitro* intestinal proteolysis of βLg

Prior to examining the impact of BS content of human bile (HB) on the degree of βLg digestion, a preliminary study was conducted – a quantitative analysis of the impact of individual (model) BS concentration on the degree of protein hydrolysis. In this approach, I used the simplified *in vitro* intestinal digestion model with trypsin and chymotrypsin (Section 3.4.1.). A previously published qualitative study, which involved the use of a mixture of six tauro- and glyco-conjugated BS (Gass et al., 2007), showed that protein digestibility increased gradually as BS concentration increased. My objective was to do a quantitative evaluation of the proteolysis process for both purified native βLg and βLg in a food-grade WPI. Importantly, in order to simulate the presence of HB in the digesting environment, I only combined two distinct BS (NaTC and NaGDC). As recently stated (Macierzanka, Torcello-Gómez, Jungnickel, & Maldonado-Valderrama, 2019), the two BS had previously been employed in a variety of *in vitro* investigations aiming to replicate the biochemical environment of the human small intestine. These particular BS, however, have never been demonstrated to have a direct effect on the intestinal digestion of milk proteins (or any other proteins). Additionally, they haven't been examined in any comparative study against HB.

Molecular interactions between BS and proteins in aqueous solutions have been the subject of several studies. The far-UV circular dichroism (CD) spectroscopy study of malate dehydrogenase and luciferase has found that the proteins were forced to significantly unfold and aggregate when they had been incubated with cholate and/or deoxycholate (Cremers, Knoefler, Vitvitsky, Banerjee, & Jakob, 2014). The detected alterations in the proteins' secondary structures pointed to an increase in the formation of random coils, which took place at the expense of α-helical fragments. According to Kimzey and Haxo (2016), BS can denature glycoproteins and make them vulnerable to enzymatic deglycosylation. Martos, Contreras, Molina, and López-Fandio (2010) explored how egg white ovalbumin (OVA) interacted with NaTC and NaGDC. Despite the fact that the molecular structure of OVA did not appear to be affected by BS, the amount of IgG that bound to the protein was

dramatically reduced. The authors suggested that OVA might interact with BS, increasing the protein's exposure to pancreatic proteases. The significantly increased digestibility of OVA in the presence of BS, as observed by Martos et al. under simulated intestinal conditions (Martos et al., 2010), was most likely the result of non-specific interactions of the protein with the BS, because BS have not been found to affect the proteolytic activity of trypsin and chymotrypsin (Gass et al., 2007). Conjugated BS can greatly improve the digestibility of a number of globular dietary proteins, including myoglobin, bovine serum albumin, and βLg, under simulated duodenal conditions with trypsin and chymotrypsin (Gass et al., 2007). The researchers hypothesised that in the case of βLg, some BS could bind into the hydrophobic interior domains of the protein, causing the protein structure to become unstable and making the domains available for the cleavage by the intestinal proteases. That study did not, however, investigate the actual influence of BS on the structure of βLg. In a different study (Maldonado-Valderrama et al., 2011), a far-UV CD was applied to check the influence of NaTC and NaGDC on the structure of bovine milk βLg. When applied at 7.4 mM concertation, the BS were discovered to bind with the protein and partially disrupt its secondary structure. In my investigation, a comparable experiment has been carried out (Fig. 19).

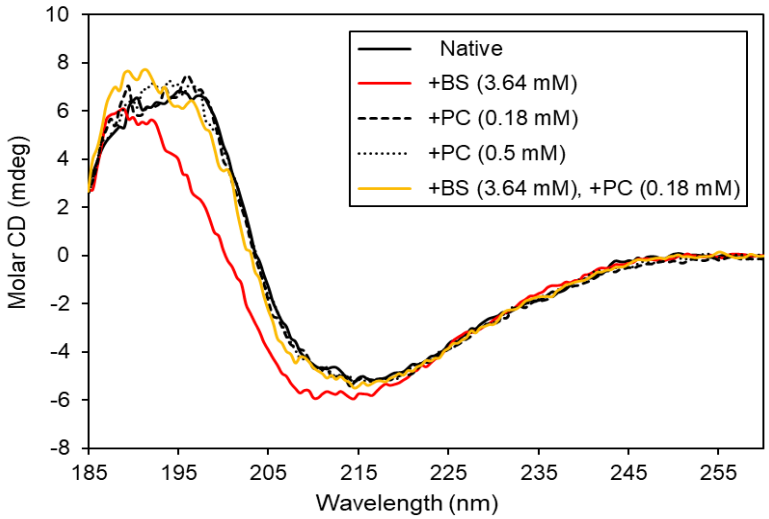

Figure 19. Far-UV circular dichroism (CD) spectroscopy of β-lactoglobulin. Prior to analysis, the native protein was incubated with vesicular phosphatidylcholine (PC; 0.18 mM or 0.5 mM) and/or individual bile salts (BS) i.e., NaTC and NaGDC (1:1, mol/mol; total 3.64 mM) as described in section 3.6. The 0.18 mM PC and 3.64 mM BS concentrations have been selected in order to reflect the PC and BS concentrations that were produced in the digestion mix with the HB sample 65(B) (see Fig. 21a). These results have been published (Dulko, et al. 2021).

Even though the total BS concentration was over two times lower and the BS/protein ratio was over four times lower than in the study by Maldonado-Valderrama et al. (2011), the incubation of βLg with an equimolar mixture of the same, individual BS (i.e., NaTC and NaGDC) resulted in a similar change in the protein's secondary structure (Fig. 19).

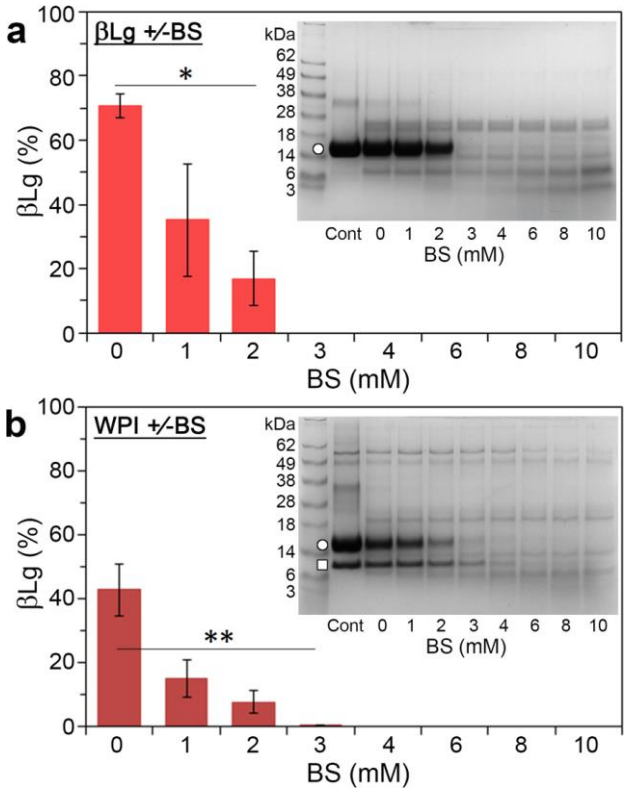

Figure 20. The *in vitro* intestinal proteolysis of (a) pure β-lactoglobulin (βLg) or (b) βLg in whey protein isolate (WPI) is affected by the total concentration of individual bile salts (BS; NaTC and NaGDC, 1:1, mol/mol). The bar graphs display HPLC data for the percentage of βLg that was still intact after 5 min of digestion with trypsin and chymotrypsin (1:1, w/w; total concentration of 0.1 mg/mL) at 37°C (mean ± SD; (a) n = 3, * $P < .01$; (b) n = 5, ** $P < .001$). The SDS-PAGE results that correlate to the HPLC data are also provided (reducing conditions; "Cont" stands for undigested control; ○, βLg; □, α-lactalbumin). These results have been published (Dulko, et al. 2021).

These BS-mediated structural alterations are likely to be the reason for the greatly increased intestinal digestibility of βLg I observed in the *in vitro* proteolysis study (Fig. 20). In the absence of BS (NaTC and NaGDC), the proportion of native βLg that was still undigested after 5 min of incubation with trypsin and chymotrypsin was decreased to 70.5±3.7% of its initial amount before digestion (Fig. 20a). However, when the proteolysis was repeated in the presence of 1 mM BS, the remaining amount of undigested protein was reduced by the factor of two. When the BS concentration was increased to 2 mM, only 16.9±8.3% of the βLg

remained undigested after 5 min. The HPLC analysis also demonstrated that no intact βLg could be seen in digestions carried out at higher concentrations of BS. It was also clear from the steadily increasing intensity of the bands corresponding to peptides ($M_r \leq 6$ kDa) formed during the digestions at increasing concentrations of BS (Fig. 20a) that the proteolysis progress was still BS-dependent at these high BS concentrations ($c \geq 3$ mM). Compared to the purified βLg, the degree of βLg digestion in WPI was higher (Fig. 20b). For instance, following 5-min digestion of WPI at 1 mM BS, 15.1±5.8% of undigested βLg was still present (Fig. 20b), as opposed to 35.2±17.4% in the experiment on purified βLg with the same BS dose (Fig. 20a). However, the control proteolysis experiments (i.e., without BS) also revealed a higher digestibility of βLg in WPI, i.e., 42.7±8.2% remained intact in the experiment on WPI (Fig. 20b) vs. 70.5±3.7% in the experiment on purified βLg (Fig. 20a). Here, the increased susceptibility of βLg in WPI to enzymatic hydrolysis might have been caused by the method through which food-grade WPI is made. βLg can partially denature during the moderate heat-treatment processing used in the conventional manufacturing of WPI, which could result in the observed, higher susceptibility of the protein to the proteolysis. Purified βLg and βLg in WPI have been proven to be more easily digested after they had been heat-treated (Kitabatake & Kinekawa, 1998). However, the extent of protein unfolding and aggregation depends on the heating conditions, which in turn have a significant impact on such a heat-induced enhancement of protein digestibility (Macierzanka et al., 2012). The type and extent of food processing is often an important determinant of protein digestibility (Asensio-Grau, Peinado, Heredia, & Andrés, 2019; Asensio-Grau, Calvo-Lerma, Heredia, & Andrés, 2021). For instance, a previous *in vitro* study of cheese digestion revealed that the properties of the cheese matrix made from cow, sheep, or goat milk were the main factors that affected the gastrointestinal degradation of the protein fraction (Peinado, et al., 2019).

4.1.2. *In vitro* intestinal proteolysis of βLg in the presence of human bile

After analysing how the concentration of individual BS affected protein digestion, I conducted *in vitro* intestinal proteolysis studies with real HB. This aimed to determine whether the BS-mediated impact may also be seen in HB samples that (i) varied in the overall BS contents and (ii) had BS compositions that were more complex than the simple mixture of two individual BS.

I used HB that had been aspirated from patients that suffered from a medical condition affecting the physiological function of the liver, the pancreas, or the bile duct (Tab. 2) and that could impact, therefore, the chemical composition of HB. Selection of this diverse group of patients was intentional as I required HB samples that differed substantially in chemical composition. The concentrations of two important biliary surfactants (BS and PC) have been found to change substantially between the collected HB samples, as revealed by quantitative analysis (Fig. 15d). This made it possible to choose a number of HB samples that would meet the following requirements: (i) different BS concentrations, (ii) comparable and low PC concentrations, and (iii) lack of any residual proteolytic activity (e.g., deriving from contamination with pancreatic proteases). Following the above criteria, three HB samples (i.e., 46(B), 65(B), and 51(A), Fig. 21a) were selected for the *in vitro* intestinal proteolysis experiments. The final concentrations of BS and PC that would be produced in an experimental digestion mixture after the selected HB samples have been applied – which required their 20-fold dilution in a digestion mix (see Section 3.4.1) – are shown in Fig. 21a.

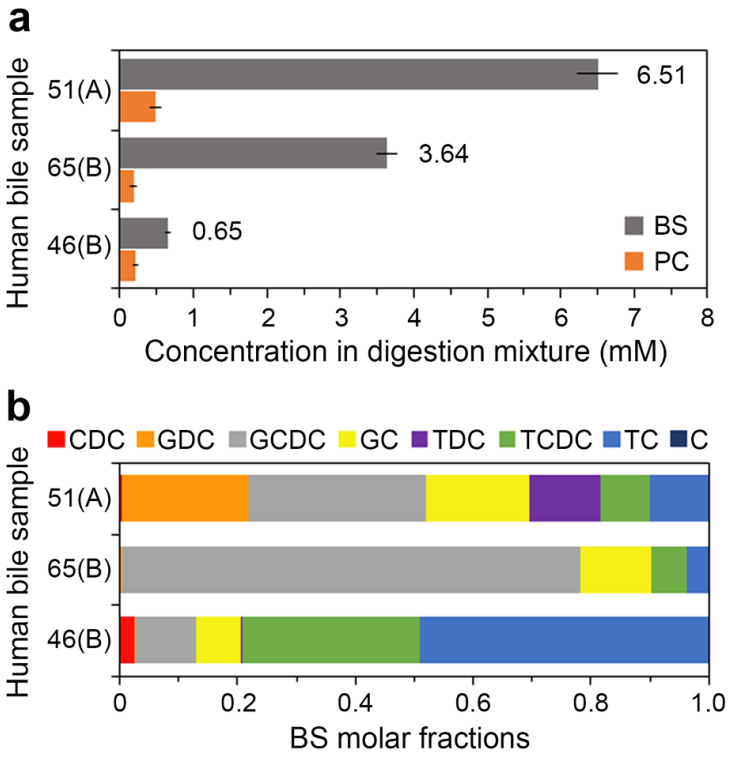

Figure 21. The samples of human bile (HB) utilised for *in vitro* proteolysis experiments. (a) The amounts of total bile salt (BS) and phosphatidylcholine (PC) in the *in vitro* digestion environment with the selected HB samples (i.e., following their 20-fold dilution in a digestion mix). (b) The BS profiles of the HB samples; individual BS molar fractions in total BS examined (chenodeoxycholate, CDC; glycodeoxycholate, GDC; glycochenodeoxycholate, GCDC; glycocholate, GC; taurodeoxycholate, TDC; taurochenodeoxycholate, TCDC; taurocholate, TC; cholate, C). These results have been published (Dulko, et al. 2021).

By choosing those HB samples, I aimed to primarily investigate any potential effects of the total BS content of HB on proteolysis progress and extent. This is why the selected HB samples needed to have low and comparable concentrations of PC (<0.5 mM was obtained in the digestion mix with the HB samples used, Fig. 21a), but it was also crucial that they differed substantially in the total BS concentrations (BS concentrations ranging from 0.65 mM to 6.51 mM were produced in the digestion mix after the selected HB samples had been introduced, Fig. 21a). None of the three HB samples exhibited any proteolytic activity (Fig. 22), which confirmed they had not been contaminated with pancreatic proteases during the bile aspiration.

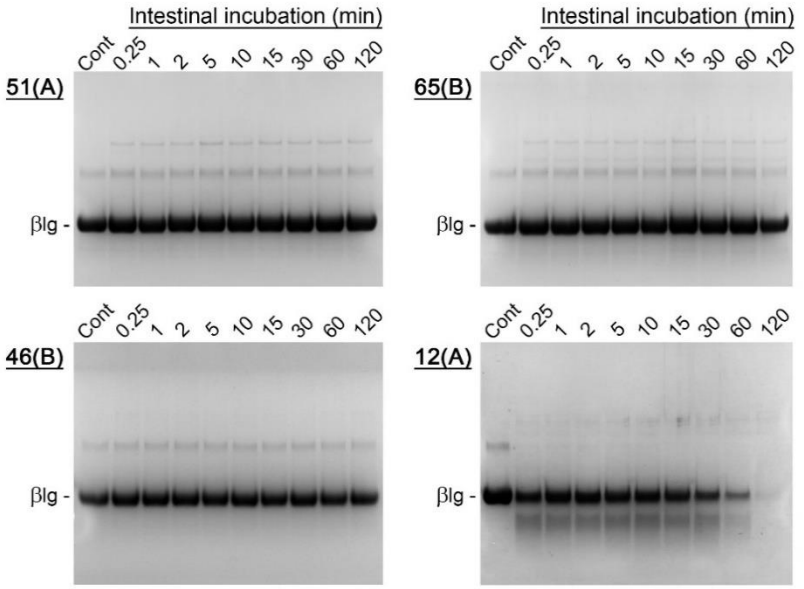

Figure 22. Representative SDS-PAGE analysis (reducing conditions) of purified β-lactoglobulin (βLg) incubated under the intestinal digestion conditions in the absence of enzymes (trypsin and chymotrypsin) but in the presence of selected human bile (HB) samples. The incubation of βLg with HB 51(A), 65(B), or 46(B) caused no change in the intensity of the protein band as compared to the control ('Cont') not incubated with HB. The same concentrations of the protein in the controls and in the protein samples incubated up to 120 min with HB 51(A), 65(B), or 46(B) were confirmed by HPLC (data not shown), which indicated the three HB samples had no proteolytic activity. For comparison, SDS-PAGE analysis of the protein incubation with HB sample 12(A) showed the HB must have been contaminated with intestinal proteases as the βLg band was observed to fade gradually during the incubation. The formation of bands corresponding to peptides with lower M_r than βLg indicates the protein was hydrolysed. These results have been published (Dulko, et al. 2021).

Similar as with the individual BS (Fig. 20), the HB samples were applied in the *in vitro* intestinal digestion of βLg. The amount of purified βLg was reduced to 56.7±8.1% of its original amount (i.e., before digestion) after 2 min of incubation with trypsin and chymotrypsin in the presence of as little as 0.65 mM BS that derived from HB (see Fig. 23a), which was substantially less than the reduction to ca. 80% of intact βLg in the control digestion without HB (Fig. 23a).

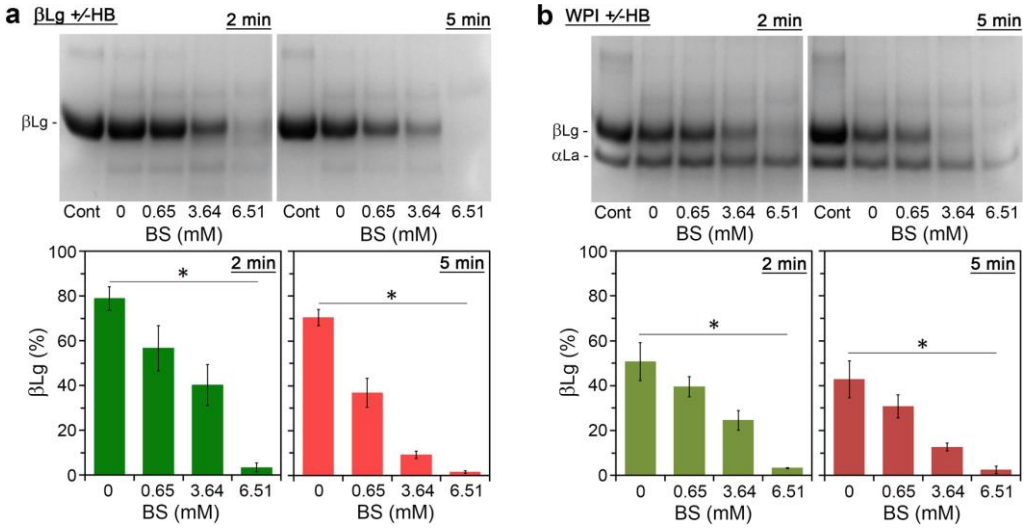

Figure 23. Effect of the total bile salt (BS) content of human bile (HB) on the *in vitro* intestinal proteolysis of either (a) purified β-lactoglobulin (βLg) or (b) β-Lg in whey protein isolate (WPI). The bar graphs show HPLC data (mean ± SD, n = 5; * *P*<.001) for the percentage of βLg that remained intact following 2 min or 5 min digestion at 37°C with trypsin and chymotrypsin (1:1, w/w; total concentration of 0.1 mg/mL) in the absence of HB or in the presence of different concentrations of BS obtained with various HB samples (see Fig. 21a). The relevant SDS-PAGE results (reducing conditions; "Cont" denotes undigested control; "αLa," α-lactalbumin) are provided along with the HPLC data. The results have been published (Dulko, et al. 2021).

The protein was hydrolysed more thoroughly when the HB samples with larger BS concentrations were used; after the 2-min proteolysis, there was 40.2%±9.1% or only 3.5%±2.0% of undigested βLg left when applying 3.64 mM BS or for 6.51 mM BS, respectively (Fig. 23a), delivered with different HB samples (see Fig. 21a). Extending the digestion to 5 min increased the degree of hydrolysis (Fig. 23a). When employing HB samples with increasing concentrations of BS, experiments on WPI demonstrated a very similar trend of the BS-depended digestibility of βLg (Fig. 23b). However, compared to the purified βLg (Fig. 23a), the degree of hydrolysis was generally greater. SDS-PAGE revealed that trypsin and

chymotrypsin appeared to impact α-lactalbumin less than βLg under the *in vitro* digestion conditions applied (Fig. 23b).

The trend seen in Fig. 23 of an increasing extent of βLg hydrolysis upon increasing the BS content in HB is similar to what is seen in Fig. 20 for the proteolysis experiment with increasing concentrations of individual BS. This is despite the fact that the employed, individual BS consisted of an equimolar mixture of just two BS (NaTC and NaGDC), whereas the three HB samples varied considerably from one another in terms of both the BS profiles and the total BS concentration (Fig. 21). This implies that in order to facilitate the intestinal digestion of protein, the total BS concentration of HB might be more important than its BS composition. However, there was a noticeable difference in the extent of βLg proteolysis between experiments with individual BS and HB – a lower concentration of individual BS, relative to the BS concentration delivered with HB, was required to exert a similar effect on protein digestibility. For example, 15.1±5.8% of intact βLg remained after 5 min of WPI digestion in the presence of just 1 mM concentration of individual BS (Fig. 20b), but 12.6±1.8% of undigested βLg remained after 5 min of WPI digestion in the presence of 3.64 mM BS from HB (Fig. 23b). In the experiments involving the individual BS, no intact βLg remained after increasing the BS concentration >3 mM (Fig. 20b). Similar differences in the degree of digestion were also observed for proteolysis of purified βLg (Fig. 20a vs. Fig. 23a; 5 min digestions).

In order to examine this effect more closely, I repeated the intestinal proteolysis of βLg with HB sample 65(B) (i.e., at 3.64 mM BS concentration created by the HB) as well as with the individual BS used at the total concentration of 3.64 mM in the digesting mix. The duration of the digesting experiment was up to 120 min (Fig. 24).

The lack of any signs of hydrolysis of the protein in the blank tests (i.e., without enzymes but with HB or individual BS) confirmed there was no proteolytic activity in such control digestion environments (Fig. 24a,b). When the intestinal proteases were used in the absence of BS, βLg gradually degraded, and after 60 min of digestion just a faint band of the protein could be visible on the SDS-PAGE gel (Fig. 24c). Addition of the HB that delivered 3.64 mM BS to the digestion mix reduced this time to 15 min (Fig. 24d). However, substituting the HB with 3.64 mM of individual BS substantially accelerated the proteolysis, and the SDS-PAGE revealed no intact βLg in the samples after 5 min of intestinal digestion (Fig. 24e). The

difference in the way an *ex vivo* HB and a mixture of individual BS can contribute to intestinal proteolysis was further explored in the *in vitro* gastrointestinal digestion model.

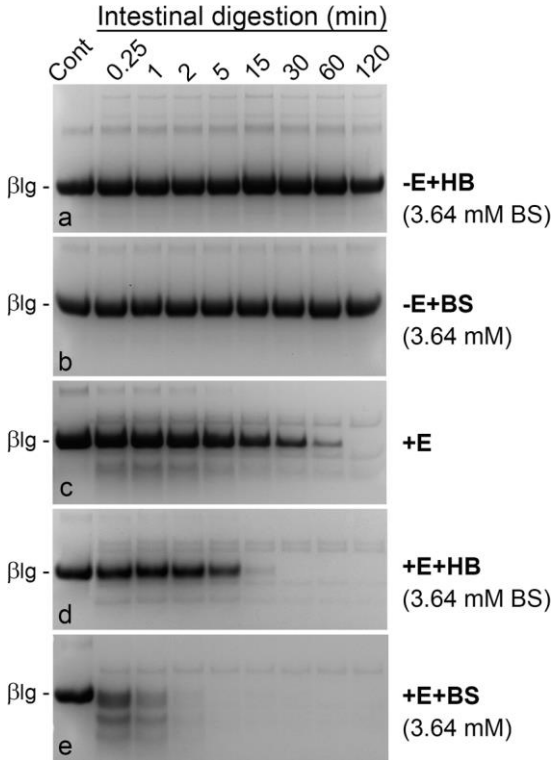

Figure 24. Representative SDS-PAGE analysis (reducing conditions) of the *in vitro* intestinal proteolysis of purified β-lactoglobulin (βLg) in the presence or absence of 3.64 mM individual bile salts (BS; NaTC and NaGDC, 1:1, mol/mol), or human bile (HB) providing 3.64 mM BS (HB sample no. 65(B), see Fig. 21). (a,b) Incubation of the protein under the intestinal digestion conditions in the absence of enzymes (-E) and in the presence of HB (a) or individual BS (b). (c–d) Intestinal proteolysis with trypsin and chymotrypsin (+E), and in the absence of BS (c), or in the presence of either HB (d) or individual BS (e). 'Cont' refers to undigested control. These results have been published (Dulko, et al. 2021).

4.1.3. *In vitro* gastrointestinal proteolysis: Simulating the impact of human bile by a mixture of individual bile salts and phospholipids

After analysing the impact of HB on the extent of proteolysis, I performed a simulated gastric followed by intestinal proteolysis to see if the effect of HB could be replicated with individual BS. This aimed to validate the use of BS as a substitute for difficult-to-obtain HB in *in vitro* simulations of the gastrointestinal proteolysis. I used the gastrointestinal model of proteolysis (Section 3.4.2.) to verify whether applying this more complex *in vitro* digestion protocol would deliver a similar pattern of βLg hydrolysis relative to the one observed in the simpler, intestinal model (Section 3.4.1). If so, it would support the robustness of my results.

This is especially important due to the fact that using different static *in vitro* gastrointestinal models for the proteolysis evaluation can produce contrasting digestibility results, despite that every *in vitro* model is deemed to be physiologically relevant. This has recently been demonstrated for the proteolysis of several food proteins (Torcello-Gómez et al., 2020).

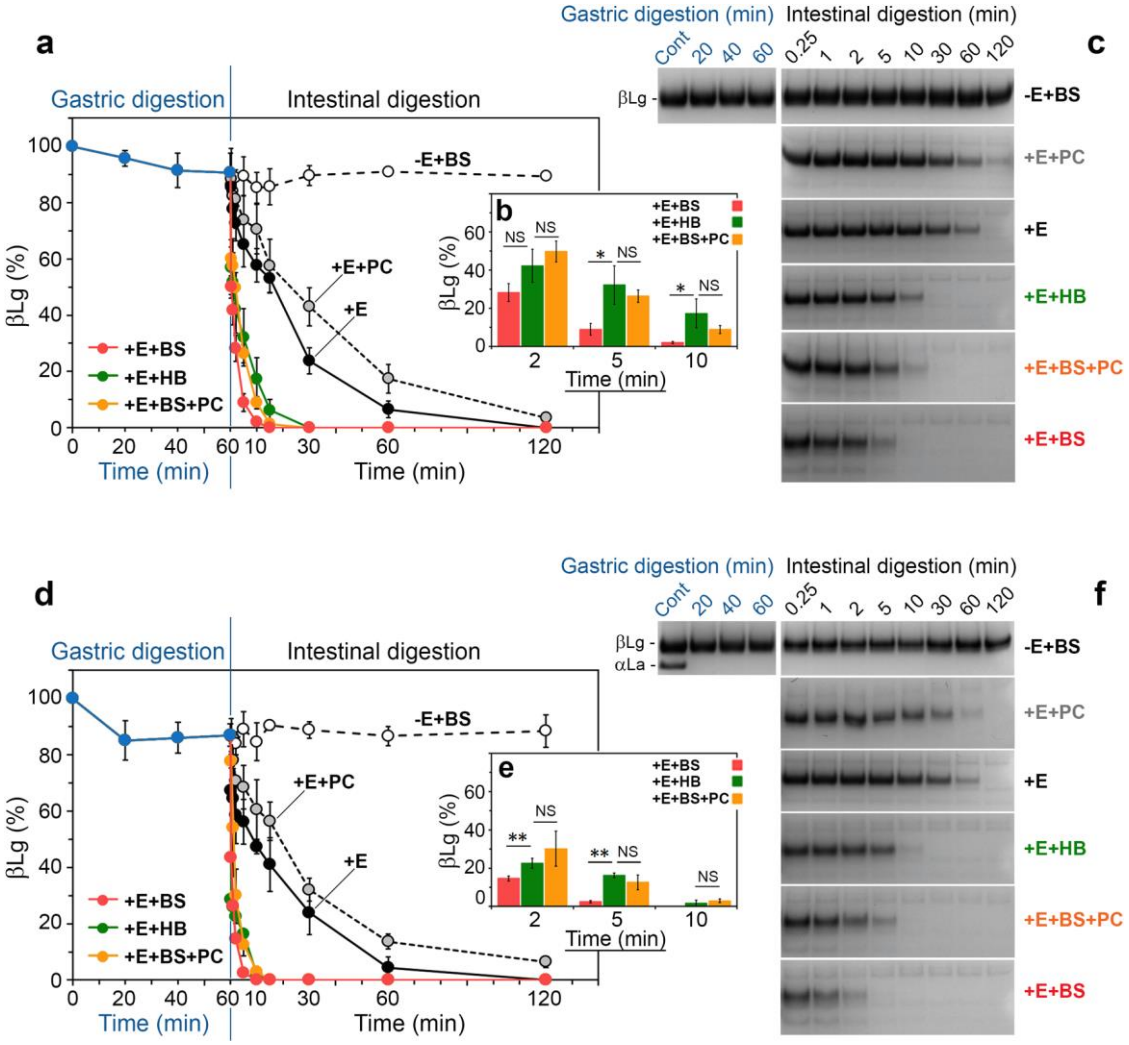

Figure 25. Effect of individual bile salts (BS), phosphatidylcholine (PC), or human bile (HB) on *in vitro* gastrointestinal proteolysis of (a–c) purified β-lactoglobulin (βLg) or (d–f) βLg in whey protein isolate (WPI). HPLC (a, b, d, e) and SDS-PAGE (c, f; reducing conditions) analyses of the digestion time-point samples. The HPLC data (mean ± SD; n = 5) show the percentage of intact βLg remaining in the digestion mix. The gastric phase of digestion was performed with pepsin, whereas the intestinal phase was carried out with trypsin and chymotrypsin (+E), and in the presence (+) or absence of individual BS (NaTC and NaGDC, 1:1, mol/mol; total concentration of 3.64 mM), PC (0.18 mM), or HB (sample no. 65(B) diluted to give 3.64 mM BS and 0.18 mM PC in the digestion mix; see Fig. 21a). Some experiments were also done in the absence of the intestinal enzymes (-E). (b,e) * P<.05; ** P<.01; NS, not significant (P>.05). (c,f) 'Cont' refers to undigested control; αLa, α-lactalbumin. These results have been published (Dulko, et al. 2021).

Both, the purified βLg and the food-grade WPI underwent a gastric phase of digestion with pepsin before the intestinal phase was carried out under various conditions (see Section 3.4.2.). HPLC analysis of the time-point samples obtained during the digestion of the purified βLg revealed that approximately 90% of the protein remained intact after 60 min pepsinolysis (Fig. 25a). This high resistance of native βLg to pepsin is in accordance with earlier research (Kitabatake & Kinekawa, 1998; Mandalari, Adel-Patient, et al., 2009) and is most likely due to the burial of potential cleavage sites between specific amino acids of the protein in the folded calyx structure of β-strands (Reddy, Kella, & Kinsella, 1988). The amount of intact, post-gastric βLg remained constant for the whole duration of the following intestinal phase of digestion (120 min) if it was done under control conditions, i.e., with individual BS but without the intestinal proteolytic enzymes (Fig. 25a; '-E+BS'). When the protein was subjected to trypsin and chymotrypsin in the absence of BS (Fig. 25a; "+E"), the results showed that βLg was gradually hydrolysed, leaving only 6.5±2.9% of undigested protein in the system after 60 min of the intestinal hydrolysis. However, when the proteolysis was repeated in the presence of BS, βLg was hydrolysed quickly and fully during the first 10-15 min of the intestinal phase of digestion (Fig. 25a; '+E+BS'). In addition to enhancing the extent of proteolysis, the presence of BS may have also affected the profile of peptides formed from βLg during the digestion with trypsin and chymotrypsin. The HPLC chromatograms obtained for the digestion time-point samples showed different patterns of the peptides produced in the absence relative to the presence of BS in the digestion environment (Fig. 26).

This general pattern of increased proteolysis in the presence of BS is in line with the SDS-PAGE results of the previous, simpler intestinal model of digestion (Fig. 24) and is most likely due to the partial denaturation of βLg by the BS (Fig. 19), which may have made the protein more susceptible to the intestinal proteases.

In order to directly compare the results obtained with the individual BS with results seen in the presence of HB sample 65(B), a 3.64 mM concentration of the individual BS was used in the gastrointestinal digestion mix – similar to what was employed in the initial assessment of the intestinal proteolysis (Section 4.1.1.). According to the HPLC and SDS-PAGE results, switching from individual BS to HB made βLg less vulnerable to the digestive enzymes (Fig. 25a–c; "+E+BS" vs. "+E+HB"). The observed discrepancy might have resulted from the presence of other components of HB, such as phospholipids, which could influence the

protein digestibility. Using the HB sample 65(B) in the digestion mix meant that, on top of 3.64 mM BS, 0.18 mM concentration of phosphatidylcholine (PC) was delivered with the HB (Fig. 21a). This meant that PC had a greater molar concentration than βLg, for which it was approx. 0.05 mM. When these exact PC and BS concentrations were replicated in the digestion environment with individual BS and egg yolk PC (Fig. 25a, '+E+BS+PC'), the protein hydrolysis extent was reduced compared to the experiment conducted only in the presence of individual BS (Fig. 25a, '+E+BS'). Importantly, statistical analysis showed that the addition of PC was essential in adjusting the protein digestibility, so that it did not differ substantially (P>.05) from that recorded in the presence of HB (Fig. 25b). This might have been because of the PC interacting with βLg and/or due to complexation of PC with BS, which would render some BS molecules unavailable to interact with βLg, as discussed below.

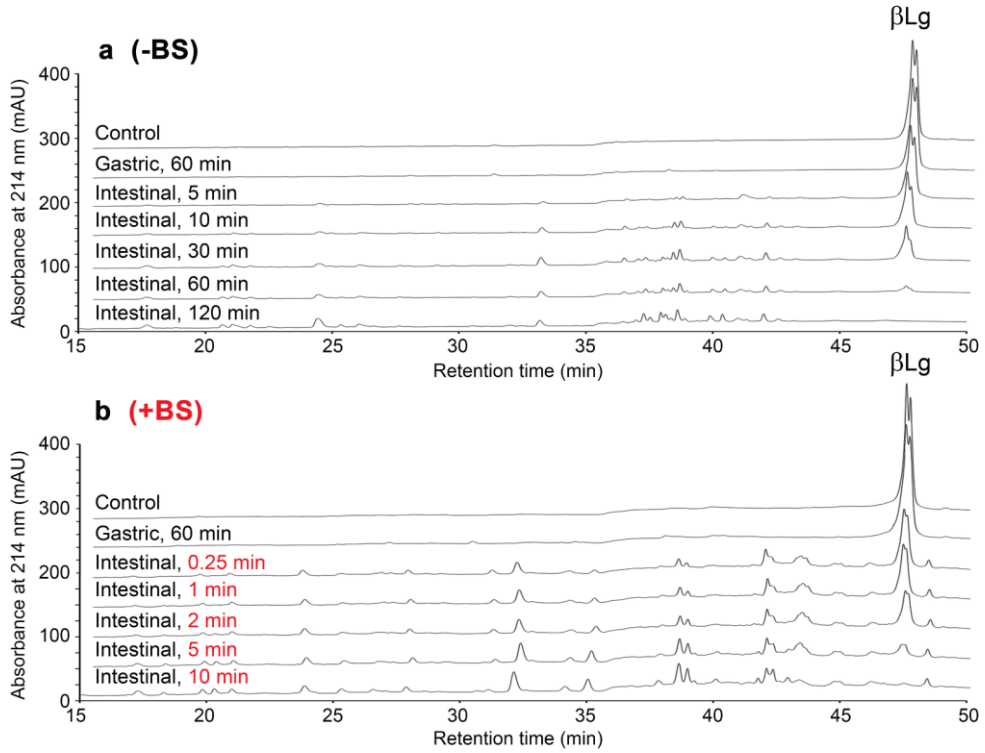

Figure 26. Representative HPLC chromatograms of undigested protein (purified β-lactoglobulin (βLg); 'Control') and the *in vitro* gastrointestinal digestion time-point samples. The *in vitro* gastric digestion of βLg with pepsin (60 min) was followed by the intestinal digestion with trypsin and chymotrypsin (up to 120 min), which was carried out in the absence (a) or presence (b) of individual bile salts (BS; NaTC and NaGDC, 1:1, mol/mol; total concentration of 3.64 mM). Formation of a range of proteolysis products can be observed for retention times ≤45 min. The results have been published (Dulko, et al. 2021).

In addition to bile salts, phospholipids are another substantial class of highly surface-active molecules in human bile; while cholesterol is the main sterol and very little diglycerides, triglycerides, or fatty acids are present in the bile (Boyer, 2013). PC is the main phospholipid of human bile – the previous study showed that it accounts for ca. 95% of the biliary phospholipids (Gilat & Sömjen, 1996). In this study, the HPLC-ELSD analysis revealed that the PC concentrations in the HB samples used were considerably lower than the relevant total BS concentrations (Fig. 21a). In addition, phosphatidylethanolamine was not detected in the HB samples (Fig. 27), which confirmed the abovementioned finding of PC being the most abundant phospholipid in human bile.

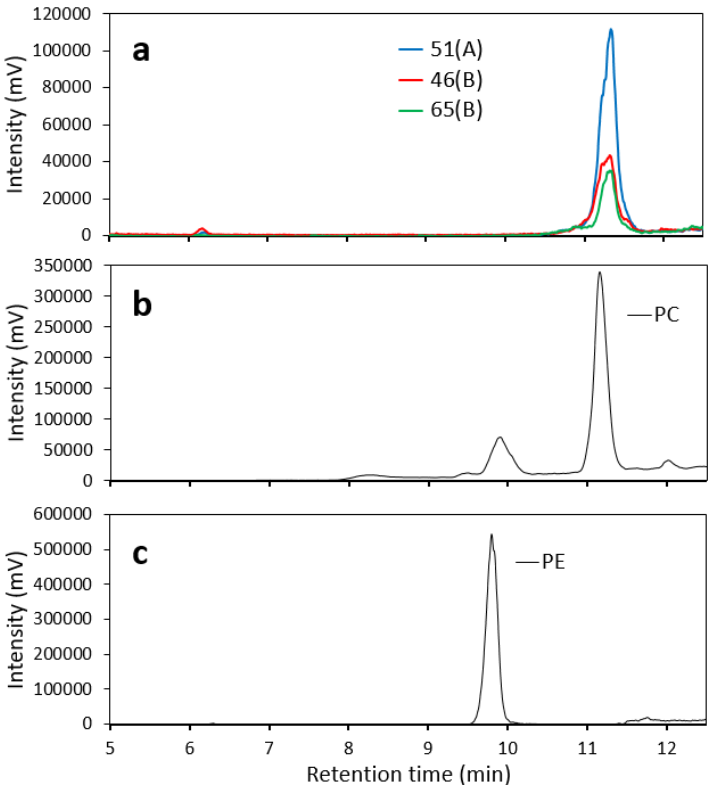

Figure 27. HPLC-ELSD analysis of human bile (HB). (a) Representative chromatograms of HB samples 51(A), 65(B) and 46(B), analysed for the presence/concentration of phosphatidylcholine (PC) and phosphatidylethanolamine (PE). Phospholipids were identified by retention times matching with PC and PE standards (b and c, respectively). The concentrations of individual phospholipids in HB were determined from a calibration curve, as explained in Section 3.2. The results have been published (Dulko, et al. 2021).

The influence of PC on the resistance of bovine βLg to *in vitro* gastrointestinal proteolysis has previously been investigated (Mandalari, Mackie, Rigby, Wickham, & Mills, 2009; Bossios et al., 2011). It has been found that PC was able to reduce the extent of protein hydrolysis by trypsin and chymotrypsin. It has been suggested the effect was brought about by monomeric PC binding to a secondary fatty acid binding site along the single strand of α-helix in βLg, causing steric hindrance that prevented the cleavage by the intestinal proteases. Several research studies (Berecz et al., 2013; Moreno et al., 2005; Vassilipoulou et al., 2006) have demonstrated that the PC–protein interaction can drastically lower the *in vitro* gastrointestinal digestibility of a number of different globular proteins. The improved stability and rigidity of the protein scaffold provided by the formation of extra hydrogen bonds between the PC ligand and protein have been thought to be related to the lower rate of proteolysis. Incubating βLg (1 mg/mL) with PC (2.32 mg/mL) showed no direct impact on the protein secondary structure, according to a previous study that used far-UV CD spectroscopy (Maldonado-Valderrama et al., 2011). However, if βLg had been incubated with PC and BS (7.4 mM) under *in vitro* gastrointestinal conditions, the lipid appeared to prevent the protein from structural reorganisations that could otherwise be recorded after exposing βLg to BS alone. In my present study, a similar CD experiment was carried out, but with a total 3.64 mM concentration of the individual BS (NaTC and NaGDC) and 0.18 mM PC (Fig. 19) in order to represent the BS and PC concentrations produced in the digestion mix with the HB sample 65(B) (Fig. 21a). The protein structure, when incubated with PC alone, was not altered, even if the PC concentration was increased to 0.5 mM (Fig. 19). However, in the experiment with BS and PC, 0.18 mM PC was enough to prevent structural alterations of βLg brought about by BS. The protein was only partially denatured after being treated with the BS on its own (Fig. 19). As suggested in the previous study (Maldonado-Valderrama et al., 2011), the underlying mechanism might have involved either (i) non-specific interactions of PC with the protein, which reduced the denaturing effect of BS, or (ii) a reduction in the concentration of monomeric BS due to binding of the BS and PC into mixed micelles, which decreased the number of monomeric BS molecules available for interacting with βLg. The protective effect of PC has been confirmed also under the *in vitro* intestinal proteolysis conditions applied in my work. The concentrations of undigested βLg were consistently greater in the time-point samples taken during the proteolysis in the presence of PC (Fig. 25a, '+E+PC') than in the digestion without PC (Fig. 25a, '+E').

Interaction of emulsified triglycerides with BS and/or PC can also affect the digestion of proteins. According to previous *in vitro* proteolysis studies, interfacial adsorption appears to give rise to a pepsin-susceptible form of βLg in protein-stabilised emulsions (Macierzanka et al., 2009; Sarkar et al., 2009) – only about 40% of βLg has been observed to remain intact in emulsion after 60 min of pepsinolysis relative to >90% intact protein in a control experiment, where βLg was exposed to pepsin in solution (Macierzanka et al., 2009). The remaining, adsorbed βLg was quickly removed from the interface by the BS present in the digestion mix in a subsequent, duodenal stage of digestion described in that research, and the protein was fully hydrolysed in the aqueous phase of emulsion by trypsin and chymotrypsin within 30 min. However, in the presence of BS and PC, the intestinal proteolysis was reduced, and after 30 min there was >30% undigested βLg in the digestion environment (Macierzanka et al., 2009). It has been proposed that, after βLg is removed from the interface, the protection can be caused by the ability of the protein to interact with PC in an aqueous solution (Mandalari, Mackie, et al., 2009).

Other lipids that are present in the intestinal lumen can modify intestinal proteolysis too. A combined effect of a mixture of conjugated BS (12 mM) with monoglycerides (monoolein; 6 mM) and fatty acids (oleic acid; 12 mM) on simulated duodenal proteolysis of βLg has been studied by Gass and co-workers (Gass et al., 2007). That lipid composition was used to simulate the mixture of the small intestinal lipolysis products with the biliary surfactants – BS – that together would be able to form mixed micelles in the simulated postprandial small intestine. The SDS-PAGE examination of a control experiment (i.e., conducted solely in the presence of 12 mM BS) has demonstrated that during the first 5 min under the *in vitro* duodenal conditions, trypsin and chymotrypsin were able to completely hydrolyse βLg (Gass et al., 2007). It has also been found that this enhancing effect of BS was significantly attenuated after monoglycerides and fatty acids had been introduced into the digestion mixture, although protein degradation was still accelerated relative to proteolysis performed in the presence of trypsin and chymotrypsin alone. According to the authors of that cited study, the attenuation effect could be explained by the competition for BS incorporation into the mixed micelles that might have reduced the concentration of free BS available to interact with βLg molecules.

In my research, gastrointestinal digestion experiments were also performed on WPI (Fig. 25d–f). In general, all the above conclusions from the results obtained for purified βLg (Fig.

25a–c) also apply to the digestion of βLg with WPI. However, the relative concentrations of undigested βLg in the WPI samples assessed at different stages of the gastrointestinal proteolysis (Fig. 25d,e) were up to 15–20% lower than those observed in corresponding experiments on purified βLg (Fig. 25a,b). This effect was consistent with or without BS, PC, or HB. The most probable explanation is the aforementioned, higher susceptibility of βLg to the enzymatic action of proteases caused by the production process of food-grade WPI that involves limited denaturation of some βLg molecules. Another clear effect was the rapid hydrolysis of αLa during the gastric proteolysis by pepsin (Fig. 25f). Unlike βLg, αLa is known for its high susceptibility to digestion by pepsin (Sah, McAinch & Vasiljevic, 2016).

In my study, the *in vitro* digestibility of other milk proteins has also been evaluated for comparison with βLg. Purified β-casein as well as a food-grade casein concentrate (sodium caseinate) and a casein food supplement (Micellar Casein) were placed through the gastric followed by intestinal proteolysis, according to the procedure outlined in Section 3.4.2. As expected, in all three cases, the caseins were fully hydrolysed by pepsin during the first 10–20 min of the gastric digestion (Fig. 28), and only low molecular weight peptides were transferred to the intestinal phase of digestion for further hydrolysis under the simulated intestinal conditions (data not shown). Interactions of the peptides with BS or PC were not studied. The fact of the caseins expressing low resistance to pepsin is well-documented in the scientific literature (Mandalari, Adel-Patient, et al., 2009; Dupont et al., 2009; Böttger et al., 2019). This is because the enzyme has a preference of cleaving loosely structured polypeptides, which are typical of caseins (Dupont & Tomé, 2020). The results for digestibility of caseins presented in my report are very much in line with those earlier findings.

Together, my results and the findings of the other studies mentioned above suggest that the extent of βLg proteolysis can be influenced by the presence of BS and other polar lipids, such as phospholipids, in the aqueous environment of intestinal digestion. However, to my knowledge, this is the first time that the significance of taking into account a combined influence of two key surface-active components of human bile – BS and PC – on the progress of gastrointestinal proteolysis has been demonstrated. This is also the first time when analogous effects have been shown for a real HB and a BS/PC mixture, the latter being applied in order to simulate the bile. The results obtained in this study can validate the usage

of a mixture of individual BS and PC as a human-relevant alternative to real HB for future *in vitro* proteolysis experiments.

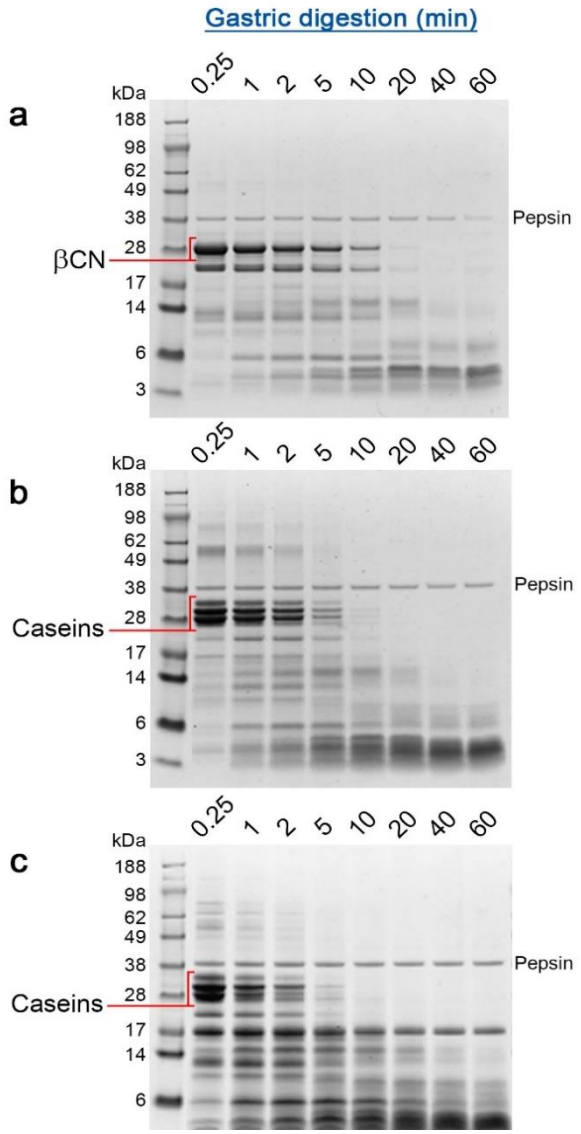

Figure 28. Representative SDS-PAGE analysis (reducing conditions) of simulated gastric pepsinolysis of (a) β-casein (βCN), (b) sodium caseinate, and (c) Micellar Casein food supplement. The results have been published (Dulko, et al. 2021).

The data gathered in my study also suggest that using mixtures of individual BS and PC may be a more convenient solution than using animal bile (e.g., fresh bovine or porcine bile, or commercially available bile extracts) for simulating the impact of HB on gastrointestinal proteolysis. Animal bile extracts have widely been used in *in vitro* digestion models because they are thought to reflect the complexity of the BS profile in HB and are advised to be used in quantities sufficient to achieve a predefined total BS concentration (Brodkorb et al., 2019).

Much less attention has been paid to other ingredients (such as phospholipids) that are introduced to the digestive environment with such animal bile formulations. My findings suggest that, at least for the proteolysis of βLg, it is both – the BS/PC ratio and the overall BS concentration – that define the extent of digestion process and is important for replicating the physiological influence of HB. Applying individual BS and PC allows for a straightforward and accurate control of the BS/PC ratio.

The results presented in Section 4.1 and other related contents have been published in research article:

Dulko, D., Staroń, R., Krupa, L., Rigby, N.M., Mackie, A.R., Gutkowski, K., Wasik, A., & Macierzanka, A. (2021). The bile salt content of human bile impacts on simulated intestinal proteolysis of β-lactoglobulin. Food Research International, 145, 110413

4.2. *In vitro* lipolysis: Emulsion study

4.2.1. Effect of the concentration of individual bile salts on *in vitro* intestinal lipolysis in emulsion

Before investigating any influence of the BS content of human bile (HB) on the lipolysis progress, I first focused on how the presence and the concentration of individual BS affected the extent of TG hydrolysis in the emulsion used. Intestinal lipolysis is an interfacial enzymatic reaction carried out by the pancreatic lipase adsorbed onto the TG-water interface, and the rate of TG conversion to MGs and FFAs has been shown to largely depend on the emulsion droplet size, and thus the overall interfacial area available for the enzyme action (Armand et al., 1992), (Torcello-Gómez, Maldonado-Valderrama, Martín-Rodríguez, & McClements, 2011), (J. Li, Ye, Lee, & Singh, 2012). The mean droplet size of the oil-in-water emulsion used in my study was 736±82 nm.

After 2h of intestinal lipolysis under control conditions (i.e., with pancreatin but in the absence of BS), 30.6±0.7% of FFAs was released from the TG substrate (Fig. 29), although the majority (ca. 25%) was produced within the first 30 min. This is an expected result as the digestion mixture did not contain BS that could effectively solubilise the surface-active lipolysis products from the interface, potentially limiting the lipolysis progress after the initial saturation of the interface with the lipolysis products. Thus, the interfacial mechanism of the likely product inhibition of the enzymatic reaction might have been similar to what had been reported by Pafumi et al. (Pafumi et al., 2002) for the gastric lipolysis of lipid droplets, where the FFAs and MGs produced during the lipolysis accumulated at the droplets' surface and diminished the access of gastric lipase to the TG substrate, effectively retarding further production of FFAs.

In the next step, I looked at whether and how increasing the concentration of BS can influence the extent of lipolysis. An equimolar mixture of two individual BS (NaTC and NaGDC) was utilised as these BS had been used before in numerous studies on simulated intestinal proteolysis, lipolysis and transmucosal transport, with assumption they could reliably mimic physiological effects of human bile in the small intestine (Moreno, Mackie, & Mills, 2005), (Dupont et al., 2009), (Chu et al., 2009), (Böttger et al., 2019), (Krupa et al., 2020), (Macierzanka, Mackie, & Krupa, 2019). However, the HB-relevance of applying the two individual BS in *in vitro* lipolysis studies has not been validated so far.

In this study, I used a broad concentration range of the individual BS (2.5–15 mM) to reflect the varying physiological concentrations of BS in the adult human small intestine. The concentration range of 0.57–6.0 mM has been reported for the fasting state (Bourlieu et al., 2014). Here, my main focus was on mimicking the postprandial conditions, where the total BS concentration in the luminal content is, in general, higher (8–16 mM according to (Bourlieu et al., 2014)). Other authors have also reported the postprandial BS concentration to be well above 3 mM in adult humans (Sjövall, 1959), (Hernell, Staggers, & Carey, 1990), (Lindahl, Ungell, Knutson, & Lennernäs, 1997). The Infogest *in vitro* digestion protocols (Minekus et al., 2014), (Brodkorb et al., 2019) recommend applying 10 mM BS for the small intestinal digestion experiments to reflect "the typical concentration in the fed state" in the younger adult (<65 years), and a reduced concentration of 6.7 mM for the older adult (>65 years) digestion model (Menard et al., 2023).

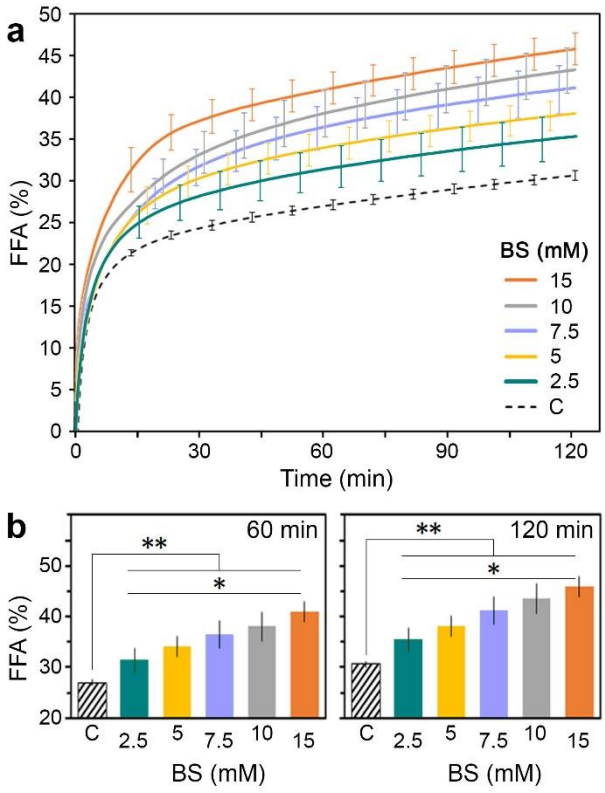

Figure 29. (a) Effect of the total concentration of individual bile salts (BS; NaTC and NaGDC, 1:1, mol/mol) in the digestion mix on the *in vitro* intestinal lipolysis progress: the amount free fatty acids (FFA) released from TG emulsion as a function of digestion time (mean ± SD; n = 3). Control digestion experiments (C; mean ± SD, n = 3) were done in the absence of BS. (b) The lipolysis progress after 60 and 120 min; * $P<0.05$, by ANOVA; ** $P<0.01$, by Student's *t* test.

According to the data presented in Fig. 29, addition of BS to the digestion mix resulted in more substantial conversion of TGs to FFAs. For the lowest BS concentration used (2.5 mM), the amounts of produced FFAs reached 31.4±2.4% and 35.4±2.8% after 60 and 120 min of lipolysis, respectively, which was significantly more (P<0.01) than in the control experiment, i.e., in the absence of these physiological surfactants (Fig. 29b). Further increase in concentration of the BS introduced to the digestion environment (5–15 mM) yielded a progressive increase in the overall conversion of TGs to FFAs. The extent of the FFA release was proportional to the BS concentration across the entire BS concentration range tested (2.5–15 mM, P < 0.05; Fig. 29b). By applying the highest BS concentration (i.e., 15 mM) it was possible to increase the lipolysis extent by approx. 50% relative to the control conditions (e.g., 45.8±1.9 vs 30.6±0.7% of FFAs released after 120 min, Fig. 29).

The positive effect of increasing BS concentrations on enhancing the lipolysis extent has been demonstrated previously (Sarkar, Ye, & Singh, 2016), (Calvo-Lerma, Fornés-Ferrer, Heredia, & Andrés, 2019). My objective here was (i) to verify this anticipated trend under the specific experimental conditions employed in this study, and (ii) to produce a purified-BS benchmark of lipolysis progress for the comparison against any impact caused by real HB samples with varying BS contents.

4.2.2. *In vitro* emulsion lipolysis in the presence of human bile

Following the analysis of the impact of individual BS on lipid digestion, I conducted *in vitro* intestinal lipolysis experiments using real human bile (HB) to explore whether the observed BS concentration-mediated effect could be replicated for HB samples with (i) varying total BS contents and (ii) distinct complexities of BS composition.

As explained in Sections 3.7 and 3.1., I collected HB samples from patients with diverse health conditions that could influence bile composition. Based on the analysis of the major biliary surfactants, BS and PC (Fig. 15d), I selected for this *in vitro* lipolysis study three HB samples with contrasting BS contents. It was necessary the chosen HB samples had low and comparable PC concentrations (ca. 0.5–0.7 mM PC was eventually produced in the digestion environment after a 10-fold dilution of HB in the digestion mix, Fig. 30a), so I could primarily investigate the potential impact of the BS content of bile on lipolysis. As required, the three HB samples differed considerably in total BS concentrations (ranging from 4.16 mM to 7.43

mM when in the digestion mix, Fig. 30a). They also showed a striking difference in BS composition, e.g., HB–5.35 was dominated by GCDC, whereas in the other two HB samples the content of GCDC was balanced by other BS species, especially TC and TCDC in HB–4.16, and GC and GDC in HB–7.43 (Fig. 30b). The selected HB samples also met the requirement of having no, or very limited, proteolytic and lipolytic activities (Tab. 3, Fig. 31), confirming they were essentially not contaminated with pancreatic enzymes during collection.

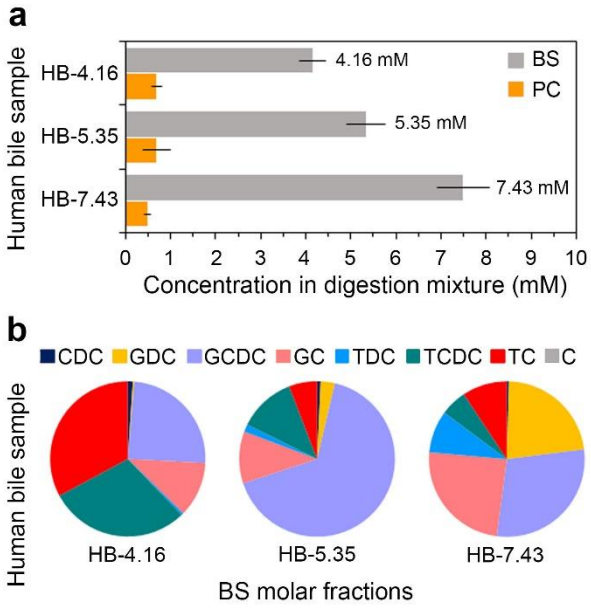

Figure 30. The human bile (HB) samples selected for the *in vitro* lipolysis study in emulsion. (a) Total bile salt (BS) and phosphatidylcholine (PC) concentrations obtained in digestion mixture with the individual HB samples (i.e., after their 10-fold dilution in the digestion mix). (b) BS profiles of the HB samples; individual BS molar fractions in the total BS tested (chenodeoxycholate, CDC; glycodeoxycholate, GDC; glycochenodeoxycholate, GCDC; glycocholate, GC; taurodeoxycholate, TDC; taurochenodeoxycholate, TCDC; taurocholate, TC; cholate, C).

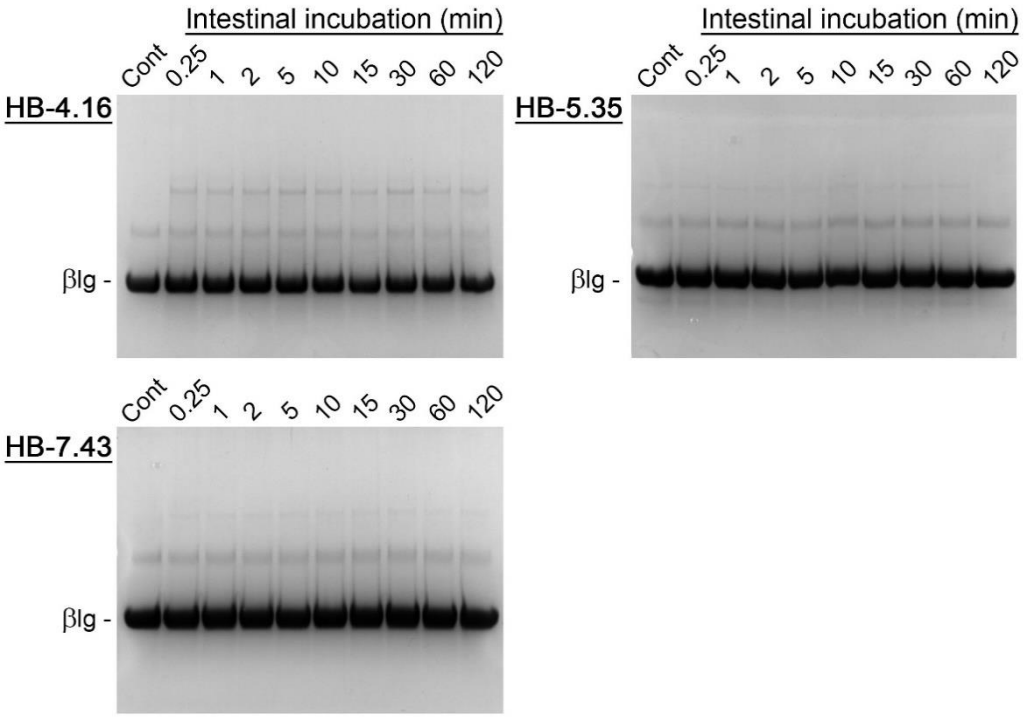

Figure 31. Representative SDS-PAGE analysis (reducing conditions) of purified β-lactoglobulin (βLg) incubated under *in vitro* intestinal digestion conditions without proteolytic enzymes (trypsin and chymotrypsin), but in the presence of selected human bile (HB) samples. The incubation of βLg with HB-4.16, HB-5.35, or HB-7.43 showed no change in the intensity of the protein band compared to the control ('Cont') not incubated with HB. HPLC analysis confirmed the same protein concentrations in the controls and the protein samples incubated up to 120 min with HB-4.16, HB-5.35, or HB-7.43 (data not shown), indicating that these three HB samples had no proteolytic activity.

Similar to the experiments with individual BS (Fig. 29), the chosen HB samples were used in the *in vitro* intestinal lipolysis experiments (Fig. 32). After subjecting emulsified TGs to the digestion conditions in the presence of 4.16 mM BS from HB, the amounts of liberated FFAs reached 32.2±2.6% and 36.8±2.7% after 60 and 120 min, respectively; significantly more (P<0.01) than in the control digestion without HB (Fig. 32b). As the HB samples contained higher concentrations of BS, the enhancement of the TG hydrolysis became increasingly profound; with 38.8±1.0% of FFAs released after 120 min for HB–5.35, and 41.7±3.0% for HB–7.43. The difference between experiments with various HB samples was significant (P<0.05, Fig. 32b).

The overall effect of significantly heightened TG hydrolysis with an increasing content of BS in HB (Fig. 32) is in line with the observations from the lipolysis experiments involving increasing concentrations of individual BS (Fig. 29). However, it is worth noting that the individual BS consisted of a simple mixture of just two BS (NaTC and NaGDC), while the three

HB samples varied greatly not only in total BS concentration (Fig. 30a) but also in the complexity of BS composition (Fig. 30b). This indicates that the overall BS content in HB may hold more significance than the specific BS composition in facilitating lipid digestion.

I explored this possibility in the final part of my study (Section 4.2.3) by replicating the precise total concentrations of BS introduced into the digestion environment by the HB samples, with the identical BS concentrations achieved through the use of the individual BS.

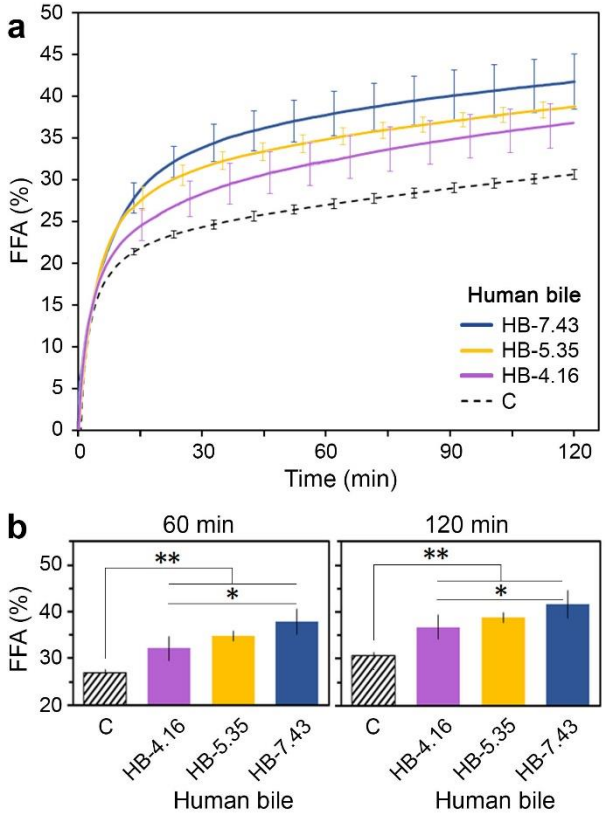

Figure 32. (a) Effect of the total bile salt (BS) content of human bile (HB) on the *in vitro* intestinal lipolysis progress: the amount free fatty acids (FFA) released from TG emulsion as a function of digestion time (mean ± SD; n = 3). The HB samples HB-4.16, HB-5.35 and HB-7.43 were used in quantities that produced 4.16 mM, 5.35 mM or 7.43 mM BS and 0.48–0.69 mM PC in the digestion mix; see Fig. 30a. Control digestion experiments (C; mean ± SD, n = 3) were done in the absence of HB. (b) The lipolysis progress after 60 and 120 min; * P<0.05, by ANOVA; ** P<0.01, by Student's t test.

4.2.3. Simulating the effect of human bile on the emulsion lipolysis extent by mixtures of individual bile salts and phospholipids

After examining the influence of HB on the lipolysis progress, I also explored whether the exact effect of HB could be replicated by using individual BS. The main goal was to validate the suitability of the individual BS as a substitute for a difficult-to-obtain bile in *in vitro*

simulations of the small intestinal lipolysis of emulsified TGs. I conducted the lipolysis experiments using the individual BS in the quantities necessary to precisely replicate the BS concentrations obtained when applying the HB samples (Fig. 30a). This allowed for a direct comparison of the new results obtained with individual BS to the observations made in the presence of corresponding HB samples (Fig. 33).

Replacing HB with the individual BS resulted in variations in the lipolysis progress and extent compared to when HB was present. However, the difference was only significant (P<0.05) for specific time-points of the digestions (Fig. 33b). The observed variance might have been caused by other surface-active components of HB, e.g., phospholipids, which could have impacted the digestibility of TGs. Phospholipids were present in HB but not when the individual BS were applied. As mentioned earlier, apart from BS, phospholipids form another significant group of surfactants in HB (Boyer, 2013), with PC being the most abundant species (approx. 95%) (Gilat & Sömjen, 1996). In the digestion experiments conducted in the presence of HB, 0.48–0.69 mM concentration of PC was introduced to the digestion mix by HB, alongside 4.16 mM, 5.35 mM, or 7.43 mM BS (Fig. 30a). When these precise PC and BS concentrations were replicated in the digestion environment by using egg yolk PC and the individual BS, the extent of lipolysis increased relative to the digestion conducted only with individual BS (Fig. 33). Crucially, the statistical analysis of the results demonstrated that the addition of PC played a decisive role in fine-tuning the digestibility of emulsified TGs, making it highly comparable (P>0.05) to that observed in the presence of HB (Fig. 33b).

Several early studies (reviewed by (Brockman, 2000)) have indicated that the binding of pancreatic lipase to the oil-water interface and subsequent interfacial lipolysis might be partially hindered by phospholipids. However, this inhibition has been suggested to depend greatly on the interfacial composition, particularly in complex systems. For example, lipolysis restoration can be accomplished by fatty acids (e.g., produced *in situ* from TGs during the lipolysis), which enhance the adsorption and catalysis of lipase/colipase in the presence of phospholipids, or through the presence of colipase at the interface, as it forms more effective associations with the lipolysis substrates and products compared to phospholipids, thus increasing the availability of the substrate to the enzyme (Brockman, 2000). The study conducted by Lykidis and co-workers (Lykidis, Avranas, & Arzoglou, 1997) has suggested that phospholipids cannot be definitively classified as inhibitors or activators of pancreatic lipase. When combined with BS, phospholipids can create synergistic effects by forming mixed

micelles, facilitating the solubilisation of lipolysis products and enabling further hydrolysis. In that study, the overall impact on lipase activity was observed to depend on the molar ratio of phospholipid to BS (using dipalmitoylphosphatidylcholine (DPPC, 0–32 mM) and sodium deoxycholate (DOC, 5–35 mM)). Lower ratios (< ca. 0.6) were found to enhance enzyme activity, while higher ratios (> ca. 0.7) resulted in inhibition. However, according to the authors, the presence of DPPC did not considerably modify the enzyme activity when the DOC concentration was as little as 5 mM. In my study, the PC/BS molar ratios generated by either the HB samples or the corresponding mixtures of individual BS and PC were relatively low, ranging from 0.06 to 0.17. The results presented in Fig. 33 demonstrate that in each instance where PC was introduced to the digestion mixture alongside the individual BS (BS/PC mixtures), the addition led to an increase in the lipolysis extent, matching the extent observed with HB. As explained in Section 3.10, I took into account any possible release of small quantities of FFAs from PC due to the action of pancreatic phospholipase in experiments with BS/PC mixtures and HB samples. Therefore, the data included in Figs. 32 and 33 represent solely the release of FFAs from TGs.

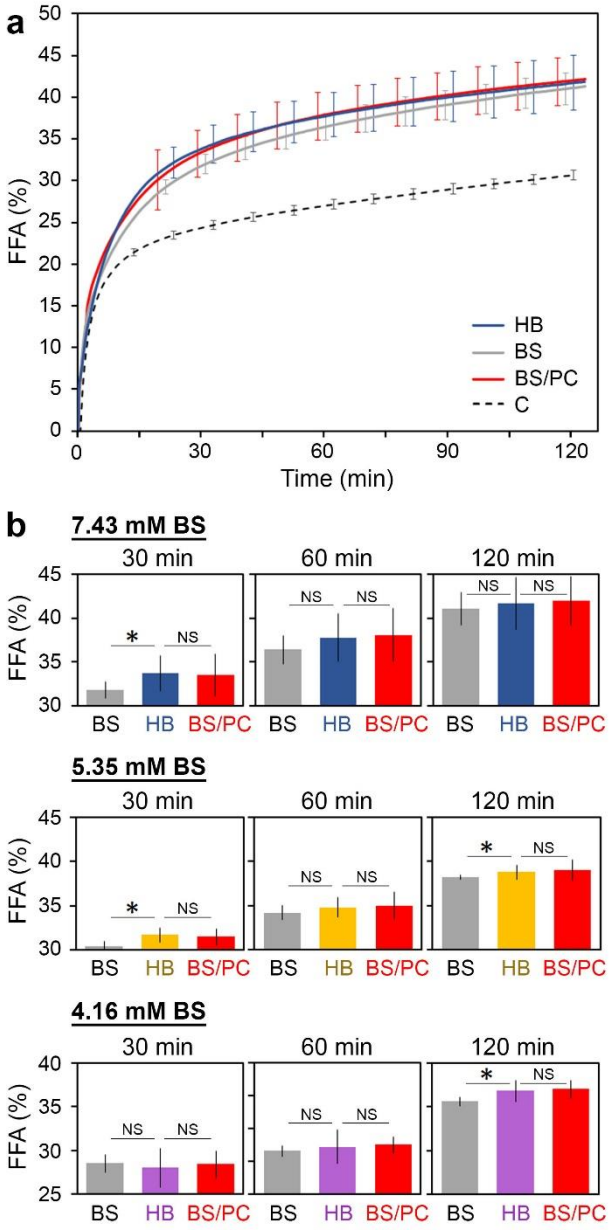

Figure 33. Comparison of the effect of individual bile salts (BS), bile salts/phosphatidylcholine mixtures (BS/PC) or human bile samples (HB) on the release of free fatty acids (FFA) from TG emulsion during the *in vitro* intestinal lipolysis (mean ± SD; n = 3). (a) The HB sample HB-7.43 was used in quantities that produced 7.43 mM BS and 0.48 mM PC in the digestion mix; see Fig. 30a). The HB was then substituted in lipolysis experiments with individual BS (NaTC and NaGDC, 1:1, mol/mol; total concentration of 7.43 mM in the digestion mix, or BS/PC mixture (the individual BS total concentration of 7.43 mM and PC concentration of 0.48 mM in the digestion mix). Control digestion experiments (C) were performed in the absence of HB, BS, or BS/PC. (b) The lipolysis progress after 30, 60, and 120 minutes for different concentrations of BS (7.43 mM, 5.35 mM, and 4.16 mM) achieved with individual BS, HB samples, or BS/PC mixtures (when applying HB samples and BS/PC mixtures, 0.48–0.69 mM PC was also generated in the digestion mix; see Fig. 30a). * P<0.05, NS (not significant, P>0.05), by Student's t test.

My findings, together with the previous research mentioned above, confirm that the BS and phospholipids can influence the extent of intestinal lipolysis. However, this study is the first to demonstrate analogous effects between complex HB and a simple mixture of BS and PC, which was used to mimic bile. My results support the use of a combination of individual BS and PC as a human-relevant substitute for HB in *in vitro* lipolysis studies of TG emulsions.

As mentioned earlier, the surface-active constituents of bile are frequently recommended for *in vitro* simulations of the small intestinal digestion environment. However, these recommendations typically only focus on the source (e.g., fresh bovine or porcine bile, or commercially available animal bile extracts) and/or specific concentrations of BS (Brodkorb et al., 2019), (Menard et al., 2023), (Macierzanka, Torcello-Gómez, Jungnickel, & Maldonado-Valderrama, 2019). Less attention has been devoted to the presence and concentration of other biliary surfactants, such as phospholipids. My findings indicate that the impact of real HB on emulsion lipolysis progress might be influenced not only by the total BS concentration achieved with bile but also by its BS/PC ratio. This ratio can be very accurately controlled by employing individual BS and PC, especially as the need to replicate the complexity of the BS profile of HB seems to be of lesser significance, as suggested by my results. Therefore, the use of mixtures comprising individual BS and PC presents a more convenient approach to simulate precisely the effects of a difficult-to-obtain HB on intestinal lipolysis of TG emulsions compared to relying on animal bile preparations.

The results presented in Section 4.2 and other related contents are being used in the preparation of a research article for publication in a scientific journal.

4.3. *In vitro* lipolysis: Interfacial study

The central objective of this part of my research was to examine the influence of real human bile (HB) on the evolution of oil-water interfacial tension (IFT) during the simulated intestinal lipolysis of triglycerides (TGs). Furthermore, the study aimed to determine if the interfacial behaviour exhibited by complex HB could be replicated through the substitution of HB with simplified combinations of its major surface-active constituents, specifically bile salts (BS) and phospholipids. Achieving this objective would enable a reliable and physiologically relevant *in vitro* simulation of HB using these biliary surfactants, which are commercially accessible and readily obtainable for scientific applications. This holds particular importance, as procuring genuine HB for research requires ethical authorisation, alongside access to advanced clinical facilities and proficient medical practitioners. These requirements often render the acquisition of HB very challenging for scientific purposes.

4.3.1. Analysis of adsorption and desorption at the oil-water interface

Before using HB samples in experiments simulating intestinal lipolysis, I initially examined how their BS contents influenced the oil-water IFT. Additionally, I conducted a comparison of the adsorption-desorption patterns of the selected HB samples with the patterns obtained for individual BS (i.e., an equimolar mixture of NaTC and NaGDC) and for blends of individual BS with phosphatidylcholine (BS/PC). This part of the study aimed to pinpoint any similarities or distinctions in the interfacial behaviour of HB in relation to the individual BS and BS/PC preparations, under the premise that all three analysed systems contained an equal total amount of BS.

In line with the aforementioned information (Sections 4.1. and 4.2.), the mixture of two individual BS, NaTC and NaGDC, was also chosen for this interfacial study, as these compounds have been extensively employed in previous *in vitro* investigations of intestinal digestion and transmucosal transport; it has often been assumed that these BS could effectively replicate the physiological impacts of HB within the small intestine (Moreno, Mackie, & Mills, 2005), (Dupont et al., 2009), (Chu et al., 2009), (Böttger et al., 2019), (Krupa et al., 2020), (Macierzanka, Mackie, & Krupa, 2019). However, the HB-relevance of utilising the two individual BS for investigating *in vitro* lipolysis of TG emulsion has only been examined in my current PhD project (Section 4.2.). The application of PC in the present study

was driven by the fact that this phospholipid represents the most prevalent species of phospholipids in HB (Gilat & Sömjen, 1996), as it was mentioned earlier too.

In this interfacial study, I opted for three distinct HB samples with varying BS contents (HB-2.23, HB-5.35, and HB-7.81; see Section 3.12. for all selection criteria). It was crucial that the chosen HB samples possessed low and comparable PC concentrations – a maximum PC concentration of about 0.5–0.7 mM PC was ultimately generated in the experimental setup following a 10-fold dilution of HB, as illustrated in Fig. 17a. This selection allowed me to primarily explore the potential influence of the BS content of HB on the oil-water IFT. As stipulated, the three HB samples exhibited substantial differences in overall BS concentrations (ranging from 2.23 mM to 7.81 mM when the samples were used in maximum quantities, Fig. 17a). Furthermore, they showcased evident disparities in BS composition. For instance, GCDC was the most abundant BS in HB-5.35, but the content of this BS in HB-2.23 was considerably lower than the individual contents of GC, TCDC, or TC (Fig. 17b). Importantly, the selected HB samples met the prerequisite of having negligible lipolytic and proteolytic activities (Tab. 4 and Fig. 34), indicating the lack of contamination by pancreatic enzymes. This precaution was essential to avoid introducing uncontrolled digestive enzymes with HB, which could have considerably complicated the outcomes of the interfacial examinations.

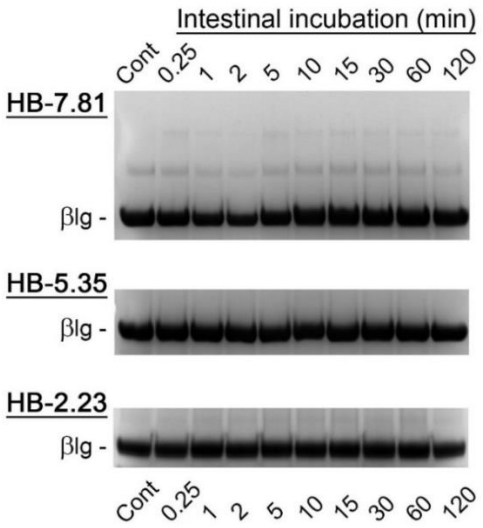

Figure 34. Representative SDS-PAGE analysis (under reducing conditions) of purified β-lactoglobulin (βLg) incubated under *in vitro* small intestinal conditions, following the methodology previously described (Section 3.12.2, and Dulko et al., 2021). Proteolytic enzymes (trypsin and chymotrypsin) were absent, but selected human bile (HB) samples were present. Incubation of βLg for up to 120 min with HB-7.81, HB-5.35, or HB-2.23 demonstrated no discernible alteration in the intensity of the protein band when compared to the control ('Cont'), which was not exposed to HB. HPLC analysis validated identical protein concentrations in both the control samples and the protein samples

incubated with HB-7.81, HB-5.35, or HB-2.23 (data not shown), affirming the absence of proteolytic activity in these three HB samples.

I initially conducted adsorption-desorption experiments for the individual BS and the BS/PC mixtures to examine the impact of increasing BS concentration and the inclusion of PC on the evolution of the IFT. The individual BS and PC were used in quantities that mirrored the total BS and PC concentrations in the selected HB samples (Fig. 17a), as explained in Section 3.14.3. This allowed me to assess the independent effects of these model biliary surfactants and compare them to the influence exerted by real HB.

The sole use of individual BS in the interfacial adsorption experiments led to a rapid decrease in IFT, dropping from 23.5 ± 1.5 mN/m for the plain oil-water interface (as detailed in Section 3.14.2.) to less than 10 mN/m in the presence of individual BS (Fig. 35a). BS are recognised for their high surface activity and have been documented to adsorb rapidly onto interfaces, achieving a stable interfacial tension almost immediately after the formation of a pendant droplet (Maldonado-Valderrama et al., 2008). NaTC and NaGDC have been demonstrated to achieve a stable surface pressure in under 10 s, even at a bulk concentration as low as 1–3 mM (Maldonado-Valderrama, Wilde, Macierzanka, & Mackie, 2011). This very swift adsorption kinetics has been linked to the planar conformation of BS, signifying a substantial affinity of these surfactants for interfaces. In my experiments, the final IFT, recorded after 32 min of adsorption at 37°C, only marginally decreased with increasing the concentration of individual BS from 2.23 mM to 5.35 and up to 7.81 mM (Fig. 36a). Notably, the impact of BS concentration became markedly more pronounced after 10-fold and 100-fold reductions in the BS concentrations (Fig. 36a), indicating that the BS concentration must have fallen well below the CMC. Isothermal titration calorimetry revealed that the CMC of the equimolar mixture of the two individual BS utilised in this study was 3.3 ± 0.4 mM (n = 3; Fig. 37). This explains why the IFT profiles shown in Fig. 35 for the concentrations above the CMC essentially coincide.

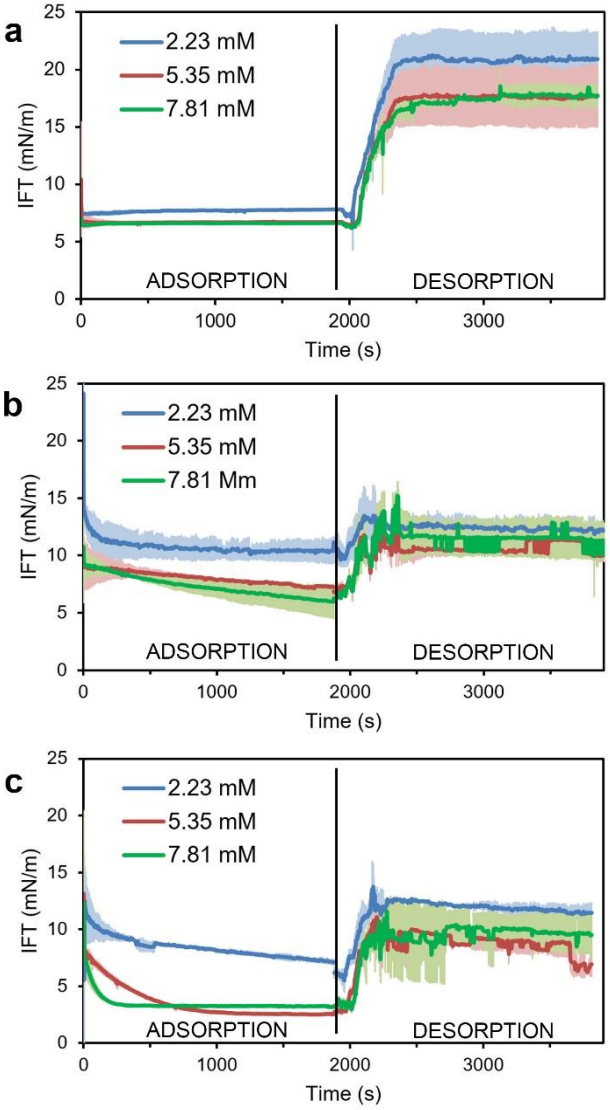

Figure 35. Time-dependent evolution of the sunflower oil–water interfacial tension (IFT) during the 'ADSORPTION' phase succeeded by the 'DESORPTION' phase (mean ± SD, n = 3 for each condition). Experiments were conducted at 37 ± 0.1°C for total BS concentrations of 2.23 mM, 5.35 mM, and 7.81 mM achieved using (a) individual BS, (b) BS/PC mixtures, or (c) HB samples (HB-2.23, HB-5.35, and HB-7.81). When examining the BS/PC mixtures, PC was used in quantities adjusted to mirror the PC concentrations of the corresponding HB samples (refer to Fig. 17a and Section 3.14.3).

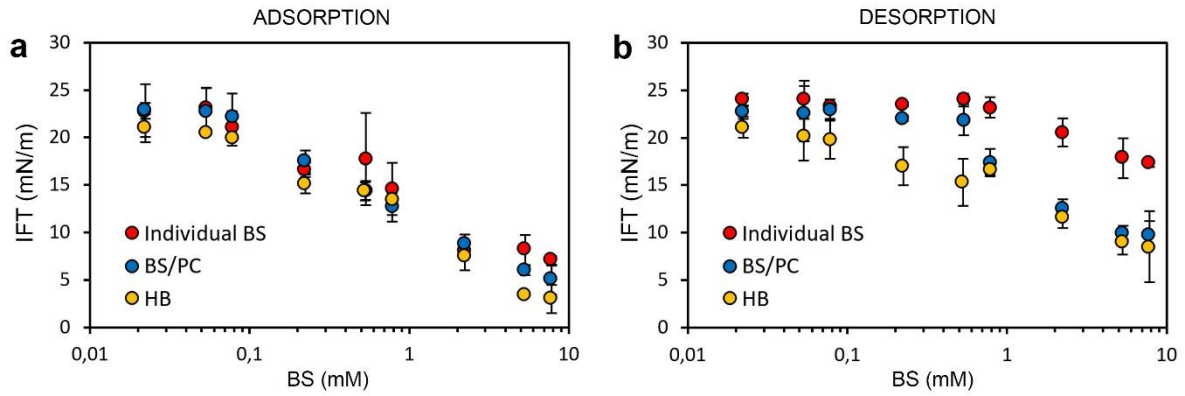

Figure 36. IFT values of (a) adsorbed layers formed at the oil-water interface using individual BS, BS/PC, and HB samples, and (b) subsequent to subphase exchange by SIF and completion of the desorption phase. The IFT assessment initially encompassed the total BS concentrations (x-axis) of 2.23 mM, 5.35 mM and 7.81 mM (achieved using individual BS, BS/PC mixtures, or HB samples), followed by 10-fold and 100-fold dilutions and the resulting reductions in the total BS concentrations (as outlined in Section 3.14.3). The results are presented as the mean ± SD (n = 3). Measurements were conducted at 37 ± 0.1°C.

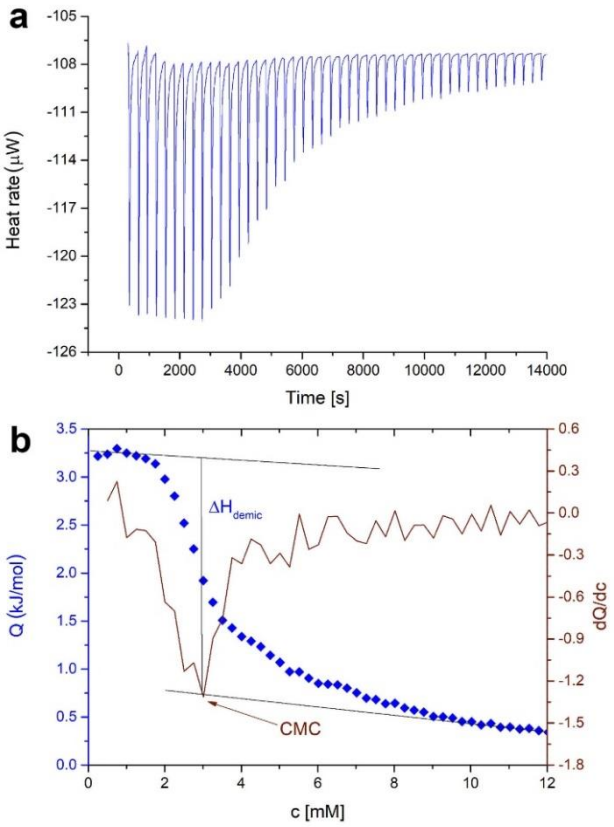

Figure 37. Representative isothermal titration calorimetry (ITC) data for determining CMC of the equimolar mixture of two individual BS, NaGDC and NaTC. (a) Exemplary heat-flow versus time results for the titration of the mixture of individual BS (48 mM stock) into SIF at 37°C. (b) Typical enthalpogram of the ITC titration detailing the determination of CMC and ΔH for demicellisation (ΔH_{demic}).

Incorporating PC into systems with BS concentrations exceeding the CMC (namely, for 5.35 mM and 7.81 mM BS) led to a more substantial IFT decrease (to ca. 5 mN/m, following 32 min of adsorption; Figs. 35b and 36a) compared to the solitary use of individual BS (Figs. 35a and 36a). This result was consistent with previous findings (Torcello-Gómez et al., 2011), and may suggest a synergistic effect of BS and PC at these BS concentrations. Importantly, this BS/PC-related trend in IFT reduction was also evident in the adsorption experiments involving the three different HB samples with varying total BS concentrations (Figs. 35c and 36a). However, the final IFT values noted for the HB samples were slightly lower by 2-3 mN/m in comparison to the values measured for the corresponding BS/PC mixtures. This implies a modest involvement of other surface-active components of HB (distinct from the biliary BS and PC) in the IFT reduction process (e.g., partial glycerides and/or cholesterol esters, (Boyer, 2013)).

I also examined the dilatational rheology of the formed adsorbed layers, evaluating the dilatational modulus at frequencies of 0.01, 0.1, and 1 Hz. In this context, I present outcomes specifically for 0.1 Hz (Table 5), as this oscillation frequency has been suggested to roughly correspond to the peristaltic frequency in the small intestine during digestion (11.7 per min in the duodenum (Kellow, Borody, Phillips, Tucker, & Haddad, 1986)). The dilatational rheology results at 0.01 and 1 Hz (not shown) mirrored the trend observed at 0.1 Hz.

BS are considered facial amphiphiles, exhibiting a distinct hydrophobic and hydrophilic face rather than the conventional head-tail surfactant configuration (Parekh, Patel, Khimani, & Bahadur, 2023). Although this planar arrangement facilitates rapid interfacial adsorption, leading to a swift reduction in IFT (Fig. 35a), it also results in a notably fluid-like interface characterised by low dilatational moduli (Maldonado-Valderrama et al., 2008), which may stem from weak lateral interactions between BS molecules within adsorbed films (Matubayasi, Kanzaki, Sugiyama, & Matuzawa, 1996). My study has confirmed this aspect for the individual BS used (Tab. 5). The dilatational moduli measured for the adsorbed individual BS were in the low range of 1–1.5 mN/m at 0.1 Hz, likely attributed to the rapid exchange of BS molecules between the interface and the bulk during the oscillation period (Maldonado-Valderrama et al., 2011). In contrast, the interfacial layers formed in the presence of BS and phospholipids (i.e., in adsorption experiments with BS/PC or HB samples) were characterised by dilatational moduli that were 5–8 times higher, indicating the formation of more elastic films of adsorbed surfactants compared to when solely individual BS were used (Tab. 5). This

distinction was apparent regardless of the total BS concentrations delivered through individual BS, BS/PC blends, or HB samples.

When used alone, PC tends to form condensed and elastic interfacial films of interacting adsorbed molecules, resulting in a densely packed layer due to the double-tail anchoring group of the phospholipid (De Vleeschauwer & Van der Meeren, 1999), (Torcello-Gómez et al., 2011). However, in the presence of BS, the interfacial organisation of BS-PC mixed films has been shown to be less compact and more disorganised (Chu et al., 2010), (Pabois et al., 2019), which can lead to lower dilatational modulus values (Torcello-Gómez, Jódar-Reyes, Maldonado-Valderrama, & Martín-Rodríguez, 2012). Moreover, the actual molar ratio of adsorbed BS and PC, and consequently the microstructure of the resulting interfacial film, has been found to significantly depend on the type and the bulk concentration of the BS used, as observed for NaTC and NaTDC (Pabois et al., 2019). These previous findings suggest that the formation and structure of BS-PC interfacial films might be particularly intricate when multiple species of BS simultaneously compete with PC for the interface, as is likely the case in the presence of HB. Nevertheless, the dilatational modulus data obtained for the adsorbed interfacial films produced with the three HB samples (Tab. 5), which varied substantially in BS characteristics and concentrations (Fig. 17), indicate that these interfacial films were more elastic than those produced with individual BS in the absence of PC. These results align with those obtained for the simpler BS/PC blends (Tab. 5) and strongly suggest the coexistence of both BS and PC at the interface after the adsorption phase of the experiment was conducted for either the HBs or the BS/PC mixtures.

Table 5. Dilatational modulus (E, mN/m; mean ± SD, n = 3) of the oil-water interface recorded at 0.1 Hz after the adsorption phase of experiments involving individual BS, PS/PC, and HB samples at 2.23 mm, 5.35 mm, and 7.81 mm BS concentrations, and after the subsequent desorption phase (refer to section 3.14.3 for experimental details)

Analysed system	BS concentration, mM	E, mN/m (**Adsorption**)	E, mN/m (**Desorption**)
Individual BS	2.23	1.4 ± 0.2	5.9 ± 0.4
	5.35	1.1 ± 0.3	6.7 ± 0.08
	7.81	1.0 ± 0.13	4.1 ± 0.14
BS/PC [a]	2.23	5.4 ± 0.6	25 ± 6
	5.35	8.8 ± 0.2	24 ± 6
	7.81	7.0 ± 0.2	15 ± 4
HB	2.23 [b]	7.5 ± 0.2	16.2 ± 0.4
	5.35 [c]	5.5 ± 0.7	15.4 ± 0.6
	7.81 [d]	6.1 ± 0.9	18 ± 2

[a] Corresponding PC concentrations as shown in Fig. 17a.
[b,c,d] HB samples HB-2.23, HB-5.35, and HB-7.81, respectively (Fig. 17).

Following the adsorption phase, the content of the pendant droplet was repeatedly exchanged with SIF, and the IFT was continuously monitored as described in Section 3.14.3. This process aimed to explore the potential of interfacial materials to desorb from the interface. The degree of ease in removing surface-active compounds would be reflected in an increase in the IFT (Maldonado-Valderrama et al., 2015).

In the absence of PC, i.e., when employing only individual BS during the adsorption phase, the subphase exchange led to a substantial elevation in the IFT, reaching up to ca. 20 mN/m for the 2.23 mM BS condition (Figs. 35a and 36b). Considering that the IFT of the plain oil-water interface (i.e., not occupied by surface-active materials) was approx. 23.5 mN/m, this suggests that the individual BS could have been relatively efficiently and effectively removed from the interface. This observation aligns with previous findings on the behaviour of NaGDC and NaTC at interfaces, wherein these two BS were found to almost entirely desorb from the air-water (Maldonado-Valderrama et al., 2011) and the oil-water (Maldonado-Valderrama et al., 2013) interfaces upon replacing the BS subphase with pure buffer. As a compact interfacial layer does not form during the oil-water adsorption of NaTC and NaGDC (Maldonado-Valderrama et al., 2008), (Maldonado-Valderrama et al., 2013), subsequent subphase exchange and the consequent desorption of diluted interfacial BS networks leads to elevated IFT values (Fig. 36b). The desorption profiles depicted in Fig. 35a underscore the reversible adsorption of individual BS onto the oil–water interface, as evident by the swift and significant recovery of IFT, alongside sustained low dilatational modulus (Tab. 5).

The desorption patterns of the HB samples were most accurately replicated by the BS/PC preparations, mirroring the findings from the adsorption phase. A moderate yet comparable rise in the IFT during the desorption step was observable in both the experiments involving the HB samples and the BS/PC blends (Figs. 35b,c and 36b). The inclusion of phospholipids alongside BS in these two types of systems bolstered the resistance of the adsorbed layer to desorption. This suggests the formation of a complex interface owing to the coexistence of these two biliary surfactant types, which are capable of enduring at the interface and forming a more strongly adhered BS–phospholipid layer than that of the individual BS.

The alignment in the interfacial behaviour of HB and BS/PC was further underscored by the results of dilatational rheology, wherein the partial desorption of adsorbed material led to a substantial elevation in the values of dilatational moduli (to ca. 15–25 mN/m, Tab. 5). This stands in contrast to the lower dilatational moduli noted for the individual BS (ca. 4–7

mN/m, Tab. 5), hinting at the pivotal role of phospholipids in conferring elasticity to the interfacial layer. The observed increase could potentially be attributed to the preferential desorption of BS over PC. The subphase exchange with pure SIF created conditions conducive to the facilitated desorption of easily removable BS, thereby leaving the interfacial layer dominated by PC, which might have exhibited greater resistance to desorption. The elevated values of the dilatation moduli (Tab. 5) and relatively low IFT values (Fig. 35b,c) observed for the BS/PC blends and HB samples after desorption suggest the formation of a compact arrangement of interfacial molecules driven by strong intermolecular interactions. Such properties have been demonstrated in a previous study on dilatational rheology for the PC interfacial layer adsorbed onto the n-decane-water interface (Mekkaoui et al., 2021). The same study also showed that interfaces occupied by BS (sodium cholate) or the BS in combination with PC were characterised by substantially lower dilatational modulus values.
The impeded desorption of the interfacial material in the presence of phospholipids could potentially have ramifications for the results of the experiments carried out in the presence of lipase. Any such potential effects were further investigated in Section 4.3.2.

4.3.2. Simulating the interfacial behaviour of human bile during the *in vitro* lipolysis

Following the assessment of adsorption and desorption for the individual BS, BS/PC blends, and HB samples, I carried out interfacial experiments aimed at investigating the utilisation of these three sources of BS within simulated intestinal lipolysis conditions. My primary objective was to evaluate the suitability of individual BS and/or BS/PC mixtures as substitutes for difficult-to-obtain HB in *in vitro* simulations of small intestinal lipolysis. Through the analysis of interfacial phenomena, my goal was also to attain knowledge applicable to exploring the lipolysis of oil-in-water emulsions. Once again, I conducted the experiments using individual BS and PC in quantities precisely reproducing the BS and PC concentrations achieved when employing the HB samples (Fig. 17a). This approach allowed for a direct comparison of results obtained from individual BS, BS/PC blends, and HB samples.
The interfacial experiments commenced with the adsorption of βLg onto the oil-water interface, simulating the creation of the interfacial membrane of TG droplets within a protein-stabilised emulsion. Following the protein adsorption phase, the lipolysis phase was

initiated through subphase exchange involving the addition of pancreatic lipase. The experiments were finalised with the desorption phase, after the droplet content had been substituted with pure SIF (Fig. 18a). Oscillations were performed on a solution droplet and the dilatational modulus was measured after each phase (Fig. 18b).

The initial protein adsorption step was conducted uniformly across all interfacial experiments, resulting in the reduction of the oil-water IFT to 12.0 ± 0.5 mN/m after 62 min of incubation with βLg at 37°C (Fig. 38). Subsequent introduction of lipase under the control lipolysis conditions (i.e., in the absence of BS, PC, or HB) led to a modest decrease in the IFT (to approx. 11 mN/m, Fig. 38). This suggests that the adsorbed βLg layer restricted the access of lipase to the interface, resulting in only limited hydrolysis of TGs into surface-active products of lipolysis (MGs, DGs, and FFAs). My parallel *in vitro* investigation of intestinal lipolysis in βLg-stabilised sunflower oil-in-water emulsions (Section 4.2) demonstrated that TG hydrolysis can occur to some extent in the absence of biliary surfactants. However, the emulsion study utilised pancreatin containing both lipolytic and proteolytic enzymes, with the latter potentially degrading the adsorbed βLg, thereby facilitating easier access of lipase to the TG substrate. Results of earlier interfacial studies have implied that enzymatic degradation of interfacial protein can contribute to enhancing the subsequent TG hydrolysis at the oil-water interface by facilitating the interfacial adsorption of lipase (Maldonado-Valderrama et al., 2015). This is particularly relevant when the adsorbed protein exhibits substantial resistance to gastric pepsinolysis, only yielding peptides with a lower surface activity than the activity of a parent protein upon the action of intestinal proteases in the small intestinal environment. Such a gastrointestinal digestion pattern has been observed for interfacial βLg (Macierzanka, Sancho, Mills, Rigby, & Mackie, 2009). However, it is important to keep in mind that the aforementioned scenario remains applicable only to control intestinal lipolysis conditions in the absence of BS. It has been demonstrated that physiologically relevant quantities of BS introduced into the intestinal environment are highly effective in displacing both native (undigested) βLg and post-digestion βLg peptides from the oil-water interface (Maldonado-Valderrama et al., 2008), (Macierzanka et al., 2009). In this study, I intentionally omitted the use of intestinal proteases, as my objective was to compare the efficacy of HB and isolated biliary surfactants in displacing interfacial protein under simulated intestinal lipolysis conditions.

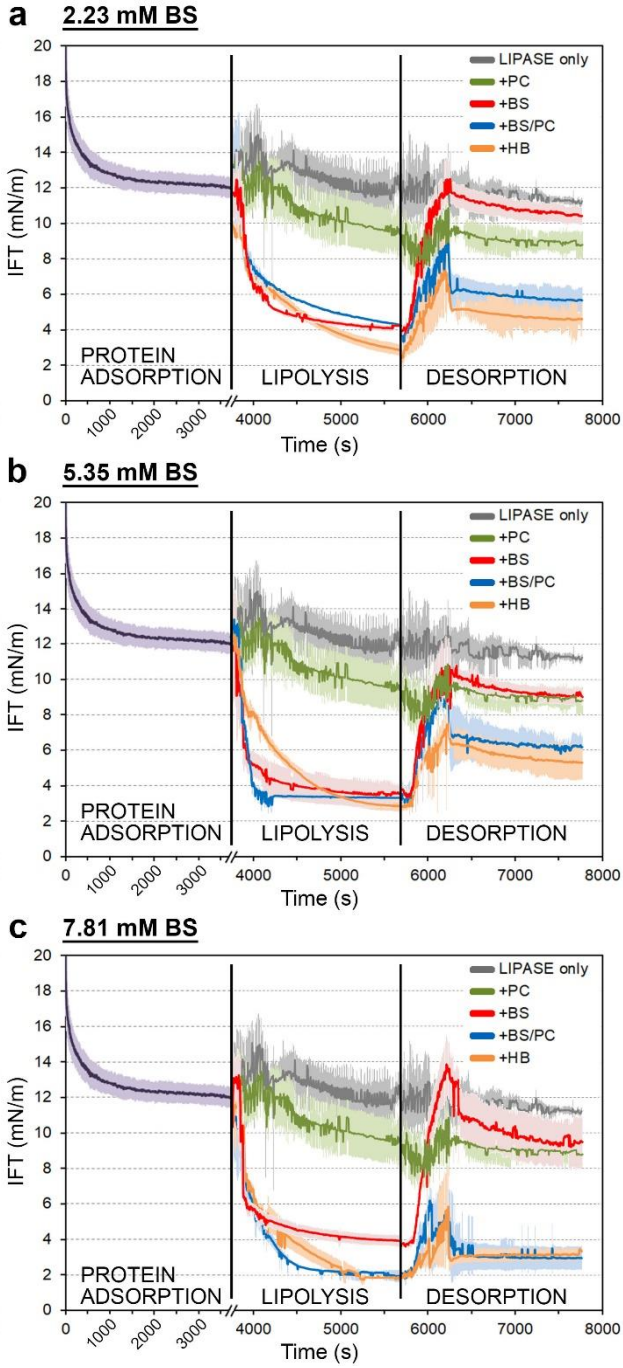

Figure 38. Time-dependent evolution of the sunflower oil–water interfacial tension (IFT) during the βLg 'PROTEIN ADSORPTION' phase (mean ± SD, n = 15), succeeded by the simulated intestinal 'LIPOLYSIS' phase with pancreatic lipase (mean ± SD, n = 3 for each condition), and concluding with the 'DESORPTION' phase (mean ± SD, n = 3 for each condition) (refer to Fig. 18 for a diagrammatic representation of the experimental sequence). The lipolysis phase was conducted either solely with the lipase or in conjunction with (i) HB ('+HB'; encompassing (a) HB-2.23 sample diluted to 2.23 mM BS, (b) HB-5.35 sample diluted to 5.35 mM BS, or (c) HB-7.81 sample diluted to 7.81 mM BS in the experimental setup; as depicted in Fig. 17a), (ii) individual BS ('+BS', NaTC and NaGDC, 1:1, mol/mol; overall concentration of (a) 2.23 mM, (b) 5.35 mM, or (c) 7.81 mM), (iii) PC ('+PC'; 0.6 mM in all (a), (b), and (c) scenarios), or (iv) the individual BS combined with PC ('+BS/PC'; using quantities of these biosurfactants adjusted to mirror the BS and PC concentrations in the corresponding HB samples, i.e., (a) 2.23 mM, (b) 5.35 mM, or (c) 7.81 mM BS and 0.5–0.7 mM PC; refer to Fig. 17a). All stages were carried out at 37 ± 0.1°C.

During the lipolysis phase conducted in the presence of 0.6 mM PC, a gradual and limited reduction of the IFT was observed, and the IFT decreased to approx. 9 mN/m by the end of this experimental phase (Fig. 38). PC has been demonstrated previously to effectively displace βLg from oil-water interfaces due to the higher interfacial activity of the lipid relative to the protein (Macierzanka et al., 2009). However, PC has also been shown to only slightly enhance the efficiency of *in vitro* intestinal lipolysis of TGs in oil-in-water emulsions (Ahn & Imm, 2023). Consequently, the observed IFT reduction in my study might primarily result from the displacement of the interfacial protein by PC, rather than the formation of substantial quantities of surface-active lipolysis products and their adsorption onto the interface. This suggestion can be supported by a previous atomic force microscopy (AFM) study, which has demonstrated that lipase tends to adsorb preferentially to the mixed BS-PC regions at the interface (NaGDC, NaTC, and dipalmitoylphosphocholine, DPPC, were investigated), rather than the PC condensed phase (Chu et al., 2010).

The IFT results obtained for PC stand in stark contrast to those observed after the application of individual BS, BS/PC mixtures, or HB samples during the lipolysis phase. In these cases, the combined action of biliary surfactants and lipase led to much more efficient reduction of the IFT, with a substantial drop observed within the first several minutes (Fig. 38). This implies that βLg has been replaced at the interface by BS with/without PC (depending on the analysed system). Importantly, the final IFT was comparable amongst experiments involving individual BS, BS/PC mixtures, and HB samples, reaching values as low as 2–4 mN/m, regardless of the BS concentration analysed. These values were generally lower than those observed during the adsorption of biliary surfactants in the absence of lipase (Fig. 35). This implies a contribution from the surface-active lipolysis products formed *in situ* during the lipolysis phase, which aided in lowering the IFT.

However, it is crucial to emphasise that the *in vitro* interfacial lipolysis experiments cannot directly ascertain the extent to which individual BS, BS/PC mixtures, or HB samples effectively facilitate the enzymatic hydrolysis of TGs and their conversion into lipolysis products. These experiments solely illustrate the evolution of the IFT during lipolysis, resulting from the combined action of BS, PC, and lipase generating MGs, DGs, and FFAs. Nonetheless, it is worth noting that every lipolysis experiment performed with any of the three analysed sources of BS and across all three analysed BS concentrations demonstrated

a substantially greater reduction in the IFT compared to the control lipolysis (conducted without added biosurfactants), as discussed earlier.

The effectiveness of individual BS, BS/PC mixtures, and HB samples in enhancing the rate and extent of *in vitro* lipolysis in emulsions has been demonstrated in my parallel work (Section 4.2) by assessing the yields of FFA release from emulsified TGs. This study has indicated that to accurately mimic the effect of HB on the progress of lipolysis in emulsions, it was essential to employ individual BS combined with PC (BS/PC) – rather than using individual BS alone – and in quantities that replicated the total concentrations of BS and PC in HB. This might have been attributed to the combination of these two types of biliary surfactants, which together allowed for mimicking both the interfacial and bulk behaviours of HB.

BS are known to enhance the lipolysis progress through their facilitation of lipase interfacial adsorption, boosting enzyme interaction with the TG substrate, and through their role in solubilising lipolysis products at the oil-water interface, subsequently transporting them into the bulk phase in the form of mixed micelles (Macierzanka, Torcello-Gómez, Jungnickel, & Maldonado-Valderrama, 2019). This desorption mechanism prevents the accumulation of surface-active lipolysis products at the interface, thus enabling continued lipolysis until completion, as the enzyme remains proximal to the TGs. The desorption of BS from oil-water interfaces has been studied previously (Maldonado-Valderrama et al., 2011), (Maldonado-Valderrama et al., 2013), (Pabois et al., 2019). However, this is not the case for BS-PC mixtures, particularly in the context of simulating HB behaviour using individual biliary surfactants under the intestinal lipolysis conditions.

The interfacial experiments in my present study revealed that the desorption profiles of HB could be closely replicated only by using BS in conjunction with PC (BS/PC, Fig. 38). This finding aligns with the desorption results shown in Figs. 35b,c and 36b for scenarios lacking lipase. However, the generally lower IFT values depicted in Fig. 38 for the BS/PC blends and HB samples suggest the presence of surface-active lipolysis products, which could have remained to some extent at the interface along with PC, despite the subphase exchange after the lipolysis phase, and contributed to the lower IFT observed.

When I examined the post-lipolysis desorption for individual BS, the IFT rebounded to much higher values than those observed for HB or BS/PC (Fig. 38). This confirmed that BS could be relatively easily removed from the interface in the absence of PC. However, the steady-state

desorption values of the IFT shown in Fig. 38 for individual BS ranged from approx. 9 to 11 mN/m, depending on the BS concentration. These values are lower than the corresponding values presented in Figs. 35a and 36b for the desorption of individual BS in the absence of lipase (i.e., ca. 17–21 mN/m). Once again, this suggests that, even with the solitary use of individual BS during the lipolysis phase, some surface-active lipolysis products produced *in situ* could remain adsorbed to a certain extent at the interface after the exchange of the droplet content with pure SIF and the resulting desorption of BS.

To compare the efficiency of interfacial material desorption amongst the analysed systems, I calculated the difference between the final IFT value of the desorption phase and the final IFT value of the lipolysis phase (ΔIFT) for each experiment involving individual BS, BS/PC blends or HB samples. The results indicated that the extent of this relative difference was primarily influenced by the presence of phospholipids, decreasing by at least a factor of two between experiments with individual BS and those with BS/PC or HB (P<0.01, Fig. 39). Importantly, the disparities in the ΔIFT values between BS/PC and HB were not statistically significant (P>0.05) for any of the three total BS concentrations analysed. This observation remained consistent despite the considerably more complex compositions of BS in the HB samples (Fig. 17b) compared to the BS/PC blends, where only two BS – NaTC and NaGDC – were utilised to mimic biliary BS.

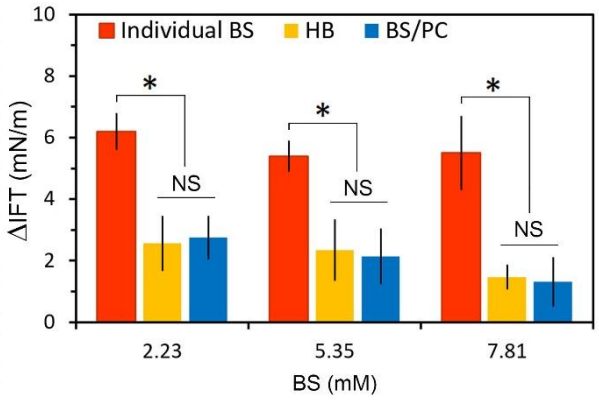

Figure 39. Relative difference (ΔIFT) between the oil-water interfacial tension values recorded at the final stages of the desorption and the lipolysis phases, depicted as a function of the total BS concentration introduced into the lipolysis experimental setup, using individual BS, BS/PC mixtures, or HB samples (mean ± SD, n = 3 for each condition). * P<0.01; NS, not significant (P>0.05).

The measurement of the dilatational modulus after the lipolysis phase conducted in the presence of 0.6 mM PC returned a value of 8.4 ± 0.9 mN/m (Tab. 6), which was very similar to the value previously obtained for a phospholipid-stabilised olive oil-water interface

treated with lipase (Torcello-Gómez et al., 2011), and suggested limited lipolysis under the applied experimental conditions. The dilatational modulus only slightly increased to 11 ± 2 mN/m after the subsequent desorption phase (Tab. 6), indicating that the interfacial PC, and any lipolysis products that might have formed, largely remained at the interface following the subphase exchange with SIF. This is confirmed by the results of the static measurements showing that the final IFT recorded during the lipolysis phase with PC remained largely unchanged after the completion of the desorption phase (Fig. 38).

Table 6 also presents the dilatational modulus results for the experiments involving individual BS, BS/PC blends, and HB samples. In general, the trend in the evolution of interfacial rheology aligns with the findings presented in Table 5 (and discussed in Section 4.3.1) for the experiments that did not employ lipase. This underscores the significance of including PC in blends with BS to reliably replicate the interfacial behaviour of HB during *in vitro* lipolysis studies. These results further bolster the conclusions drawn from the static experiments (Fig. 38) concerning the similar interfacial behaviour of the complex HB samples and the simpler BS/PC mixtures during *in vitro* lipolysis.

Table 6. Dilatational modulus (E, mN/m; mean ± SD, n = 3) of the oil-water interface recorded at 0.1 Hz after the lipolysis phase of interfacial experiments involving either PC, individual BS, PS/PC, or HB, and after the subsequent desorption phase (refer to section 3.14.4 for experimental details)

Analysed system	BS concentration, mM	E, mN/m (**Lipolysis**)	E, mN/m (**Desorption**)
PC [a]	0	8.4 ± 0.9	11 ± 2
Individual BS	2.23	1.2 ± 0.2	5.1 ± 0.8
	5.35	0.9 ± 0.2	4 ± 1
	7.81	0.8 ± 0.06	4.5 ± 0.9
BS/PC [b]	2.23	2.6 ± 0.2	13 ± 2
	5.35	5.4 ± 0.2	23 ± 1
	7.81	5.1 ± 0.1	21 ± 4
HB	2.23 [c]	3.7 ± 0.2	15.6 ± 0.8
	5.35 [d]	2.5 ± 0.3	13 ± 2
	7.81 [e]	4.3 ± 0.6	15 ± 1

[a] PC concentration, 0.6 mM.
[b] Corresponding PC concentrations as shown in Fig. 17a.
[c,d,e] HB samples HB-2.23, HB-5.35, and HB-7.81, respectively (Fig. 17).

The results presented in Section 4.3 and other related contents are being used in the preparation of a research article for publication in a scientific journal.

5. Summary and conclusions

The conducted research and the obtained results have enabled to draw several general conclusions.

1. Quantitative analysis demonstrated that the concentration of BS strongly influences the extent of the proteolysis of bovine milk βLg by trypsin and chymotrypsin under simulated small intestinal conditions, with a significant increase in the proteolysis already observed for as little as 1 mM BS. The impact was observed for simple mixtures of two different BS as well as for real HB samples with complex BS compositions, and its magnitude increased upon increasing the overall BS concentration. The total BS content of HB appeared to be more important in determining the extent of βLg proteolysis than the BS profile of HB, according to the results of the simulated intestinal digesting experiments performed in the presence of various HB samples. This suggests that the kinetics of protein digestion in the small intestine may rely on the overall luminal BS concentration, which is dependent on the amount of BS secreted with bile into the intestinal lumen. My investigation also showed that using individual BS combined with PC allowed for reliable replication of the effect of HB on the *in vitro* gastrointestinal proteolysis of βLg (purified and in a food-grade whey protein isolate). However, a follow-up study, including a larger number of HB samples with various BS and PC contents, is required to corroborate this.

The findings of the *in vitro* proteolysis study may help to define the full physiological function of HB. They also provide an insight into the potential effects of BS deficiency on the efficiency of food digestion. This study also demonstrates how a difficult-to-obtain HB could be successfully substituted by BS/PC mixtures for *in vitro* human-relevant proteolysis models that mimic the small intestinal environment.

2. My research has also revealed a clear relationship between the concentration of BS and the *in vitro* intestinal lipolysis of emulsified TGs. I observed a consistent enhancement of the lipolysis extent as the total concentrations of applied BS increased, both in simple mixtures of two individual BS and in real HB samples with more complex BS compositions. The results also suggest that the overall luminal concentration of BS may have a more pivotal role in determining the extent of lipolysis compared to the specific profile of BS delivered with HB. This observation aligns with the previous conclusion from the *in vitro* proteolysis

investigation, where the simulated intestinal digestibility of βLg was found to be dependent on the total BS concentration in the digestion environment rather than the BS composition. Most importantly, also the emulsion lipolysis study has demonstrated that the impact of HB on intestinal lipolysis could be most accurately replicated *in vitro* using individual BS mixed with PC. This has showcased how difficult-to-obtain HB can be reliably mimicked in *in vitro* human-relevant lipolysis models simulating small intestinal conditions.

3. The results of the time-dependent evolution of the IFT offered insights into the interfacial behaviours of individual BS and their blends with PC during the lipolysis and subsequent desorption of interfacial material. These findings have shed light on why BS-PC mixtures are more suitable candidates than pure BS preparations for reliably mimicking the function of real HB in investigations simulating the physiological processes of TG digestion in the small intestine.

Nevertheless, it is crucial to acknowledge that all the conclusions are derived from static *in vitro* digestion models. Indeed, the conclusions can contribute in improving the existing *in vitro* static models of digestion that are used world-wide in many research laboratories. However, in order to precisely identify the physiological functions of HB in protein and lipid digestion, and the ability of individual BS and PC to replicate such functions, more research is needed. This should be carried out using dynamic *in vitro* digestion models, as well as, if possible, *in vivo* models. My research, presented in this PhD thesis, offers a strong foundation for such future digestion studies.

6. Literature

Aguilera-Garrido, A., del Castillo-Santaella, T., Galisteo-González, F., José Gálvez-Ruiz, M., & Maldonado-Valderrama, J. (2021). Investigating the role of hyaluronic acid in improving curcumin bioaccessibility from nanoemulsions. *Food Chemistry*, *351*(February), 129301. https://doi.org/10.1016/j.foodchem.2021.129301

Ahn, N., & Imm, J.-Y. (2023). Effect of phospholipid matrix on emulsion stability, microstructure, proteolysis, and in vitro digestibility in model infant formula emulsion. *Food Research International*, *163*(July), 112218. https://doi.org/10.1016/j.foodres.2022.112218

Alegría, A., Garcia-Llatas, G., & Cilla, A. (2015). Static digestion models: General introduction. In *The Impact of Food Bioactives on Health: In Vitro and Ex Vivo Models* (pp. 3–12). https://doi.org/10.1007/978-3-319-16104-4_1

Alric, M., & Denis, S. (2009). Dispositif de simulation d'un estomac d'un mammifere monogastrique ou d'un être humain. *Patent NW02009087314*.

Anderson, J. M., & Van Itallie, C. M. (2009). Cite this article as. *Cold Spring Harb Perspect Biol*, *1*, 2584–2585. https://doi.org/10.1101/cshperspect.a002584

Armand, M. (2007). Lipases and lipolysis in the human digestive tract: Where do we stand? *Current Opinion in Clinical Nutrition and Metabolic Care*, *10*(2), 156–164. https://doi.org/10.1097/MCO.0b013e3280177687

Armand, M., Borel, P., Ythier, P., Dutot, G., Melin, C., Senft, M., … Lairon, D. (1992). Effects of droplet size, triacylglycerol composition, and calcium on the hydrolysis of complex emulsions by pancreatic lipase: an in vitro study. *The Journal of Nutritional Biochemistry*, *3*(7), 333–341. https://doi.org/10.1016/0955-2863(92)90024-D

Asensio-Grau, A., Calvo-Lerma, J., Heredia, A., & Andrés, A. (2021). In vitro digestion of salmon: Influence of processing and intestinal conditions on macronutrients digestibility. *Food Chemistry*, *342*, 128387. https://doi.org/10.1016/j.foodchem.2020.128387

Asensio-Grau, A., Peinado, I., Heredia, A., & Andrés, A. (2019). In vitro study of cheese digestion: Effect of type of cheese and intestinal conditions on macronutrients digestibility. *LWT*, *113*, 108278. https://doi.org/10.1016/j.lwt.2019.108278

Bellmann, S., Lelieveld, J., Gorissen, T., Minekus, M., & Havenaar, R. (2016). Development of an advanced in vitro model of the stomach and its evaluation versus human gastric physiology. *Food Research International*, *88*, 191–198. https://doi.org/10.1016/j.foodres.2016.01.030

Berecz, B., Mills, C. E. N., Parádi, I., Láng, F., Tamás, L., Shewry, P. R., & Mackie, A. R. (2013). Stability of sunflower 2S albumins and LTP to physiologically relevant in vitro gastrointestinal digestion. *Food Chemistry*, *138*(4), 2374–2381. https://doi.org/10.1016/j.foodchem.2012.12.034

Bhutia, Y. D., & Ganapathy, V. (2018). Protein Digestion and Absorption. In *Physiology of the Gastrointestinal Tract: Sixth Edition* (Vols. 2–2, pp. 1063–1086). Elsevier Inc. https://doi.org/10.1016/B978-0-12-809954-4.00047-5

Bornhorst, G. M., & Singh, R. P. (2012). Bolus Formation and Disintegration during Digestion of Food Carbohydrates. *Comprehensive Reviews in Food Science and Food Safety*, *11*(2), 101–118. https://doi.org/10.1111/j.1541-4337.2011.00172.x

Bornhorst, G. M., & Singh, R. P. (2013). Kinetics of in Vitro Bread Bolus Digestion with Varying Oral and Gastric Digestion Parameters. *Food Biophysics*, *8*(1), 50–59. https://doi.org/10.1007/s11483-013-9283-6

Bossios, A., Theodoropoulou, M., Mondoulet, L., Rigby, N. M., Papadopoulos, N. G., Bernard, H., … Papageorgiou, P. (2011). Effect of simulated gastro-duodenal digestion on the allergenic reactivity of beta-lactoglobulin. *Clinical and Translational Allergy*, *1*(1), 6. https://doi.org/10.1186/2045-7022-1-6

Böttger, F., Dupont, D., Marcinkowska, D., Bajka, B., Mackie, A., & Macierzanka, A. (2019). Which casein in sodium caseinate is most resistant to in vitro digestion? Effect of emulsification and enzymatic structuring. *Food Hydrocolloids*, *88*, 114–118. https://doi.org/10.1016/j.foodhyd.2018.09.042

Bourlieu, C., Ménard, O., Bouzerzour, K., Mandalari, G., Macierzanka, A., Mackie, A. R., & Dupont, D. (2014). Specificity of Infant Digestive Conditions: Some Clues for Developing Relevant In Vitro Models. *Critical Reviews in Food Science and Nutrition*, *54*(11), 1427–1457. https://doi.org/10.1080/10408398.2011.640757

Boyer, J. L. (2013). Bile Formation and Secretion. In *Comprehensive Physiology* (Vol. 3, pp. 1035–1078). Hoboken, NJ, USA: John Wiley & Sons, Inc. https://doi.org/10.1002/cphy.c120027

Brockman, H. (2000). Kinetic behavior of the pancreatic lipase-colipase-lipid system. *Biochimie*, *82*(11), 987–995. https://doi.org/10.1016/S0300-9084(00)01185-8

Brodkorb, A., Egger, L., Alminger, M., Alvito, P., Assunção, R., Ballance, S., Bohn, T., Bourlieu-Lacanal, C., Boutrou, R., Carrière, F., Clemente, A., Corredig, M., Dupont, D., Dufour, C., Edwards, C., Golding, M., Karakaya, S., Kirkhus, B., Le Feunteun, S., … Recio, I. (2019). INFOGEST static in vitro simulation of gastrointestinal food digestion. *Nature Protocols*, *14*(4), 991–1014. https://doi.org/10.1038/s41596-018-0119-1

Brooks, S., & Kalmokoff, M. (2012). (No Title). *Journal of Aoac InternatIonal*, *95*(1). https://doi.org/10.5740/jaoacint.SGE_Macfarlane

Buettner, A., Beer, A., Hannig, C., & Settles, M. (2001). Observation of the swallowing process by application of videofluoroscopy and real-time magnetic resonance imaging-consequences for retronasal aroma stimulation. *Chemical Senses*, *26*(9), 1211–1219. https://doi.org/10.1093/chemse/26.9.1211

Calvo-Lerma, J., Fornés-Ferrer, V., Heredia, A., & Andrés, A. (2019). In vitro digestion models

to assess lipolysis: The impact of the simulated conditions on gastric and intestinal pH, bile salts and digestive fluids. *Food Research International*, *125*, 108511. https://doi.org/10.1016/j.foodres.2019.108511

Camilleri, M., & Vazquez Roque, M. I. (2014). Gastrointestinal Functions. *Encyclopedia of the Neurological Sciences*, *2*(phase III), 411–416. https://doi.org/10.1016/B978-0-12-385157-4.00501-7

Carey, M. C., & Small, D. M. (1972). Micelle Formation by Bile Salts: Physical-Chemical and Thermodynamic Considerations. *Archives of Internal Medicine*, *130*(4), 506–527. https://doi.org/10.1001/archinte.1972.03650040040005

Chen, J. (2009). Food oral processing-A review. *Food Hydrocolloids*, *23*(1), 1–25. https://doi.org/10.1016/j.foodhyd.2007.11.013

Chu, B. S., Rich, G. T., Ridout, M. J., Faulks, R. M., Wickham, M. S. J., & Wilde, P. J. (2009). Modulating pancreatic lipase activity with galactolipids: Effects of emulsion interfacial composition. *Langmuir*, *25*(16), 9352–9360. https://doi.org/10.1021/la9008174

Costi, R., Gnocchi, A., Di Mario, F., & Sarli, L. (2014). Diagnosis and management of choledocholithiasis in the golden age of imaging, endoscopy and laparoscopy. *World Journal of Gastroenterology*, *20*(37), 13382–13401. https://doi.org/10.3748/wjg.v20.i37.13382

Cremers, C. M., Knoefler, D., Vitvitsky, V., Banerjee, R., & Jakob, U. (2014). Bile salts act as effective protein-unfolding agents and instigators of disulfide stress in vivo. *Proceedings of the National Academy of Sciences of the United States of America*, *111*(16). https://doi.org/10.1073/pnas.1401941111

Cotten, S. W. (2020). Evaluation of exocrine pancreatic function. *Contemporary Practice in Clinical Chemistry*, 573–585. https://doi.org/10.1016/B978-0-12-815499-1.00033-8

Dawes, C., Pedersen, A. M. L., Villa, A., Ekström, J., Proctor, G. B., Vissink, A., Aframian, D., McGowan, R., Aliko, A., Narayana, N., Sia, Y. W., Joshi, R. K., Jensen, S. B., Kerr, A. R., & Wolff, A. (2015). The functions of human saliva: A review sponsored by the World Workshop on Oral Medicine VI. *Archives of Oral Biology*, *60*(6), 863–874. https://doi.org/10.1016/j.archoralbio.2015.03.004

De Carvlho, K. G., Kruger, M. F., Nader Furtado, D., Todorov, S. D., & Gombossy De Melo Franco, B. D. (2009). Evaluation of the role of environmental factors in the human gastrointestinal tract on the behaviour of probiotic cultures ofLactobacillus casei Shirota andLactobacillus casei LC01 by the use of a semi-dynamicin vitro model. *Annals of Microbiology*, *59*(3), 439–445. https://doi.org/10.1007/BF03175128

De, E., Phanie Blanquet-Diot, S., Jarrige, J.-F.-O., Denis, S., Beyssac, E., & Alric, M. (2009). Combining the Dynamic TNO-Gastrointestinal Tract System with a Caco-2 Cell Culture Model: Application to the Assessment of Lycopene and r-Tocopherol Bioavailability from a Whole Food. *J. Agric. Food Chem*, *57*, 11314–11320. https://doi.org/10.1021/jf902392a

De Vleeschauwer, D., & Van der Meeren, P. (1999). Colloid chemical stability and interfacial

properties of mixed phospholipid–non-ionic surfactant stabilised oil-in-water emulsions. *Colloids and Surfaces A: Physicochemical and Engineering Aspects*, *152*(1–2), 59–66. https://doi.org/10.1016/S0927-7757(98)00617-7

Duerksen, D. R., Fallows, G., & Bernstein, C. N. (2006). *Vitamin B12 malabsorption in patients with limited ileal resection*. https://doi.org/10.1016/j.nut.2006.08.017

Dulko, D., Staroń, R., Krupa, L., Rigby, N. M., Mackie, A. R., Gutkowski, K., … Macierzanka, A. (2021). The bile salt content of human bile impacts on simulated intestinal proteolysis of β-lactoglobulin. *Food Research International*, *145*, 110413. https://doi.org/10.1016/j.foodres.2021.110413

Dupont, D., Mandalari, G., Molle, D., Jardin, J., Léonil, J., Faulks, R. M., … Mackie, A. R. (2009). Comparative resistance of food proteins to adult and infant *in vitro* digestion models. *Molecular Nutrition & Food Research*, *54*(6), 767–780. https://doi.org/10.1002/mnfr.200900142

Dupont, D., & Tomé, D. (2020). Milk proteins: Digestion and absorption in the gastrointestinal tract. In *Milk Proteins (3rd ed.)* (pp. 701–714). Elsevier. https://doi.org/10.1016/B978-0-12-815251-5.00020-7

Falasca, M., Stokes, K. Y., Prasad, S., Bhat, A. A., Uppada, S., Achkar, I. W., Hashem, S., Yadav, S. K., Shanmugakonar, M., Al-Naemi, H. A., Haris, M., & Uddin, S. (2019). *Tight Junction Proteins and Signaling Pathways in Cancer and Inflammation: A Functional Crosstalk*. https://doi.org/10.3389/fphys.2018.01942

Gass, J., Vora, H., Hofmann, A. F., Gray, G. M., & Khosla, C. (2007). Enhancement of Dietary Protein Digestion by Conjugated Bile Acids. *Gastroenterology*, *133*(1), 16–23. https://doi.org/10.1053/j.gastro.2007.04.008

Gibson, G. L. E. Y. Y. R., & Roberfroid, M. B. (1995). *Critical Review Dietary Modulation of the Human Colonie Microbiota : Introducing the Concept of Prebiotics*. *August 1994*.

Giglio, E., Loreti, S., & Pavel, N. V. (1988). EXAFS: A new approach to the structure of micellar aggregates. *Journal of Physical Chemistry*, *92*(10), 2858–2862. https://doi.org/10.1021/j100321a032

Gilat, T., & Sömjen, G. J. (1996). Phospholipid vesicles and other cholesterol carriers in bile. *Biochimica et Biophysica Acta - Reviews on Biomembranes*, *1286*(2), 95–115. https://doi.org/10.1016/0304-4157(96)00005-6

Głazowska, J., Stankiewicz, U., & Bartoszek, A. (2017). Absorpcja, metabolizm i rola biologiczna kwasów nukleinowych obecnych w żywności. *Zywnosc. Nauka. Technologia. Jakosc/Food. Science Technology. Quality*, *24*(1), 18–32. https://doi.org/10.15193/zntj/2017/110/170

Guerra, A., Etienne-Mesmin, L., Livrelli, V., Denis, S., Blanquet-Diot, S., & Alric, M. (2012). Relevance and challenges in modeling human gastric and small intestinal digestion. *Trends in Biotechnology*, *30*(11), 591–600. https://doi.org/10.1016/J.TIBTECH.2012.08.001

Guo, Q., Ye, A., Lad, M., Ferrua, M., Dalgleish, D., & Singh, H. (2015). Disintegration kinetics of food gels during gastric digestion and its role on gastric emptying: An in vitro analysis. *Food and Function*, *6*(3), 756–764. https://doi.org/10.1039/c4fo00700j

Gupta, M. K., Sunflower oil. In: Gunstone, F. D. (Ed.) Vegetable Oils in Food Technology: Composition, Properties and Uses, CRC Press LLC, 2002 .

Hanasaki, K., Ono, T., Saiga, A., Morioka, Y., Ikeda, M., Kawamoto, K., Higashino, K. I., Nakano, K., Yamada, K., Ishizaki, J., & Arita, H. (1999). Purified Group X Secretory Phospholipase A2 Induced Prominent Release of Arachidonic Acid from Human Myeloid Leukemia Cells. *Journal of Biological Chemistry*, *274*(48), 34203–34211. https://doi.org/10.1074/JBC.274.48.34203

Havenaar, R., Anneveld, B., Hanff, L. M., De Wildt, S. N., De Koning, B. A. E., Mooij, M. G., Lelieveld, J. P. A., & Minekus, M. (2013). In vitro gastrointestinal model (TIM) with predictive power, even for infants and children? *International Journal of Pharmaceutics*, *457*(1), 327–332. https://doi.org/10.1016/J.IJPHARM.2013.07.053

Hebanowska, A. (2010). *Biosynteza kwasów żółciowych i jej regulacja * Bile acid biosynthesis and its regulation*. 544–554.

Helander, H. F., & Fändriks, L. (2014). Surface area of the digestive tract-revisited. *Scandinavian Journal of Gastroenterology*, *49*(6), 681–689. https://doi.org/10.3109/00365521.2014.898326

Hernández-Ledesma, B., Dávalos, A., Bartolomé, B., & Amigo, L. (2005). Preparation of antioxidant enzymatic hydrolysates from α-lactalbumin and β-lactoglobulln. Identification of active peptides by HPLC-MS/MS. *Journal of Agricultural and Food Chemistry*, *53*(3), 588–593. https://doi.org/10.1021/jf048626m

Hernell, O., Staggers, J. E., & Carey, M. C. (1990). Physical-chemical behavior of dietary and biliary lipids during intestinal digestion and absorption. 2. Phase analysis and aggregation states of luminal lipids during duodenal fat digestion in healthy adult human beings. *Biochemistry*, *29*(8), 2041–2056. https://doi.org/10.1021/bi00460a012

Hinsberger, A., & Sandhu, B. K. (2004). Digestion and absorption. *Current Paediatrics*, *14*(7), 605–611. https://doi.org/10.1016/j.cupe.2004.08.004

Hoebler, C., Karinthi, A., Devaux, M. F., Guillon, F., Gallant, D. J. G., Bouchet, B., Melegari, C., & Barry, J. L. (1998). Physical and chemical transformations of cereal food during oral digestion in human subjects. *British Journal of Nutrition*, *80*(5), 429–436. https://doi.org/10.1017/s0007114598001494

Hofmann, A. F., & Hagey, L. R. (2014). Key discoveries in bile acid chemistry and biology and their clinical applications: History of the last eight decades. In *Journal of Lipid Research* (Vol. 55, Issue 8, pp. 1553–1595). American Society for Biochemistry and Molecular Biology Inc. https://doi.org/10.1194/jlr.R049437

Hooton, D., Lentle, R., Monro, J., Wickham, M., Simpson, R., Hooton, D., Lentle, R., Monro, J.,

Simpson, R., & Wickham, M. (2015). The Secretion and Action of Brush Border Enzymes in the Mammalian Small Intestine. *Rev Physiol Biochem Pharmacol*, *168*, 59–118. https://doi.org/10.1007/112_2015_24

Hornbuckle, W. E., Simpson, K. W., & Tennant, B. C. (2008). *Gastrointestinal Function SALIVARY SECRETIONS FUNCTION*. *1*, 413–457.

ISO 12966-2:2017(E), Animal and Vegetable Fats and Oils – Gas Chromatography of Fatty Acid Methyl Esters – Part 2: Preparation of Methyl Esters of Fatty Acids. ISO 2017, Geneva, Switzerland.

Jenkins, J. M. W. W. and D. J. A. (2007). Carbohydrate Digestibility and. *Clinical Nutrition*, *4*, 2539–2546.

Johnston, N., Dettmar, P. W., Bishwokarma, B., Lively, M. O., & Koufman, J. A. (2007). *Activity / Stability of Human Pepsin : Implications for Reflux Attributed Laryngeal Disease*. *June*, 1036–1039. https://doi.org/10.1097/MLG.0b013e31804154c3

Kellow, J. E., Borody, T. J., Phillips, S. F., Tucker, R. L., & Haddad, A. C. (1986). Human interdigestive motility: Variations in patterns from esophagus to colon. *Gastroenterology*, *91*(2), 386–395. https://doi.org/10.1016/0016-5085(86)90573-1

Kimchi, E. T., Gusani, N. J., & Kaifi, J. T. (2019). Anatomy and Physiology of the Small Intestine. *Greenfield's Surgery: Scientific Principles and Practice: Fifth Edition*, 817–841. https://doi.org/10.1016/B978-0-323-40232-3.00071-6

Kimzey, M. J., & Haxo, F. T. (2016). Use of bile detergents to denature glycoproteins prior to enzymatic digestion. US 2016/0348139A1 Patent Application.

Kitabatake, N., & Kinekawa, Y.-I. (1998). Digestibility of Bovine Milk Whey Protein and β-Lactoglobulin in Vitro and in Vivo. *Journal of Agricultural and Food Chemistry*, *46*(12), 4917–4923. https://doi.org/10.1021/jf9710903

Kong, F., & Singh, R. P. (2008). A model stomach system to investigate disintegration kinetics of solid foods during gastric digestion. *Journal of Food Science*, *73*(5), 202–210. https://doi.org/10.1111/j.1750-3841.2008.00745.x

Kozarek, R. A. (2017). The past, present, and future of endoscopic retrograde cholangiopancreatography. *Gastroenterology and Hepatology*, *13*(10), 620–622.

Krupa, L., Bajka, B., Staroń, R., Dupont, D., Singh, H., Gutkowski, K., & Macierzanka, A. (2020). Comparing the permeability of human and porcine small intestinal mucus for particle transport studies. *Scientific Reports*, *10*(1), 20290.

Kudo, I., & Murakami, M. (2002). Phospholipase A2 enzymes. *Prostaglandins & Other Lipid Mediators*, *68–69*, 3–58. https://doi.org/10.1016/S0090-6980(02)00020-5

Li, T., & Apte, U. (2015). Bile Acid Metabolism and Signaling in Cholestasis, Inflammation, and Cancer. *Advances in Pharmacology*, *74*, 263–302.

https://doi.org/10.1016/bs.apha.2015.04.003

Li, J., Ye, A., Lee, S. J., & Singh, H. (2012). Influence of gastric digestive reaction on subsequent in vitro intestinal digestion of sodium caseinate-stabilized emulsions. *Food & Function*, *3*(3), 320. https://doi.org/10.1039/c2fo10242k

Li, Y., & McClements, D. J. (2010). New Mathematical Model for Interpreting pH-Stat Digestion Profiles: Impact of Lipid Droplet Characteristics on in Vitro Digestibility. *Journal of Agricultural and Food Chemistry*, *58*(13), 8085–8092. https://doi.org/10.1021/jf101325m

Lindahl, A., Ungell, A. L., Knutson, L., & Lennernäs, H. (1997). Characterization of fluids from the stomach and proximal jejunum in men and women. *Pharmaceutical Research*, *14*(4), 497–502. https://doi.org/10.1023/A:1012107801889

Liu, Y., Zhang, Y., Dong, P., An, R., Xue, C., Ge, Y., Wei, L., & Liang, X. (2015). Digestion of Nucleic Acids Starts in the Stomach. *Nature Publishing Group*. https://doi.org/10.1038/srep11936

Lykidis, A., Avranas, A., & Arzoglou, P. (1997). Combined Effect of a Lecithin and a Bile Salt on Pancreatic Lipase Activity. *Comparative Biochemistry and Physiology Part B: Biochemistry and Molecular Biology*, *116*(1), 51–55. https://doi.org/10.1016/S0305-0491(96)00153-8

Łuczak, J., Jungnickel, C., Joskowska, M., Thöming, J., & Hupka, J. (2009). Thermodynamics of micellization of imidazolium ionic liquids in aqueous solutions. *Journal of Colloid and Interface Science*, *336*(1), 111–116. https://doi.org/10.1016/j.jcis.2009.03.017

Macierzanka, A., Böttger, F., Lansonneur, L., Groizard, R., Jean, A. S., Rigby, N. M., … Mackie, A. R. (2012). The effect of gel structure on the kinetics of simulated gastrointestinal digestion of bovine β-lactoglobulin. *Food Chemistry*, *134*(4), 2156–2163. https://doi.org/10.1016/j.foodchem.2012.04.018

Macierzanka, A., Bo, F., Rigby, N. M., Lille, M., Poutanen, K., Mills, E. N. C., & Mackie, A. R. (2012). *Enzymatically Structured Emulsions in Simulated Gastrointestinal Environment : Impact on Interfacial Proteolysis and Di ff usion in Intestinal Mucus*. https://doi.org/10.1021/la302194q

Macierzanka, A., Torcello-gómez, A., & Maldonado-valderrama, J. (2019). Jo ur na l P re ro of. *Advances in Colloid and Interface Science*, 102045. https://doi.org/10.1016/j.cis.2019.102045

Macierzanka, A., Sancho, A. I., Mills, E. N. C., Rigby, N. M., & Mackie, A. R. (2009). Emulsification alters simulated gastrointestinal proteolysis of β-casein and β-lactoglobulin. *Soft Matter*, *5*(3), 538–550. https://doi.org/10.1039/B811233A

Macierzanka, A., Mackie, A. R., & Krupa, L. (2019). Permeability of the small intestinal mucus for physiologically relevant studies: Impact of mucus location and ex vivo treatment. *Scientific Reports*, *9*(1), 17516. https://doi.org/10.1038/s41598-019-53933-5

Mackie, A., & Rigby, N. (2015). InfoGest Consensus Method, in: Verhoeckx K. et al. (Eds.), The

Impact of Food Bioactives on Health: in vitro and ex vivo models, Springer Open, pp. 13–22. https://doi.org/10.1007/978-3-319-16104-4

Maldonado-Valderrama, J. (2019). Probing in vitro digestion at oil–water interfaces. In *Current Opinion in Colloid and Interface Science* (Vol. 39, pp. 51–60). Elsevier Ltd. https://doi.org/10.1016/j.cocis.2019.01.004

Maldonado-Valderrama, J., Wilde, P., MacIerzanka, A., & MacKie, A. (2011). The role of bile salts in digestion. *Advances in Colloid and Interface Science*, *165*(1), 36–46. https://doi.org/10.1016/j.cis.2010.12.002

Maldonado-Valderrama, J., Woodward, N. C., Patrick Gunning, A., Ridout, M. J., Husband, F. A., Mackie, A. R., Morris, V. J., & Wilde, P. J. (2008). Interfacial characterization of β-lactoglobulin networks: Displacement by bile salts. *Langmuir*, *24*(13), 6759–6767. https://doi.org/10.1021/la800551u

Maldonado-Valderrama, J., Muros-Cobos, J. L., Holgado-Terriza, J. A., & Cabrerizo-Vílchez, M. A. (2014). Bile salts at the air-water interface: Adsorption and desorption. *Colloids and Surfaces B: Biointerfaces*, *120*, 176–183. https://doi.org/10.1016/j.colsurfb.2014.05.014

Maldonado-Valderrama, J., Terriza, J. A. H., Torcello-Gómez, A., & Cabrerizo-Vílchez, M. A. (2013). In vitro digestion of interfacial protein structures. *Soft Matter*, *9*(4), 1043–1053. https://doi.org/10.1039/C2SM26843D

Maldonado-Valderrama, Julia, del Castillo Santaella, T., Holgado-Terriza, J. A., & Cabrerizo-Vílchez, M. Á. (2022). In vitro Digestion of Emulsions in a Single Droplet via Multi Subphase Exchange of Simulated Gastrointestinal Fluids. *Journal of Visualized Experiments*, *2022*(189). https://doi.org/10.3791/64158

Maldonado-Valderrama, Julia, Torcello-Gómez, A., del Castillo-Santaella, T., Holgado-Terriza, J. A., & Cabrerizo-Vílchez, M. A. (2015). Subphase exchange experiments with the pendant drop technique. *Advances in Colloid and Interface Science*, *222*, 488–501. https://doi.org/10.1016/j.cis.2014.08.002

Mandalari, G., Mackie, A. M., Rigby, N. M., Wickham, M. S. J., & Mills, E. N. C. (2009). Physiological phosphatidylcholine protects bovine β-lactoglobulin from simulated gastrointestinal proteolysis. *Molecular Nutrition & Food Research*, *53*(S1), S131–S139. https://doi.org/10.1002/mnfr.200800321

Martos, G., Contreras, P., Molina, E., & López-Fandiño, R. (2010). Egg White Ovalbumin Digestion Mimicking Physiological Conditions. *Journal of Agricultural and Food Chemistry*, *58*(9), 5640–5648. https://doi.org/10.1021/jf904538w

Matubayasi, N., Kanzaki, M., Sugiyama, S., & Matuzawa, A. (1996). Thermodynamic study of gaseous adsorbed films of sodium taurocholate at the air/water interface. *Langmuir*, *12*(7), 1860–1862. https://doi.org/10.1021/la950832o

Mekkaoui, A., Liu, Y., Zhang, P., Ullah, S., Wang, C., & Xu, B. (2021). Effect of bile salts on the interfacial dilational rheology of lecithin in the lipid digestion process. *Journal of Oleo*

Science, *70*(8), 1069–1080. https://doi.org/10.5650/jos.ess21081

Ménard, O., Cattenoz, T., Guillemin, H., Souchon, I., Deglaire, A., Dupont, D., & Picque, D. (2014). Validation of a new in vitro dynamic system to simulate infant digestion. *Food Chemistry*, *145*, 1039–1045. https://doi.org/10.1016/j.foodchem.2013.09.036

Menard, O., Lesmes, U., Shani-Levi, C. S., Araiza Calahorra, A., Lavoisier, A., Morzel, M., … Dupont, D. (2023). Static in vitro digestion model adapted to the general older adult population: an INFOGEST international consensus. *Food & Function*, *14*(10), 4569–4582. https://doi.org/10.1039/D3FO00535F

Meyer, V. R. (1995). Quantitation of chromatographic peaks in the 0.1 to 1.0% range. *Chromatographia*, *40*(1–2), 15–22. https://doi.org/10.1007/BF02274601

Minekus, M., Marteau, P., Havenaar, R., & Veld, J. H. J. H. in't. (1995). A multicompartmental dynamic computer-controlled model simulating the stomach and small intestine. *Alternatives to Laboratory Animals*, *23*(2), 197–209.

Minekus, M., Alminger, M., Alvito, P., Ballance, S., Bohn, T., Bourlieu, C., … Brodkorb, A. (2014). A standardised static in vitro digestion method suitable for food-an international consensus. *Food and Function*, *5*(6), 1113–1124. https://doi.org/10.1039/c3fo60702j

Mnasri, T., Hérault, J., Gauvry, L., Loiseau, C., Poisson, L., Ergan, F., & Pencréac'H, G. (2017). Lipase-catalyzed production of lysophospholipids. *OCL - Oilseeds and Fats, Crops and Lipids*, *71*(4), 0–5. https://doi.org/10.1051/ocl/2017011

Molendi-Coste, O., Legry, V., & Leclercq, I. A. (2011). Why and How Meet n-3 PUFA Dietary Recommendations? *Gastroenterology Research and Practice*, *2011*, 11. https://doi.org/10.1155/2011/364040

Molly, K., Vande Woestyne, M., & Verstraete, W. (1993). Development of a 5-step multi-chamber reactor as a simulation of the human intestinal microbial ecosystem. *Applied Microbiology and Biotechnology*, *39*(2), 254–258. https://doi.org/10.1007/BF00228615

Moreno, F. J., Mackie, A. R., & Mills, E. N. C. (2005). Phospholipid Interactions Protect the Milk Allergen α-Lactalbumin from Proteolysis during in Vitro Digestion. *Journal of Agricultural and Food Chemistry*, *53*(25), 9810–9816. https://doi.org/10.1021/jf0515227

Mulet-Cabero, A.-I., Egger, L., Portmann, R., Ménard, O., Marze, S., Minekus, M., Le Feunteun, S., Sarkar, A., M-L Grundy, M., Carrière, F., Golding, M., Dupont, D., Recio, I., Brodkorb, A., & Mackie, A. (2020). *Cite this: Food Funct*. *11*, 1702. https://doi.org/10.1039/c9fo01293a

Mun, S., Decker, E. A., Park, Y., Weiss, J., & McClements, D. J. (2006). Influence of interfacial composition on in vitro digestibility of emulsified lipids: Potential mechanism for chitosan's ability to inhibit fat digestion. *Food Biophysics*, *1*(1), 21–29. https://doi.org/10.1007/s11483-005-9001-0

Nagadome, S., Okazaki, Y., Lee, S., Sasaki, Y., & Sugihara, G. (2001). Selective solubilization of

sterols by bile salt micelles in water: A thermodynamic study. *Langmuir*, *17*(14), 4405–4412. https://doi.org/10.1021/la010087h

Nater, U. M., Rohleder, N., Gaab, J., Berger, S., Jud, A., Kirschbaum, C., & Ehlert, U. (2005). Human salivary alpha-amylase reactivity in a psychosocial stress paradigm. *International Journal of Psychophysiology*, *55*(3), 333–342. https://doi.org/10.1016/j.ijpsycho.2004.09.009

Ntemiri, A., Ní Chonchuír, F., O, T. F., Stanton, C., Paul Ross, R., & O, P. W. (2017). *Glycomacropeptide Sustains Microbiota Diversity and Promotes Specific Taxa in an Artificial Colon Model of Elderly Gut Microbiota*. https://doi.org/10.1021/acs.jafc.6b05434

O'Connor, C. J., Ch'ng, B. T., & Wallace, R. G. (1983). Studies in bile salt solutions. 1. Surface tension evidence for a stepwise aggregation model. *Journal of Colloid And Interface Science*, *95*(2), 410–419. https://doi.org/10.1016/0021-9797(83)90200-X

Olivares-Morales, A., Lennernäs, H., Aarons, L., & Rostami-Hodjegan, A. (2015). Translating Human Effective Jejunal Intestinal Permeability to Surface-Dependent Intrinsic Permeability: a Pragmatic Method for a More Mechanistic Prediction of Regional Oral Drug Absorption. *AAPS Journal*, *17*(5), 1177–1192. https://doi.org/10.1208/s12248-015-9758-0

Pabois, O., Lorenz, C. D., Harvey, R. D., Grillo, I., Grundy, M. M. L., Wilde, P. J., … Dreiss, C. A. (2019). Molecular insights into the behaviour of bile salts at interfaces: a key to their role in lipid digestion. *Journal of Colloid and Interface Science*, *556*, 266–277. https://doi.org/10.1016/j.jcis.2019.08.010

Pafumi, Y., Lairon, D., De La Porte, P. L., Juhel, C., Storch, J., Hamosh, M., & Armand, M. (2002). Mechanisms of inhibition of triacylglycerol hydrolysis by human gastric lipase. *Journal of Biological Chemistry*, *277*(31), 28070–28079. https://doi.org/10.1074/jbc.M202839200

Parekh, P. Y., Patel, V. I., Khimani, M. R., & Bahadur, P. (2023). Self-assembly of bile salts and their mixed aggregates as building blocks for smart aggregates. *Advances in Colloid and Interface Science*, *312*(January), 102846. https://doi.org/10.1016/j.cis.2023.102846

Persson, E., Löfgren, L., Hansson, G., Abrahamsson, B., Lennernäs, H., & Nilsson, R. (2007). Simultaneous assessment of lipid classes and bile acids in human intestinal fluid by solid-phase extraction and HPLC methods. *Journal of Lipid Research*, *48*(1), 242–251. https://doi.org/10.1194/jlr.D600035-JLR200

Reddy, I. M., Kella, N. K. D., & Kinsella, J. E. (1988). Structural and Conformational Basis of the Resistance of β-Lactoglobulin to Peptic and Chymotryptic Digestion. *Journal of Agricultural and Food Chemistry*, *36*(4), 737–741. https://doi.org/10.1021/jf00082a015

Reynaud, Y., Couvent, A., Manach, A., Forest, D., Lopez, M., Picque, D., Souchon, I., Rémond, D., & Dupont, D. (2021). Food-dependent set-up of the DiDGI® dynamic in vitro system: Correlation with the porcine model for protein digestion of soya-based food. *Food Chemistry*, *341*, 128276. https://doi.org/10.1016/J.FOODCHEM.2020.128276

Rosenthal, R., Heydt, M. S., Amasheh, M., Stein, C., Fromm, M., & Amasheh, S. (n.d.).

Analysis of absorption enhancers in epithelial cell models. *Ann. N.Y. Acad. Sci*. https://doi.org/10.1111/j.1749-6632.2012.06562.x

Sah, B. N. P., McAinch, A. J., & Vasiljevic, T. (2016). Modulation of bovine whey protein digestion in gastrointestinal tract: A comprehensive review. *International Dairy Journal*, *62*, 10–18. https://doi.org/10.1016/j.idairyj.2016.07.003

Sarkar, A., Li, H., Cray, D., & Boxall, S. (2018). Composite whey protein–cellulose nanocrystals at oil-water interface: Towards delaying lipid digestion. *Food Hydrocolloids*, *77*, 436–444. https://doi.org/10.1016/j.foodhyd.2017.10.020

Sarkar, A., Ye, A., & Singh, H. (2016). On the role of bile salts in the digestion of emulsified lipids. *Food Hydrocolloids*, *60*, 77–84. https://doi.org/10.1016/j.foodhyd.2016.03.018

Schaafsma, G. (2005). The Protein Digestibility-Corrected Amino Acid Score (PDCAAS)-A Concept for Describing Protein Quality in Foods and Food Ingredients: A Critical Review. *Journal of AOAC International, 88*(3), 988-994. ttps://academic.oup.com/jaoac/article/88/3/988/5657545

Singh, H., & Ye, A. (2013). Structural and biochemical factors affecting the digestion of protein-stabilized emulsions. *Current Opinion in Colloid and Interface Science*, *18*(4), 360–370. https://doi.org/10.1016/j.cocis.2013.04.006

Sjövall, J. (1959). On the Concentration of Bile Acids in the Human Intestine during Absorption. Bile Acids and Steroids 74. *Acta Physiologica Scandinavica*, *46*(4), 339–345. https://doi.org/10.1111/j.1748-1716.1959.tb01763.x

Somaratne, G., Ferrua, M. J., Ye, A., Nau, F., Floury, J., Dupont, D., & Singh, J. (2020). Food material properties as determining factors in nutrient release during human gastric digestion: a review. *Critical Reviews in Food Science and Nutrition*, *60*(22), 3753–3769. https://doi.org/10.1080/10408398.2019.1707770

Stankiewicz, U., & Bartoszek, A. (2017). *ABSORPCJA , METABOLIZM I ROLA BIOLOGICZNA KWASÓW*. *1*(110), 18–32. https://doi.org/10.15193/zntj/2017/110/170

Szefel, J., Kruszewski, W. J., & Buczek, T. (2015). Enteral feeding and its impact on the gut immune system and intestinal mucosal barrier. *Przegląd Gastroenterologiczny*, *10*(2), 71–77. https://doi.org/10.5114/pg.2015.48997

Taylor, L. A., Pletschen, L., Arends, J., Unger, C., & Massing, U. (2010). Marine phospholipids-a promising new dietary approach to tumor-associated weight loss. *Support Care Cancer*, *18*(2), 159-170. https://doi.org/10.1007/s00520-009-0640-4

Tharakan, A., Norton, I. T., Fryer, P. J., & Bakalis, S. (2010). *Mass Transfer and Nutrient Absorption in a Simulated Model of Small Intestine*. https://doi.org/10.1111/j.1750-3841.2010.01659.x

Torcello-Gómez, A., Dupont, D., Jardin, J., Briard-Bion, V., Deglaire, A., Risse, K., … Mackie, A. (2020). The pattern of peptides released from dairy and egg proteins is highly dependent on

the simulated digestion scenario. *Food & Function, 11,* 5240-5256. https://doi.org/10.1039/D0FO00744G

Torcello-Gómez, A., Maldonado-Valderrama, J., Martín-Rodríguez, A., & McClements, D. J. (2011). Physicochemical properties and digestibility of emulsified lipids in simulated intestinal fluids: Influence of interfacial characteristics. *Soft Matter*, *7*(13), 6167–6177. https://doi.org/10.1039/c1sm05322a

Torcello-Gómez, A., Jódar-Reyes, A. B., Maldonado-Valderrama, J., & Martín-Rodríguez, A. (2012). Effect of emulsifier type against the action of bile salts at oil–water interfaces. *Food Research International*, *48*(1), 140–147. https://doi.org/10.1016/j.foodres.2012.03.007

Torcello-Gómez, A., Maldonado-Valderrama, J., de Vicente, J., Cabrerizo-Vílchez, M. A., Gálvez-Ruiz, M. J., & Martín-Rodríguez, A. (2011). Investigating the effect of surfactants on lipase interfacial behaviour in the presence of bile salts. *Food Hydrocolloids*, *25*(4), 809–816. https://doi.org/10.1016/j.foodhyd.2010.09.007

Value, N., & Used, P. (2010). *Ranges of Normal Values in Human Whole Blood (B), Plasma (P), or Serum (S) a Normal Value (Varies with Procedure Used) Determination Traditional Units SI Units* (p. 727).

Vassilopoulou, E., Rigby, N., Moreno, F. J., Zuidmeer, L., Akkerdaas, J., Tassios, I., … Mills, C. (2006). Effect of in vitro gastric and duodenal digestion on the allergenicity of grape lipid transfer protein. *Journal of Allergy and Clinical Immunology*, *118*(2), 473–480. https://doi.org/10.1016/j.jaci.2006.04.057

Venema, K. (2015). The TNO in vitro model of the colon (TIM-2). In *The Impact of Food Bioactives on Health: In Vitro and Ex Vivo Models*. https://doi.org/10.1007/978-3-319-16104-4_26

Venema, K., Van Nuenen, M. H. M. C., Van Den Heuvel, E. G., Pool, W., & Van Der Vossen, J. M. B. M. (2003). The Effect of Lactulose on the Composition of the Intestinal Microbiota and Short-chain Fatty Acid Production in Human Volunteers and a Computer-controlled Model of the Proximal Large Intestine. *Microbial Ecology in Health and Disease*, *15*, 94–105. https://doi.org/10.1080/08910600310019895

Verhoeckx, K., Cotter, P., Kleiveland, C., Lea, T., Mackie, A., & Requena, T. (2015). The Impact of Food Bioactives on Health. In *The Impact of Food Bioactives on Health*. https://doi.org/10.1007/978-3-319-16104-4

Verwei, M., Freidig, A. P., Havenaar, R., & Groten, J. P. (2006). Predicted Serum Folate Concentrations Based on In Vitro Studies and Kinetic Modeling are Consistent with Measured Folate Concentrations in Humans. In *The Journal of Nutrition Methodology and Mathematical Modeling J. Nutr* (Vol. 136). https://academic.oup.com/jn/article/136/12/3074/4664015

Vincent, D., Elkins, A., Condina, M. R., Ezernieks, V., & Rochfort, S. (2016). Quantitation and identification of intact major milk proteins for high-throughput LC-ESI-Q-TOF MS analyses. *PLoS ONE*, *11*(10), 1–21. https://doi.org/10.1371/journal.pone.0163471

Walton, K. D., Freddo, A. M., Wang, S., & Gumucio, D. L. (2016). *Generation of intestinal surface: an absorbing tale*. https://doi.org/10.1242/dev.135400

Warren, D. B., Chalmers, D. K., Hutchison, K., Dang, W., & Pouton, C. W. (2006). Molecular dynamics simulations of spontaneous bile salt aggregation. *Colloids and Surfaces A: Physicochemical and Engineering Aspects*, *280*(1–3), 182–193. https://doi.org/10.1016/j.colsurfa.2006.02.009

Wickham, M. J. S., Faulks, R. M., Mann, J., & Mandalari, G. (2012). The design, operation, and application of a dynamic gastric model. *Dissolution Technologies*, *19*(3), 15–22. https://doi.org/10.14227/DT190312P15

Woudstra, T., & Thomson, A. B. R. (2002). *Nutrient absorption and intestinal adaptation with ageing*. *16*(1), 1–15. https://doi.org/10.1053/bega.2002.0262

7. List of scientific activities of the PhD candidate

Scientific papers (published)

1. Maeda, N., **Dulko, D.**, Macierzanka, A., & Jungnickel, C. (2022). Analysis of the factors affecting static in vitro pepsinolysis of food proteins. *Molecules*, *27*(4), 1260; (IF_{2022} = 4.6; 140 pkt MEiN),
2. Krupa, Ł., Staroń, R., **Dulko, D.**, Łozińska, N., Mackie, A. R., Rigby, N. M., Macierzanka A., Markiewicz A., & Jungnickel, C. (2021). Importance of bile composition for diagnosis of biliary obstructions. *Molecules*, *26*(23), 7279; (IF_{2021} = 4.927; 140 pkt MEiN),
3. **Dulko, D.,** Staroń, R., Krupa, L., Rigby, N.M., Mackie, A.R., Gutkowski, K., Wasik, A., & Macierzanka, A. (2021). The bile salt content of human bile impacts on simulated intestinal proteolysis of β-lactoglobulin. *Food Research International*, 145, 110413; (IF_{2021} = 7.425; 140 pkt MEiN),
4. Böttger, F., Dupont, D., **Marcinkowska (Dulko), D.**, Bajka, B., Mackie, A., & Macierzanka, A. (2019). Which casein in sodium caseinate is most resistant to in vitro digestion? Effect of emulsification and enzymatic structuring. *Food Hydrocolloids*, *88*, 114-118; (IF_{2019} = 7.053; 140 pkt MEiN).

Participation in scientific conferences

1. A. Macierzanka, **D. Dulko**, I. E. Kłosowska-Chomiczewska, T. Del Castillo-Santaella, J. Maldonado-Valderrama; The complexity of human bile and how to replace it for in-vitro digestion studies (POSTER); 7th International Conference on Food Digestion (ICFD2022), Cork, Ireland, 3-5th May 2022,
2. A. Macierzanka, **D. Dulko**, Ilona E. Kłosowska-Chomiczewska, T. Del Castillo Santaella, M. A. Cabrerizo-Vilchez, Ł. Krupa, K. Gutkowski, R. Staron, J. Maldonado-Valderrama; Human bile: Interfacial characterisation during in vitro lipolysis (POSTER); 5th International Conference on Food Structures, Digestion and Health Engineering Food Structures for Optimal Nutrition and Health "Working With and Like Nature", Rotoura, New Zealand, 30th September – 3rd October 2019,
3. **D. Dulko**, I.E. Kłosowska-Chomiczewska, J. Maldonado-Valderrama, T. Del Castillo Santaella, M.A. Cabrerizo-Vílchez, R. Staron, Ł. Krupa, K. Gutkowski, A. Macierzanka;

Interfacial characterization of human bile salts and its effect on *in vitro* lipolysis (POSTER); 6th International Conference on Food Digestion, Granada, Spain, 2nd - 4th April 2019,

4. **D. Marcinkowska (Dulko)**, R. Staron, Ł. Krupa, K. Gutkowski, A. Torcello-Gomez, N. M. Rigby, A. R. Mackie, A. Wasik, G. Aleksiejuk, A. Jankowska, J. Parzych, A. Macierzanka; Wpływ ludzkich soli żółciowych na trawienie białek w warunkach *in vitro* (ORAL); 9th Congress of Chemical Technology, Gdańsk, Poland, 3rd -7th Sepember 2018,

5. **D. Marcinkowska (Dulko)**, R. Staron, Ł. Krupa, K. Gutkowski, A. Markiewicz, C. Jungnickel, A. Torcello-Gomez, N.M. Rigby, A.R. Mackie, A. Macierzanka; Effect of human bile salts on in vitro protein digestion (ORAL); 17th Food Colloids Conference: Application of Soft Matter Concepts, Leeds, UK, 8th - 11th April 2018,

6. C. Jungnickel, **D. Marcinkowska (Dulko)**, A. Macierzanka; Which factor is more significant in retarding pepsinolysis: additives, or colloidal matrices? (POSTER); 17th Food Colloids Conference: Application of Soft Matter Concepts, Leeds, UK, 8th - 11th April 2018.

Research visits

1. InterPhD2 internship program, November 2018 – April 2019, Department of Applied Physics, Faculty of Sciences, University of Granada, Spain,

2. Erasmus+ programme, September – October 2017, School of Food Science and Nutrition, University of Leeds, UK,

3. Erasmus+ programme, June – July 2017, School of Food Science and Nutrition, University of Leeds, UK.